

Application of Language Technologies in Biology: Feature Extraction and Modeling for Transmembrane Helix Prediction

Thesis
submitted in partial fulfilment
of the Degree of
Doctor of Philosophy
in Language and Information Technologies

Madhavi K. Ganapathiraju

CMU-LTI-07-004

Thesis Committee
Judith Klein-Seetharaman
Raj Reddy
Jaime Carbonell
Maria Kurnikova



Language Technologies Institute
School of Computer Science
Carnegie Mellon University
5000 Forbes Ave, Pittsburgh, Pennsylvania, USA

© 2007 Madhavi K. Ganapathiraju

Thesis Committee

Judith Klein-Seetharaman (co-chair)

Raj Reddy (co-chair)

Jaime G. Carbonell

Maria Kurnikova

Carnegie Mellon University

Abstract

This thesis provides new insights into the application of algorithms developed for language processing towards problems in mapping of protein sequences to their structure and function, in direct analogy to the mapping of words to meaning in natural language. While there have been applications of language algorithms previously in computational biology, most notably hidden Markov models, there has been no systematic investigation of what are appropriate word equivalents and vocabularies in biology to date. In this thesis, we consider amino acids, chemical vocabularies and amino acid properties as fundamental building blocks of protein sequence language and study n-grams and other positional word-associations and latent semantic analysis towards prediction transmembrane helices.

First, a toolkit referred to as the Biological Language Modeling Toolkit has been developed for biological sequence analysis through amino acid n-gram and amino acid word-association analysis. N-gram comparisons across genomes showed that biological sequence language differs from organism to organism, and has resulted in identification of genome signatures.

Next, we used a biologically well established mapping problem, namely the mapping of protein sequences to their secondary structures, to quantitatively compare the utility of different fundamental building blocks in representing protein sequences. We found that the different vocabularies capture different aspects of protein secondary structure best. Finally, the conclusions from the study of biological vocabularies were used, in combination with the latent semantic analysis and signal processing techniques to address the biologically important but technically challenging and unsolved problem of predicting transmembrane segments.

This work led to the development of TMpro, which achieves reduced transmembrane segment prediction error rate by 20-50% compared to previous state-of-the-art methods. The method is a novel approach of analyzing amino-acid property sequences as opposed to analyzing amino acid sequences: following our work, it has already been applied towards protein remote homology detection and protein structural type classifications by others.

Acknowledgements

I would like to express most sincere gratitude to my thesis advisors Prof. Raj Reddy and Prof. Judith Klein-Seetharaman who have influenced me greatly, and from whom I had the chance to learn throughout the course of this work.

Prof Raj Reddy's advice at every stage from identifying a problem, to the approach, implementation and even presentation of this work are most valuable. He spent many hours in shaping my research and the approach. Without these inputs, it would not have been what it is now. In spite of his very busy schedules, his students never have to wait to get an appointment! Prof Reddy has also involved me in the discussions of a number of different projects that happened during this time — I am not sure how I happened to be that fortunate. I had the benefit of listening during discussions among senior professors and gaining experience working on these projects. Each of these projects demonstrated Prof Reddy's awareness and concern to the needs of the society — Universal Library (to preserve old documents and make information freely accessible), PCtvt (to bring information and communication technologies to villagers), and distance-learning programs (for aspiring students *who missed the first bus*) are a testament to his vision and his perseverance to achieve the vision. I also found that just as a former colleague Rita Singh had told me when I came here, every idea of his is worth making into a thesis — my thesis serves as an example.

I am very fortunate that just as Prof Reddy and Prof Judith Klein-Seetharaman were discussing the seminal ideas for what was to later become biological language modeling project, I stepped into my PhD.

Prof Judith Klein-Seetharaman, my thesis (co)advisor, has influenced me greatly during this period. The first year that I worked with her on the BLM project, I had not considered making it my thesis topic — the main reason being that I had no exposure to biology. But Judith made everything so exciting that I was willing to learn the biology in order to be a part of that work. Her commitment to work is exemplary. She works hard with the students like a student, advises like a professor, gets excited with results and asks questions like a scientist. The numerous seminars she gave in the beginning for the benefit of computer science faculty and students gave us ample insight into the area of biology, that to work in computational biology there was no bridge to cross. I am grateful to her for the number of scientific discussions which lead the thesis into what it is now, for the regular research seminars, the work culture she instilled in the lab, the friendly conversations, and most importantly, hundreds of mid-nightly emails about work

(I have always looked forward to these emails!). Each of us students feel that we have her full attention, and never discovered how she manages her time. Her collaborative efforts give her students abundant opportunities to expand the approach or application of their research.

I would like to thank Prof Jaime Carbonell for allowing me to approach him for discussions even before he was on my committee — he has advised me when I was working on text processing to the time I completed this thesis work. He is a scholar who can bring to the fore his expertise to give valuable suggestions about any problem even if he is hearing it for the first time. I would like to thank Prof Maria Kurnikova for agreeing to be on my committee as an external evaluator. I have benefited from her expertise especially on channel proteins. Prof N Balakrishnan of the Indian Institute of Science is a collaborator with Prof Reddy. He was always available to us for any discussion on the signal processing techniques. I have learnt a great deal from him on these topics which were of direct use in this thesis. I thank him for that. There are a few more faculty that I would like to acknowledge. Prof Yiming Yang — least does she know, but she has influenced me in some aspects that I would remember. I would like to thank Profs Lori Levin, Eric Nyberg, Maxine Eskinazi and Alan Black for the interactions I had with them.

Moving onto the non-academic interactions, the first person I would like to mention is Ms. Vivian Lee. She is the admin contact for Prof. Reddy — but to me she is home away from home. When I first landed in US and called her from the airport, I heard her warm and friendly voice for the first time, and not once has it been different over the many years that I have known her. My friend rightly recognized that she is one person who is always giving!

Annie, fellow PhD student from ISRI, has been my best friend at CMU. We have done all the things best friends do— went to movies, shopping, dinners, travel, etc (or basically everything that was not work). Its always nice to have a friend that you can count on in need, talk to in need and have fun with when you don't need. Friends from Judith's lab at Pitt — Harpreet, Naveena, David, Yanjun, Oznur, Viji, Kalyan, Arpana, Hussein; Friends from CMU — Yan, Krishna, Rong, Ari, Yifen, Hemant — have made this period a pleasant experience. I would also like to thank Ms. Helen Higgins, Ms. Chris Koch, Ms. Stacey Young and Ms. Brooke Hyatt for their friendly supportive nature.

Thesis writing is just an excuse to acknowledge all those that you do not find chances to acknowledge otherwise. My family: my parents for their unconditional love, Padmasree who puts my welfare above hers, Gopal who is my mentor, Mythili who loves me more than she loves her daughter, Jayasree and Chiramjeevi the noble ones, Bhramaramba and Kumar whose reflection I am, Pinni and Babai who celebrate for me, and Indiratta a spiritual exemplar. My friends from my family: Mallika, Vamsee, Abhinay, Lata, Niranjana, Aparna, Chandana, Prashanth, Suvvi, Meghalu, Sadhana, Icu and Sashank. My best friend Monika, with whom I have laughed a million laughs and my best friend Preeti who makes me a better person by telling me that I am one.

In loving memory of aamma-pedananna.

Contents

Abstract	i
Acknowledgements	ii
Table of Contents	iv
List of tables	vii
List of figures	viii
Executive Summary	1
1 Human language and biological language	1
2 Proteins and transmembrane helix prediction	1
3 Unsolved challenges — previous methods	3
4 Models and methods: biological language modeling	4
5 Datasets and metrics of evaluation	4
6 Biological feature development and analysis	5
7 Algorithm for transmembrane helix prediction	7
8 Thesis contributions	8
1 Human Language and Biological Language: Analogies	9
1.1 Biology-text analogy	9
1.2 Biology-speech analogy	10
1.3 Computational Methods for Language and Speech Processing	13
1.3.1 N-grams	13
1.3.2 Yule’s q-statistic	14
1.3.3 Latent semantic analysis	14
1.3.4 Wavelet transform	16
1.4 Application to biological sequences	18
2 Introduction to Proteins	20
2.1 Amino acids: primary sequence of proteins	20
2.2 Secondary structure	23
2.3 Tertiary structure and structure-function paradigm	25
2.4 Membrane and soluble proteins	26

2.5	Membrane protein families and function	27
2.6	Proteomes	28
3	Literature Review in Transmembrane Helix Prediction	29
3.1	Segment-level distinctions between transmembrane and soluble helices . . .	29
3.2	Residue-level propensities of amino acids	30
3.3	Algorithms for transmembrane helix prediction	32
3.4	State-of-the-art and open questions	35
4	Models and Methods: Biological Language Modeling	39
4.1	Biological language modeling toolkit	39
4.1.1	Data structures used for efficient processing	39
4.1.2	Tools created	42
4.2	Adapting latent semantic analysis for secondary structure classification . .	44
4.2.1	Words and documents in proteins	45
4.2.2	Property-segment matrix	45
4.2.3	Feature construction and classification	45
4.3	Transmembrane helix feature extraction and prediction methods	47
4.3.1	Wavelet transform of a protein sequence	47
4.3.2	Rule-based method for transmembrane prediction	51
4.3.3	Transmembrane helix prediction with latent semantic analysis features	54
4.3.4	Decision trees	59
5	Datasets and Evaluations Metrics	60
5.1	Datasets	60
5.1.1	Dataset for n-gram analysis	60
5.1.2	Dataset for secondary structure classification	60
5.1.3	Dataset to compare soluble and transmembrane helices	60
5.1.4	Dataset for transmembrane segment prediction	62
5.2	Evaluation metrics	64
5.2.1	Metrics for secondary structure prediction	64
5.2.2	Metrics for transmembrane helix prediction	65
6	Biological Feature Development and Analysis	68
6.1	N-gram analysis	68
6.1.1	Biological language modeling toolkit	68
6.1.2	Distribution across organisms	72
6.1.3	Distribution across functions	77
6.1.4	Conclusions	81
6.2	Latent semantic analysis for secondary structure classification	81
6.2.1	Conclusions	84
6.3	Transmembrane helix prediction	85
6.3.1	Features to characterize transmembrane segments	85

6.3.2	Comparison of soluble and transmembrane proteins	85
6.3.3	Alternate vocabulary representation of primary sequence	90
6.3.4	Wavelet signal processing	95
7	TMpro: High-Accuracy Algorithm for Transmembrane Helix Prediction	97
7.1	TMpro	97
7.1.1	Benchmark analysis of TMpro	99
7.1.2	Performance on recent data sets	101
7.1.3	Confusion with globular proteins	102
7.1.4	Error analysis	102
7.1.5	Error recovery	105
7.2	Web server	107
7.3	Application of TMpro to specific proteins	108
7.3.1	Proteins with unconventional topology	108
7.3.2	Hypothesis for proteins with unknown transmembrane structure . .	110
8	Summary of Contributions	113
8.1	Scientific contributions	113
8.2	Biological language modeling toolkit	114
8.3	TMpro web server for transmembrane helix prediction	114
9	Future Work	115
9.1	Application of the analytical framework to other areas	115
9.2	Enhancements to TMpro	116
9.3	Genome level predictions	117
10	Publications resulting from the thesis work	118
A	Biological Language Modeling Toolkit: Source Code	121
B	TMpro Web Interface	127
C	Error Analysis Figures	132
	Bibliography	141
	Index	153

List of Tables

2.1	Amino acid properties	23
3.1	Transmembrane predictions by other methods on high resolution set.	37
4.1	Suffix array and longest common prefix array of the string <code>abaabcb</code>	40
4.2	Data Structure consisting of Suffix array, longest common prefix array and the rank array	40
4.3	Example of a genome sequence to demonstrate Suffix array construction	41
4.4	An example word-document matrix	46
5.1	List of organisms for which whole genome sequences have been analyzed	61
5.2	List of chains included in NR_TM dataset	63
5.3	Contingency table for evaluation metrics	65
6.1	Motif search in biological language modeling toolkit	71
6.2	Counts of top 10 4-grams in whole-genomes of some of the organisms studied	74
6.3	5 grams that occur in virus but not in host genome	80
6.4	Precision of secondary structure classification using vector space model	83
6.5	Recall of secondary structure classification using vector space model	83
6.6	Precision of secondary structure classification using latent semantic analysis model	83
6.7	Recall of secondary structure classification using latent semantic analysis	84
6.8	Transmembrane structure prediction on high-resolution dataset	91
6.9	Transmembrane structure prediction with decision trees	93
7.1	Transmembrane structure prediction on high-resolution dataset	100
7.2	Transmembrane structure prediction on recent and larger datasets	101
7.3	Prediction accuracies of merged predictions of TMpro and TMHMM	107

List of Figures

1	Schematic of cell and transmembrane and soluble proteins	2
1.1	Biology-language analogy	10
1.2	Spectrograms of the same sentence spoken by different speakers	12
1.3	Wavelets	17
1.4	Mexican hat wavelet at different dilations and translations	18
2.1	Amino acids	21
2.2	Chemical groups	22
2.3	An example to demonstrate the primary, secondary and tertiary structure of proteins	24
2.4	Protein function is exerted through its structure	25
2.5	Topologies of membrane proteins	27
3.1	Number of experimentally solved membrane protein structures	35
4.1	Demonstration of suffix array and rank array	42
4.2	Secondary structure annotation of a sample protein sequence	45
4.3	Wavelet analysis of <i>rhodopsin</i> protein signal	48
4.4	Wavelet coefficients for three different wavelet functions for <i>rhodopsin</i> . . .	50
4.5	Data preprocessing and feature extraction	52
4.6	Feature vectors	55
4.7	TMpro neural network architecture	56
4.8	TMpro hidden Markov model architecture	57
6.1	Example of a suffix array and its longest common prefix array and rank array, for the sequence	70
6.2	Top 20 unigrams in <i>Aeropyrum pernix</i> and <i>Neisseria meningitidis</i>	73
6.3	N-gram genome signatures	75
6.4	Random genomes versus natural genomes	76
6.5	Genome signatures standard deviations	77
6.6	Preferences between neighboring amino acids in whole genomes	78
6.7	Rare trigrams in lysozyme coincide with folding initiation sites	79

6.8	Changes in 1/f of 4-grams in mammalian rhodopsin upon mutations	80
6.9	Yule values in soluble and transmembrane helices	86
6.10	Fraction of amino acid pairs possessing strong preferences with each other .	87
6.11	Fraction of amino acid pairs possessing similar Yule values in soluble and transmembrane datasets	88
6.12	Comparison of TM prediction by rule based decision method and TMH- MMv2.0	92
6.13	Classification of protein feature vectors of the completely-membrane or completely-nonmembrane type	94
6.14	Wavelet coefficients computed for the protein sequence of <i>rhodopsin</i>	96
7.1	TMpro algorithm for TM helix prediction	98
7.2	TMpro algorithm performance on a small representative data set of high resolution proteins	103
7.3	Number of proteins as a function of observed TM segments	104
7.4	Secondary structure content in wrongly predicted segments by TMpro in globular proteins	105
7.5	TM segments wrongly predicted by TMpro in globular proteins	106
7.6	TM helix predictions on KcsA and Aquaporin by various methods	109
7.7	Annotation of PalH protein with prediction information from many sources	110
7.8	Annotation of HIV Glycoprotein gp160 with structural information	111
7.9	TM helix predictions on GP41 by various methods	112
B.1	TMpro web server - plain text output of predictions	128
B.2	TMpro web server - standardized output of TMpro predictions and addi- tional user-given data	129
B.3	TMpro web server - interactive chart	130
C.1	Number of positively charged residues	133
C.2	Number of negatively charged residues	134
C.3	Number of aromatic residues	135
C.4	Number of aliphatic residues	136
C.5	Number of nonpolar residues	137
C.6	Number of electron acceptor residues	138
C.7	Number of electron donor residues	139
C.8	Average hydrophobicity in the segment	140

Chapter 0

Executive Summary

1 Human language and biological language

Biological sequences are composed of letters (amino acids), which form words (helices, sheets or coils) that convey a meaning (structure or function), similar to natural language texts. In this thesis we apply language analysis procedures to protein sequences to predict if they are potentially membrane proteins and if yes, where in these proteins the membrane embedded segments (transmembrane segments) are located. We used algorithms for natural language processing to study classical problems pertaining to biological sequences and achieved high accuracy.

An introduction to the analogy between biology and language and also an introduction to the algorithms for language (text and speech) processing that are referred to in this thesis are presented in **Chapters 1** (next chapter) and **Publication 1** listed on page 118).

2 Proteins and transmembrane helix prediction

Amino acid sequence information has become available for hundreds of thousands of proteins in the last decade, owing to the advances in genome sequencing technologies. However, to understand the functional role played by each of these proteins in a cell, it is crucial to determine its structure, and as a first step, to determine its secondary structure. There are a class of proteins that reside embedded in the cell membrane, called membrane proteins. Parts of these proteins are found exposed to extra-cellular (ec) region and parts to the intra-cellular (cytoplasmic, cp) region, and there are segments that are embedded in the membrane (see Figure 1). These *transmembrane* (TM) segments are known to possess helical secondary structure for all plasma-membrane residing membrane proteins in eukaryotic organisms, and are characteristically different from nontransmembrane helical segments. Membrane proteins are present not only in the cellular membrane but also in membranes of organelles e.g. mitochondria, nucleus, endoplasmic reticulum.

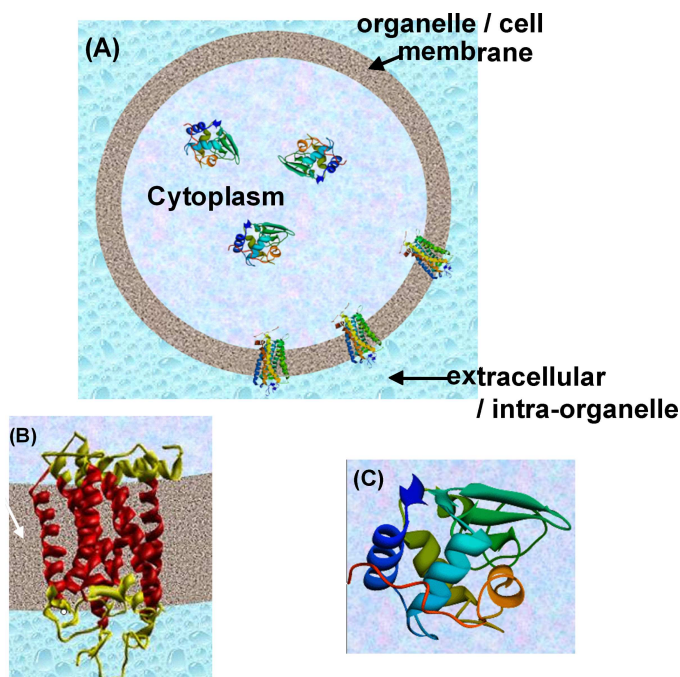


Figure 1: Schematic of cell and transmembrane and soluble proteins

(A) The cell is enveloped by a cell-membrane (brown) and is surrounded by water medium (blue bubbles). The medium inside the cell is made of water as well (blue-pink). Soluble proteins are found completely inside the cell. Membrane proteins are partly embedded in the cell-membrane. (B) Transmembrane protein rhodopsin: It starts in the cytoplasmic region (top), traverses through the cell membrane to go into the extracellular region (bottom) and then traverses the membrane again to enter the cytoplasm. It has 8 helices, 7 of which are located mostly in the *transmembrane* region. (C) Soluble protein Lysozyme: The protein is immersed in an aqueous medium.

An introduction to proteins is presented in **Chapter 2**.

The objective of this thesis is to develop computational approaches for the prediction of helical transmembrane segments in protein sequences. Accurately predicting one or more transmembrane segments in a protein in turn helps in identifying membrane proteins from soluble proteins. Focus of this work is on the more challenging problem of predicting transmembrane segments from only the primary sequence, as opposed to using evolutionary profile of the protein, in order to facilitate prediction even when such information is not available.

Membrane proteins are a large fraction ($\sim 25\%$) of all the proteins found in living organisms, and play vital roles in cellular functions such as signal transduction and transport of ions across the cell membrane.

Knowledge of the transmembrane segment locations, boundaries and the overall topology of a membrane protein can

1. give insight into the function of the protein

2. be useful in narrowing down the possible tertiary structure conformations of the protein
3. help identify other proteins related to it in order to be able to apply any knowledge known about these proteins to the protein at hand
4. can be of use in drug-design by reducing the complexity of search between drugs and their target proteins.

Experimental methods to determine the three dimensional structures of proteins such as NMR spectroscopy and x-ray crystallography are very tedious, and in case of membrane proteins, are often infeasible—transmembrane proteins aggregate in the absence of their natural hydrophobic environment, the membrane. The number of TM proteins with experimentally determined structure corresponds to only about 1.4% out of total protein structures deposited in the Protein Data Bank (PDB) as of early 2007 [1].

The importance of membrane proteins coupled with the difficulty in determining their structures by experimental methods, make it desirable and necessary to predict membrane protein structure by computational methods.

The first questions pertinent to membrane protein structures are :

1. Is the given sequence that of a membrane protein?
2. How many transmembrane segments are present in this membrane protein?
3. What is the topology of this protein with respect to the cell membrane; namely, which of the non-membrane parts are inside the cell? and which are outside?
4. What are the boundaries of the transmembrane segments?

The central component in addressing all of the questions is the identification of the locations of TM segments. Only subsequently, we can address the larger question of what are the tertiary contacts made between the amino acids in both the transmembrane and soluble portions of the protein.

3 Unsolved challenges — previous methods

There is no single method that can reliably determine the location and boundaries of transmembrane segments and the topology of the protein with respect to the cell membrane. This is primarily due to the following current limitations:

1. **Limited representation of all possible structures in training data:** Previous methods are limited by the fact that they are over trained to the limited available data, and thus are able to identify only those transmembrane proteins that have amino acid propensities similar to those of known transmembrane structure.

2. **Previous “best” methods used stringent permissible topologies:** The architecture of machine learning methods such as hidden Markov models which expect only a specific arrangement of transmembrane helices— that which is observed when the protein goes from one side of the membrane to the other side of the membrane before returning to the same side (such as shown in Figure 1). It is now known that this arrangement is not universal.

A review of literature on computational methods for characterization and prediction of transmembrane helices is presented in **Chapter 3** and **Publication 2**.

4 Models and methods: biological language modeling

The identification of transmembrane segments is a specific formulation of more general questions, namely “what are the building blocks of sequences” and “what do they infer about the structure or function of the sequence”. These questions are similar to those commonly asked pertaining to natural language texts — “what are common phrases in a language”, “what do they mean”. The specific question about transmembrane segments would correspond to a specific question in language, such as “does the style of text say something about the author”. This suggests that computational algorithms to address language related questions might be applicable to biology.

The approach adopted in this thesis is to apply the concepts of language modeling to biological sequences. Specifically, the methods of statistical n-gram analysis, Yule’s word association measure and latent semantic analysis which are methods originally developed for text processing have been adapted to study biological sequences.

Methods for adapting natural language processing algorithms to biological sequences are described in **Chapter 4**.

5 Datasets and metrics of evaluation

Analysis has been performed on benchmark datasets where available and also on “current” datasets available at the time of study. Metrics of evaluation are also standard methods used in literature.

Datasets and metrics of evaluation for all the studies performed in this thesis are described in **Chapter 5**.

6 Biological feature development and analysis

At the outset, the thesis explores the biology-language analogy, and the applicability of algorithms from natural language processing (NLP) towards answering general questions pertaining to biological sequences. Subsequently, the observations and results are applied to the study of the specific problem of transmembrane helix prediction.

N-grams in biology

Word n-gram statistical modeling is a very strong technique that captures many characteristics of language — characteristic style of an author, location of most meaningful content in a document or sentence. In the first part of this thesis, we applied the n-gram modeling techniques to biological sequences:

1. **Biological Language Modeling Toolkit:** First, a suite of tools called the Biological Language Modeling (BLM) toolkit has been developed to efficiently compute n-gram features of proteomic sequences. It preprocesses genome sequences into suffix arrays, and then computes n-gram features. More complex applications can be built over the functionality of the BLM toolkit.

BLM toolkit is described in **Publication 3** and the resulting collaborative work in **Publication 4**.

2. **Identification of genome signatures:** Analysis of most frequently occurring n-grams in one genome in comparison with the frequencies of these specific n-grams in other genomes lead to the identification of genome signatures. Further, amino acid neighbor preferences are different for different organisms.

N-gram analysis of genome sequences are presented in **Publication 10**.

3. **N-gram features in relation to protein structure and function:** We explored if the n-gram idiosyncrasies coincide with the presence of functionally or structurally relevant information in proteins:

- **Folding.** The locations of rare trigrams and experimentally determined folding initiation sites in the protein folding model system lysozyme were correlated.
- **Misfolding and Stability.** Inverse n-gram frequencies were computed for two proteins and compared with the locations known to be important for their folding and stability of the protein.
- **Host-specificity of viruses.** N-gram characteristics of specific viral proteins and the whole viral genomes were compared with the n-gram characteristics of the host species.
- **Negative charges in calcium sequestering proteins.** N-grams have been computed to infer if high abundance of charged residues can identify calcium sequestering proteins.

In these examples, amino acid n-grams alone did not consistently identify the regions with maximum biological significance. In some cases, experimental data was not available to unambiguously establish the significance of the results.

N-gram analysis of protein functions are presented in **Publication 1**. Computational analysis of misfolding and stability are described in **Publication 6**, but the n-gram analysis of the same are unpublished.

4. **Other word-association features for protein structure prediction:** In addition to n-grams, we also computed other related word association features, such as Yules association measure, and found them to capture characteristics distinguishing transmembrane helices from soluble helices.

Yule’s association measure its application to soluble and transmembrane helices is described in **Publication 11**.

Biological feature development through analysis employing n-gram and n-gram derived features are presented in Section 1 in **Chapter 6**.

Highly separable protein segment features using latent semantic analysis

We borrowed a technique from NLP, latent semantic analysis (LSA). To quantitatively compare different types of vocabularies in their ability to capture biological meaning, we investigated several different vocabularies in a well known biological context. We chose a well defined biological problem, namely that of classifying protein secondary structural segments (helix, sheet and coil). The goal of this work was to:

1. Study the utility of different vocabularies in place of amino acids in characterizing different secondary structure elements. Three separate vocabularies were considered — (i) amino acids, (ii) chemical groups and (iii) amino acid types based on their electronic property.
2. Study if latent semantic analysis is useful for the problem of protein secondary structure prediction.

We found that each vocabulary carried significant “meaning”, and that LSA is a very useful technique for biological sequence analysis.

Feature analysis using latent semantic analysis for protein sequences is described in Sections 2 and 3 in **Chapter 6** and in **Publication 7**.

7 Algorithm for transmembrane helix prediction

We then applied what we learnt from the studies described above to the challenging problem of TM helix prediction. Use of LSA for secondary structure classification established that alternate vocabularies contributed towards secondary structure prediction, and that types of secondary structure are better represented by different choice of vocabulary. Based on this, we chose to use all of the *amino acid* \leftrightarrow *property* mappings in conjunction with each other, for TM prediction. Specifically, we mapped amino acids to charge, polarity, aromaticity, size and electronic property, and constructed the LSA model over this expanded representation.

The features of transmembrane and nontransmembrane segments constructed with this adaptation of LSA were very distinct from each other, indicating possibility of high accuracy of TM segment prediction. We systematically applied different feature extraction and prediction procedures making use of the observations from our approach of language modeling of protein sequences, and developed an algorithm for transmembrane helix prediction. We refer to this algorithm as TMpro.

TMpro has been evaluated on the benchmark server and it outperformed the (previously) best of the sequence-alone methods, namely TMHMM v2.0 by 50% reduction in F-score. It is also very balanced between recall and precision of the helical segments. The Q_{ok} value, which indicates the number of proteins in which all segments are predicted correctly (with one-to-one correspondence to observed segments) is also higher by >10% w.r.t TMHMM.

The strength of TMpro comes from the fact that it does not impose architectural constraints on the topology of the protein and does not overtrain the features to amino acid propensities observed, thereby allowing it to recognize more varied types of TM segments. On evaluating the methods on NR_TM, a data set of nonredundant membrane proteins available today, TMpro achieves 20-30% reduction in segment error rate compared to the best of sequence-based prediction methods, and also outperforms in correctly distinguishing a larger number of membrane proteins from soluble proteins.

Application of TMpro to specific proteins: To estimate TMpro's ability to correctly predict TM helices in membrane proteins of unusual topology, KcsA and aquaporin, we applied TMpro to study these specific proteins. In both cases, TMpro performed favorably. TMpro was also used to predict TM structure in several membrane proteins with unknown structure.

TMpro algorithm, performance evaluations, error analysis, error recovery, application to specific proteins and availability on a web server are described in **Chapter 7** and in **Publications 8 and 9**.

8 Thesis contributions

1. A high accuracy method for TM helix prediction has been developed. It has been shown that it outperforms the current best methods, without any caveats of training data biases during evaluation.
2. Applicability of language analogy to address problems in biological sequence processing has been established through n-grams and latent semantic analysis and study of vocabularies.
3. TMpro has been applied to predict TM segments in proteins with unknown TM structure: PalH of *Botrytis cinerea* and glycoprotein GP41 of human immunodeficiency virus. Experimental studies to validate these predictions are underway.
4. The Biological Language Modeling Toolkit has been developed and released on the internet in open source¹ at <http://www.cs.cmu.edu/~blmt/source/>.
5. The TMpro algorithm has been made available on the web with novel features for analysis by expert biologists and computational scientists²: <http://linzer.blm.cs.cmu.edu/tmpro/>.

Thesis contributions are summarized in **Chapter 8** and future work is described in **Chapter 9**.

¹A web interface to the toolkit has been developed by Vijayalaxmi Manoharan with Dr. Judith Klein-Seetharaman and is available at: <http://flan.blm.cs.cmu.edu>

²The web interface and web service have been developed in collaboration with Christopher Jon Jursa and Dr. Hassan Karimi, University of Pittsburgh School of Information Sciences

Chapter 1

Human Language and Biological Language: Analogies

Genetic encoding has been referred to as a “language”, and a genome itself as “book of life” [2, 3, 4, 5]. Prior work established some characteristics that are similar between language and analogy: both follow the Zipf’s power law [6] of distribution of words which states that the rank of a word and its frequency are inversely related [7, 8]; a formal grammar is exhibited by biological sequence and structure [9, 10, 11]. Prior to this thesis, the linguistic characteristics exhibited by biological sequences have been established (mostly for DNA sequences), but little work has been done towards the application of computational language processing methods to solve specific questions pertaining to structure and function of biological sequences.

The work presented in this thesis is the first systematic application of speech and language analogies to solve specific biological questions. Parallel to the work described in this thesis, there have been other applications of the language and speech analogy to biology [12, 13, 14, 13, 15, 16, 17].

1.1 Biology-text analogy

The analogy between language and biology is outlined schematically in Figure 1.1.

1. Understanding the structure and function of proteins strongly parallels the mapping of words to meaning in natural language processing.
2. The words in text documents map to a meaning, and combine in a linear fashion to convey information. Similarly, proteins may be seen as sequences of raw text which carry higher level information about the structure of the protein. Analysis of the text documents can give further higher level information about the topic and content of the text. Analysis of protein sequences gives information on protein-protein or protein-ligand interactions, and protein functional pathways.

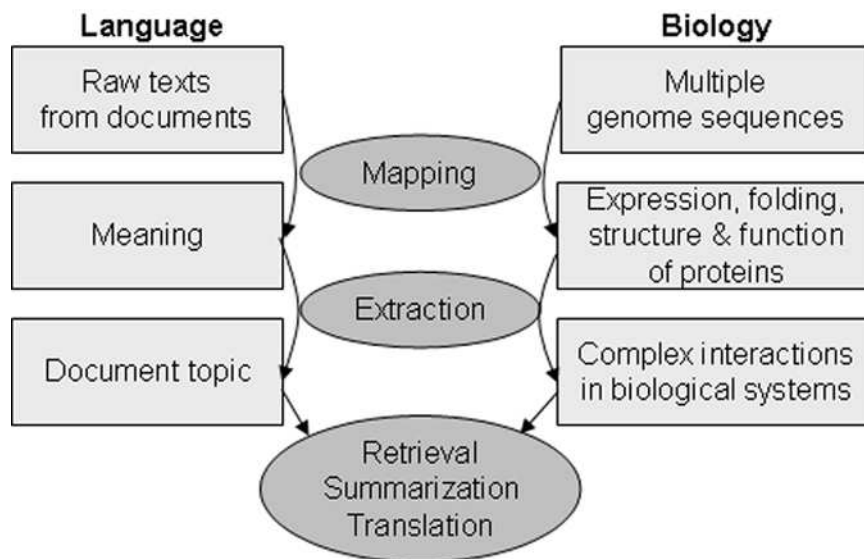


Figure 1.1: Biology-language analogy

3. Availability of large amounts of text in digital form has led to the convergence of linguistics with computational science, and has resulted in applications such as information retrieval, document summarization and machine translation. In direct analogy, transformation of protein science by data availability opened the door to convergence with computer science and information technology.

Techniques used for natural language processing find significant applications to the study of relationships between biological sequences and their functional characteristics [12]. Aside of the results presented in this thesis (see Section 10), there are a number of other examples: linguistic complexity of DNA is used to detect repetitive regions and detect functionally important messages like transcriptional terminators [13] and to determine coding and non-coding region characteristics [18, 19]; text categorization towards protein classification [14]; and n-gram counts to study evolutionary relations between species [20]. Dictionaries of motifs that represent whole genome signatures or regulatory sites have been constructed [21]. Other examples for the use of linguistic approaches for bioinformatics can be found in refs. [22, 23, 24, 25, 26, 12, 13]. Recently, probabilistic language models have been used to improve protein domain boundary detection [15] and to predict secondary structure [16] and transmembrane helix boundaries [17].

1.2 Biology-speech analogy

Segmentation is an important step in speech analysis and applications. Below we discuss examples of speech tasks that have parallels in biology.

“Word” identification by signal recognition in proteins: In a spoken sentence, words are not separated from each other by spaces as in written text. Thus, automatic speech analysis and synthesis methods have to deal with identification of meaningful units. The task therefore shifts from statistical analysis of word frequencies to a stronger focus on signal identification and differentiation in the presence of noise. The task of mapping protein sequences to their structure, dynamics and function can also be seen more generally as a signal processing task. Just as the speech signal is a waveform whose acoustical features vary with time, a protein is a linear chain amino acids whose physicochemical properties vary with respect to position in the sequence. However, while a speech sample can take unlimited continuous values, or digitized values within a given digital resolution, for proteins the value can be only one out of the possible twenty amino acids or a few possibilities of their physicochemical properties.

The goal of speech recognition is to identify the words that are spoken. There are several hundred thousand words in a typical language. These words are formed by a combination of smaller units of sound called phones. Recognizing a word in speech amounts to recognizing these phones. There are typically 50 phones in speech. For protein sequences, there are motifs of secondary structure, the secondary structure elements itself and subpatterns in the secondary structure elements (helix cap, helix core, etc). Thus, identification of structural elements in protein sequences using the signal processing approach is equivalent to phone recognition.

Application of speech analogy to transmembrane proteins: Identifying the differences between membrane and soluble secondary structure elements is analogous to the analysis of speaker variability in the signal processing field. Consider the signal characteristics of a word spoken by two different persons, especially if one is female and the other is male. Although the fundamental nature of the sounds remains the same, the overall absolute values of the signal composition are different. For example, a vowel sound has the same periodic nature, but the frequency is different. See the frequency compositions of the same sentence spoken by a male and a female speaker shown in Figures 1.2A and B.

Identifying the phones alone is not sufficient. The content of a speech signal is not dependent on the signal alone; its interpretation relies on an external entity, the listener. For example, consider the phrases:

- How to recognize speech with this new display
- How to wreck a nice beach with this nudist play

The speech signals or spectrograms showing the frequency decomposition of the sound signals for these two phrases spoken by the same speaker are shown in Figures 1.2B and 1.2C. The two very different sentences are composed of almost identical phone sequences. In this example, finding out which of the two sentences was uttered by the speaker cannot be determined from the spectrogram alone, but depends on the context in which it was

spoken. Thus the complete information for interpretation is not contained in the speech signal alone, but is also inferred from the context. In contrast, the linear strings of amino acids that make up a protein contain in principle all the information needed to fold into a 3-D shape.

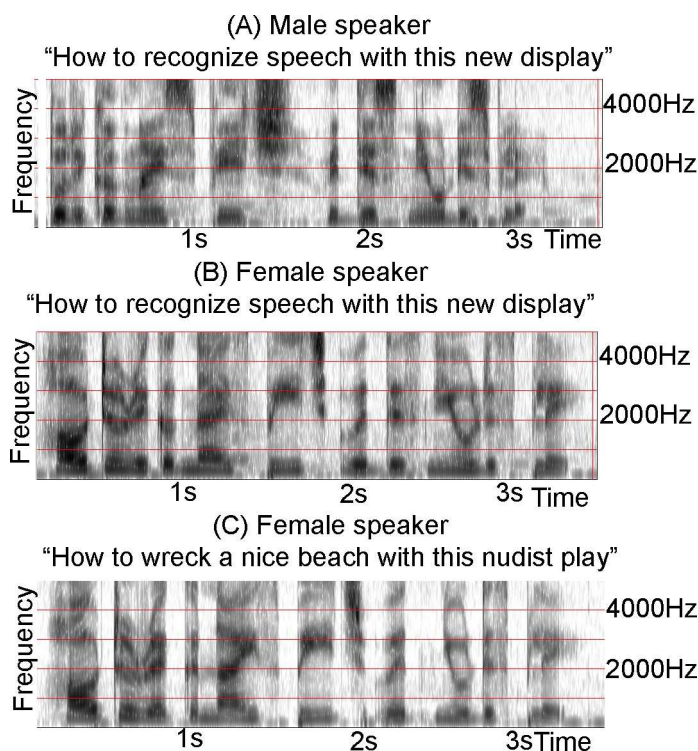


Figure 1.2: Spectrograms of the same sentence spoken by different speakers

The x-axis shows progression of time and the y-axis shows different frequency bands. The energy of the signal in different bands is shown as intensity in grayscale values with progression of time. (A) and (B) show spectrograms of the same sentence "How to recognize speech with this new display" spoken by two different speakers, male and female. Although the frequency characterization is similar, the formant frequencies are much more clearly defined in the speech of the female speaker. (C) shows the spectrogram of the utterance "How to wreck a nice beach with this nudist play" spoken by the same female speaker as in (B). (A) and (B) are not identical even though they are composed of the same words. (B) and (C) are similar to each other even though they are not the same sentences. See text for discussion.

The analogy of speaker variability in the protein world can be found in the categorization of proteins into soluble and membrane proteins. In contrast to soluble proteins, which are entirely immersed in an aqueous environment, membrane proteins have some segments that are located in an aqueous environment, while other segments are located in a chemically different environment, the membrane lipid bilayer, as shown in Figure 1C. Since the environment differs for different segments in TM proteins, the chemical and physical characteristics displayed by these segments are also different. TM helix

prediction is closely related to protein secondary structure prediction given the primary sequence. Secondary structural elements such as helix, strand, turn and loop are still the basic components of the three dimensional structure of membrane proteins; however their characteristics are different from those of the soluble proteins when they are located in the membrane embedded parts. This difference, or localization-variability, may be seen as the speaker variability in speech. The soluble and TM segments can be thought of as speech that is spoken by two different speakers, or three different speakers if the soluble portions are further separated as extracellular and cytoplasmic soluble portions.

Signal processing methods have been used for decades to capture the nuances of speech signals for speech and speaker recognition (see for example [27]). Despite the power of these mathematical tools of signal processing, their application to protein sequences has been minimal to date. The few instances where these methods have been applied are reviewed below.

One of the very first applications was in the computation of the hydrophobic moment of protein domains [28] and in detecting periodicities in secondary structure (α -helix, β -sheet and 3_{10} -helix) [29]. Wavelet analysis of the hydrophobicity signal has been used to locate the secondary structure content relating the periodicity observed in the signal to the known values of secondary structure period [30]. This is based on the fact that the period of a helix is 3.6 residues, that of a sheet is 2 to 2.3 residues and that of a 3_{10} helix is 3 residues [29]. In another application of signal processing technique, Fourier transformation was used to extract the sequence periodicities to classify structural motifs into different architectures. To this end, the Fourier spectrum is computed from the hydrophobicity and secondary structure signal of a proteins, and the power spectrum served as the feature input into a neural network [31]. Last but not the least, hidden Markov modeling, used extensively for computational biology applications such as sequence comparison, was originally applied for speech processing applications [32]

1.3 Computational Methods for Language and Speech Processing

In this chapter we present an introduction to algorithms in computational natural language processing or speech or speaker recognition that we applied to biological sequences in this thesis work. Detailed references for these fields are the books by Manning and Schutze [33] and Rabiner and Juang [34].

1.3.1 N-grams

N-grams refer to sequential occurrences of n words in a text. For example, the following 3-grams may be seen in the sentence `A party was thrown because Congress party has won the General Elections,`

`a party was, party was thrown, was thrown because, ...`

..., Congress party has, party has won, ...

For languages where a word-level dictionary is available but not computational parsers of the grammatical phrase-structure of the text, “frequency counts” of the n-grams in the texts can reveal the “meaningful content” of the text. For example, the word **party** has multiple meanings, two of them being (i) a social get-together and (ii) a group of people involved in some political activity. Construction of 3-gram counts from texts pertaining to different topics, or in other words, making a *3-gram language model* of different collections of texts, it is possible infer that in the first occurrence, the word **party** refers to the first meaning and the second occurrence refers to the second meaning.

Language technologies often use word n-grams as features to study characteristics of texts. N-grams are used in information retrieval, author recognition, plagiarism detection and word sense disambiguation.

1.3.2 Yule’s q-statistic

Yule’s q-statistic (henceforth called Yule value) is a correlation measure between two words [35]. It is used to infer from the presence *or absence* of a word, likelihood of finding another word. It takes a value between +1 and -1 corresponding to the range of “*either both words are present or both words are absent*” to “*if one occurs, the other does not occur*”. For example, the word pair **protein** and **phone** would have a Yule value close to -1, whereas the word pair **protein** and **nutrition** would have a positive value such as 0.6. Traditionally, in natural language processing, the Yule value is computed over windows of a specific length, and a word pair is said to appear together if both the words appear in the window, irrespective of which position they appear in. For example, for a window size of 6, the word pair **new** and **car** are said to occur together irrespective of whether the text is *new car* or *new blue car* or *new light blue car*. The Yule value $Y_d(x, y)$, for a pair of words x and y within in a window of a length d is given as

$$Y(x, y) = \frac{N_{00}N_{11} - N_{01}N_{10}}{N_{00}N_{11} + N_{01}N_{10}} \quad (1.1)$$

N_{11} is the number of windows in which both the words x and y occur

N_{00} is the number of windows in which neither of the words occur

N_{10} is the number of windows in which word x occurs but not word y

N_{01} is the number of windows in which word x does not occur but not word y occurs

1.3.3 Latent semantic analysis

A mathematical framework that can capture synonymy of words, is *latent semantic analysis* (LSA) [36]. Text documents are represented as bags-of-words, that is, as a vector of counts of all the words in the vocabulary.

Latent semantic analysis is performed on a collection of text documents, to infer similarities between the documents based on the similarities of distribution of words between the documents. It has the capability to infer contextual similarity of words based on their collocations across the given corpus, and hence it can recognize ‘latent’ similarities between documents when they share similar but not identical words.

Vocabulary: A list of all the unique words in the corpus is created, after removing *stop words* (e.g., *the, a, are, on, of, ...*) and after *stemming* (i.e, taking only the root of the word, e.g., stemmed version of the words *talking, talked, talk* is *talk*). This final list of words after stop word removal and stemming is referred to as **vocabulary** of the document collection.

Word-document matrix: A large matrix is created, in which rows are labeled by the different words in the vocabulary and the columns are labeled by documents in the corpus. The cell C_{ij} in the matrix corresponding to the i^{th} row and j^{th} column contains the number of times the i^{th} word appears in the j^{th} document.

Let the total number of documents be N ; let V be the vocabulary and $M = |V|$ be the total number of words in this vocabulary. Each document d_i can then be represented as a vector of length M :

$$d_i = [w_{1i} \ w_{2i} \ \dots \ w_{Mi}] \quad (1.2)$$

where w_{ji} is the number of times word j appears in the document i , and is 0 if word j does not appear in it. The entire corpus can then be represented as a matrix formed by arranging the segment vectors as its columns. The matrix would have the form

$$W = [w_{ji}], \quad 1 \leq j \leq M, \quad 1 \leq i \leq N \quad (1.3)$$

The information in the document is thus represented in terms of its constituent words; documents may be compared to each other by comparing the similarity between the document vectors. The absolute word counts are clearly related to the length of the segment and also to the overall distribution of that word in all of the corpus. To compensate for the differences in document lengths and overall counts of different words in the document collection, each word count is normalized by the length of the document in which it occurs, and the total count of the words in the corpus. This representation of words and documents is called vector space model (VSM). Documents represented this way can be seen as points in the multidimensional space spanned by the words.

Singular value decomposition: In order to capture the *latent similarity* between the documents, the matrix is subject to singular value decomposition (SVD) [37]. The matrix W is decomposed into three matrices by SVD and they are related as

$$W = USV^T \quad (1.4)$$

where U is $M \times M$, S is $M \times M$ and V is $M \times N$ (recall that M is the number of words in the original matrix and N is the number of the documents, that is, the dimension of the matrix W is $M \times N$). U and V are left and right singular matrices respectively. SVD maps the document vector into a new multidimensional space in which the corresponding vectors are the columns of the matrix SV^T . Matrix S is a diagonal matrix whose elements appear in decreasing order of magnitude along the main diagonal and indicate the energy contained in the corresponding dimensions of the M -dimensional space. Normally only the top R dimensions for which the elements in S are greater than a threshold are considered for further processing. This is achieved by setting

$$s_{jj} \forall j > R \quad (1.5)$$

Thus, the matrices U , S and V are reduced to $M \times R$, $R \times R$ and $R \times N$, respectively, leading to a data compression and noise removal. The space spanned by the R vectors is called eigenspace.

Classification: Given a corpus of documents and their topics, the goal is typically to identify the topic to which a new document belongs. A metric of “relatedness” between documents such as the cosine similarity is defined below. Classification methods (K-nearest neighbor, support vector machine, etc) are used to determine which of the training documents the new document is most similar to. The topic of the new document is assigned as that of the similar document.

Cosine similarity: This is the measure used in determining the similarity between two document vectors. For two vectors $X = [x_1 x_2 x_N]$ and $Y = [y_1 y_2 y_N]$, the cosine similarity is defined as

$$\cos(X, Y) = \frac{x_1 y_1 + x_2 y_2 + \dots + x_N y_N}{|X| \cdot |Y|} \quad \text{where, } |X| = \sqrt{x_1^2 + x_2^2 + \dots + x_N^2} \quad (1.6)$$

1.3.4 Wavelet transform

The first step in signal processing is usually the application a mathematical transform that can identify periodicities and variations in signals even in the presence of background noise. The ability to identify periodicity is applied to for example, pitch-detection in speech or to edge-detection in images.

Wavelets are functions $\psi(t)$ that can analyze a time-series signal at different scales or resolutions, and are used to locate patterns in the signal. If we look at a signal, say $p(t)$, through a large “window”, we identify gross features; if we look at the same signal with a small “window,” we differentiate detailed features. Wavelet analysis is designed to *see the forest and the trees*. A wavelet is a waveform that is localized in both time (or space) and frequency domains. A variety of different wavelet shapes have been used, of which three commonly used shapes are shown in Figure 1.3. These are (i) First derivative of

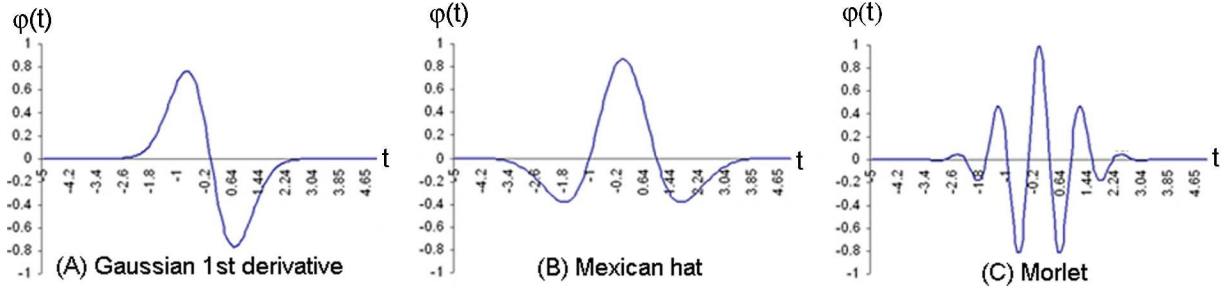


Figure 1.3: Wavelets

Three examples of analysis wavelets are shown: 1st derivative of Gaussian, Mexican Hat and Morlet wavelets, from left to right. 1st derivative of Gaussian (left) is anti-symmetric to the center, and is suitable to identify step-up or step-down nature of an input signal. Mexican hat (middle) is a symmetric wavelet with a single peak. Morlet wavelet (right) is also symmetric but is characterized by multiple peaks and is more suitable to capture ripples or multiple cycles of a periodic signal.

Gaussian, (ii) second derivative of Gaussian, called the Mexican Hat, and (iii) the Morlet wavelets. The underlying function $\psi(t)$ for the Mexican hat wavelet is shown in Equation 1.7 as an example [38].

$$\psi(t) = (1 - t^2)e^{-\frac{t^2}{2}} \quad (1.7)$$

The transformation of a time-series signal $p(t)$ using wavelets is performed as follows. The wavelet $\psi(t)$ is *convolved* with the time-series signal $p(t)$ to obtain its wavelet coefficients. This amounts to translating the wavelet to a position in the signal, and computing the product-sum of the wavelet and the signal, which would be the value of wavelet coefficient at that position. The process is repeated by translating the wavelet to all the positions of the input signal, and thus obtaining wavelet coefficients at all these positions. The original wavelet is called the *mother wavelet* or the analyzing wavelet. The mother wavelet is then scaled, a process referred to as *dilation*. The dilated wavelet is referred to as *child wavelet*. Wavelet coefficients are computed again with the child wavelet, where the child wavelet has been obtained by dilating the mother wavelet to scale a . The complete set of wavelet analysis functions in dependence of translation factor b and dilation factor a is given by Equation 1.8 [38]. A normalizing factor $1/\sqrt{a}$ is used to maintain the energy constant in the wavelet at all scales.

$$\psi_{(a,b)}(t) = \frac{1}{\sqrt{a}}\psi\left(\frac{t-b}{a}\right) \quad (1.8)$$

To illustrate, a set of mother and child wavelets for the Mexican Hat function are shown in Figure 1.4. The effect of dilation (by varying the dilation factor a) is shown in the top panel of the figure, and the effect of translation (by varying the translation factor b) is shown in the bottom panel of the figure. In each case, the mother wavelet is shown

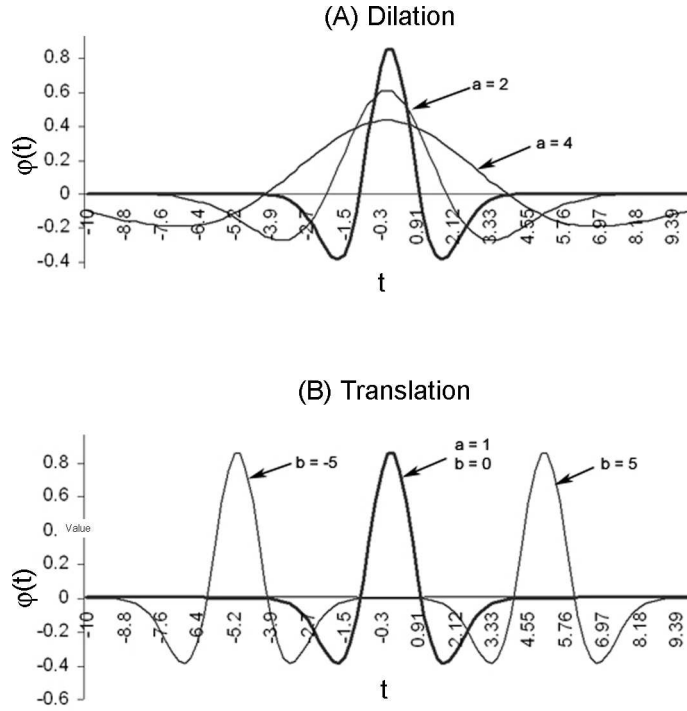


Figure 1.4: Mexican hat wavelet at different dilations and translations

The mother wavelet of Mexican hat is shown in bold in both (A) and (B). In (A), Dilation factors $a = 2$ and $a = 4$ are shown in grey shade, when translation is zero ($b = 0$). In (B) the translated wavelets of the mother wavelet are shown at $b = -5$ and $b = 5$.

in bold. Specifically, Figure 1.4 (top panel) shows the Mexican hat mother wavelet with $a = 1$, along with the dilated wavelets at scales $a = 2$ and $a = 4$. Figure 1.4 (bottom panel) shows the mother wavelet in bold at translation $b = 0$, and translated to positions $b = -5$ and $b = 5$. Finally, the wavelet transform of a given signal $p(t)$ with respect to the analyzing function $\psi(t)$ is computed as defined in Equation 1.9 [38].

$$T(a, b) = \frac{1}{\sqrt{a}} \int_{-\infty}^{\infty} p(t) \psi^* \left(\frac{t-b}{\sqrt{a}} \right) dt \quad (1.9)$$

where, a is the dilation or scale, b is the translation, and ψ^* represents complex conjugate of ψ . Note, that in the case of the Mexican hat, the wavelet function $\psi(t)$ is a real-valued function, whereby $\psi(t) = \psi^*(t)$.

1.4 Application to biological sequences

Application of n-gram analysis to biological sequences: In biological sequences, the best equivalent of words is not known. Thus, n-grams usually describe short sequences

of nucleotides or of amino acids of length n . The distributions of n -grams in genome sequences of individual organisms have been shown to follow Zipf's law [39, 40, 41, 41, 7, 8, 42, 18, 43, 11]. Other "vocabulary" that has been used includes the 61-codon types, or reduced amino acid alphabets [44, 45, 46, 47].

Prior to this thesis, N -grams were not applied to address any specific biologically relevant question about the organism. BLAST algorithm for sequence alignment ([48]) and Rosetta protein tertiary structure prediction algorithm [49] can both be viewed as applications of n -grams, albeit they are not "analogous" to how n -grams are used in language technologies.

Application of Yule's q -statistic or latent semantic analysis to biological sequences: Yule's q -statistic and LSA have not been applied to biological sequences prior to this work.

Application of wavelets to biological sequences: Wavelets have been used in place of a simple window (triangular or trapezoidal) to smooth the hydrophobicity signal to make predictions on the location of membrane spanning segments [50, 51]. Following this work, wavelet transforms have been applied for transmembrane helix prediction but the application has primarily been only to smooth the hydrophobicity signal by removing high frequency fluctuations [52, 53, 54, 55]. The other application of wavelets to protein sequences is to compare sequence similarity of proteins based on correlation between their wavelet coefficients [56].

Chapter 2

Introduction to Proteins

Proteins are complex molecules that carry out most of the important functions in the living organism—signal transduction, transport of material, defense of self from foreign bodies, are all functions carried out by thousands of different proteins in the body. Proteins also play structural roles such as forming tissues and muscular fiber. Interactions between proteins mediated by their structures form the fundamental building blocks of functional pathways in living organisms. In this chapter we present an introduction to proteins. For an in depth understanding of proteins, refer to the textbook [57].

2.1 Amino acids: primary sequence of proteins

Proteins are made up of *amino acids*. These amino acids are linked to each other in a linear fashion like beads in a chain, resulting in a protein (see Figure 2.1). There are 20 different amino acids, all of which share a common chemical composition (Figure 2.1A). There is a carbon atom called C_α at the center, which forms 4 covalent bonds—one each with (i) amino group (NH_3^+), (ii) carboxyl group (COO^-), (iii) hydrogen atom (H) and (iv) the *side chain* (R). The first three are common to all amino acids; the side chain R is a chemical group that is different for each of the 20 amino acids. Figure 2.1B shows the side chains of the 20 amino acids along with their names and the 3-letter and 1-letter codes commonly used to represent them. In most of the computational methods, the amino acids are commonly represented by the 1-letter code: A, C, D, E, F, G, H, I, K, L, M, N, P, Q, R, S, T, V, W, Y.

Two amino acids can join to each other through condensation of their respective carboxyl and amino groups, shown schematically in Figure 2.1C. The oxygen (O) from the carboxyl group on the left amino acid and two hydrogen atoms (H) from the amino group on the right amino acid get separated out as a water molecule (H_2O), leading to the formation of a covalent bond between the carbon (C) and nitrogen (N) atoms of the carboxyl and amino groups respectively. This covalent bond, which is fundamental to all proteins, is called the *peptide bond*. The peptide bond is shown in violet color in Figure 2.1C. The carboxyl group of the right amino acid is free to react with another amino

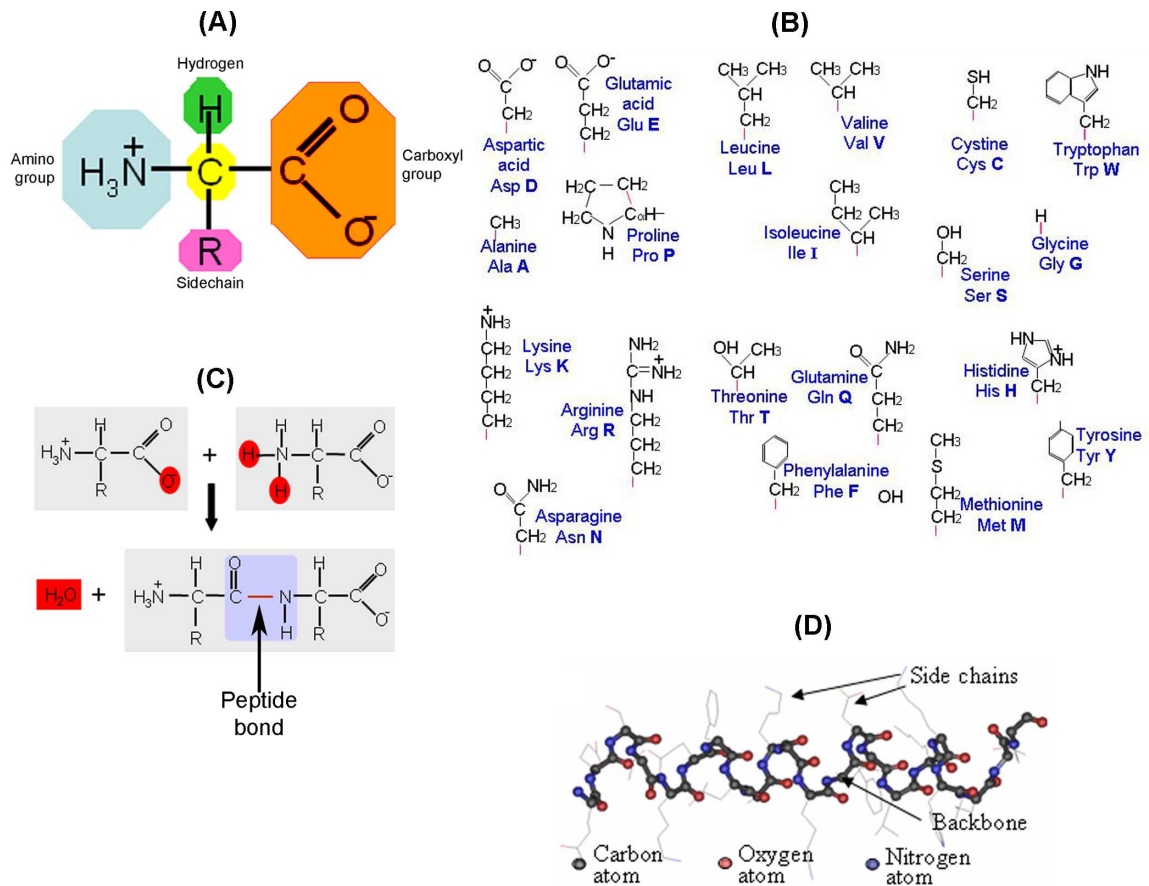


Figure 2.1: Amino acids

(A) Amino acid: there is a carbon atom at the center (C_{α} (yellow)) that forms 4 covalent bonds with: amino group (blue), carboxyl group (red), hydrogen atom (green) and the side chain R (pink). (B) There are 20 possible side chains giving rise to 20 amino acids. The names of the 20 amino acids and their 3-letter and 1-letter codes are also shown. (C) A covalent bond (called peptide bond) can form between the carboxyl group of one amino acid and amino group of the other, thereby releasing one water (H_2O) molecule. (D) Carboxyl group of the second amino acid is free to make a peptide bond with a third amino acid, thus forming a chain of amino acids called a *peptide* or a *protein*

acid in a similar fashion. The $C_\alpha H$ along with the N, C, O and H atoms that participate in the peptide bond, forms the *main chain* or *back bone* of the protein. The side chains are connected to the C_α atom. The progression of the peptide bonds between amino acids gives rise to a protein chain. A short chain of amino acids joined together through such bonds is called a *peptide*, an example of which is shown in Figure 2.1D. Synthesis of proteins in cells happens in principle in the same fashion outlined above, by joining amino acids one after the other from left to right; in the cells, each step in the formation of a protein is controlled by other enzymatic proteins. Conventionally, a protein chain is written from left to right, beginning with the NH_3^+ (amino) group on the left and ending with the COO^- (carboxyl) group on the right (same as in Figure 2.1C). Hence, the left end of a protein is called N-terminus and the right end is called C-terminus.

The term “residue” is commonly used to refer to any amino acid in the protein sequence.

Amino acid properties

The 20 amino acids have distinct physical and chemical properties because of the differences in their side chains. Many different criteria for grouping amino acids based on their properties have been proposed. Several hundred different scales relating the 20 amino acids to each other are also available (e.g. see [58], [59]). The major difficulty in classifying amino acids by a single property is the overlap in chemical properties due to the common chemical groups that the amino acid side chains are composed of (chemical groups that all 20 amino acid chains are composed of are shown in Figure 2.2).

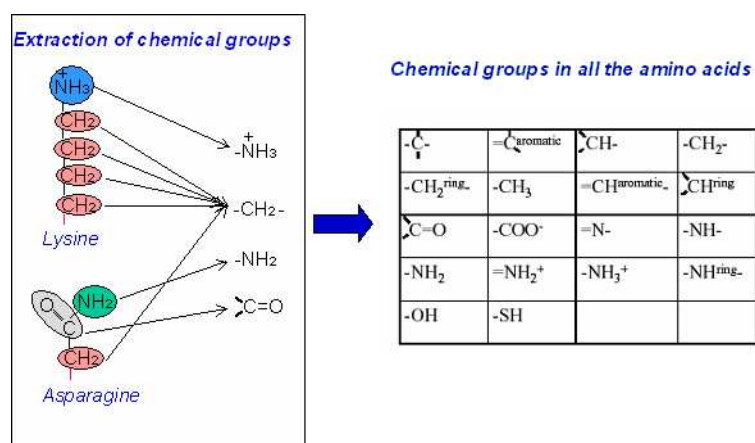


Figure 2.2: Chemical groups

Left panel shows examples of amino acid side chains, and the individual chemical groups that are constituents of the side chain. Right panel shows all the individual chemical groups that the 20 amino acids are made of.

Some commonly used properties and the set of amino acids that share the respective property are shown in Table 2.1.

Vocabulary	Words	Symbols	Amino acids	Numeric value
Charge	Positive	p	H, K, R	+1
	Negative	n	E, F	-1
	Neither	.	ACDGILMNPQSTWY	0
Polarity	Polar	p	CDEHKNQRSTY	1
	Nonpolar	n	AFGILMPVW	0 / -1
Aromaticity	Aromatic	R	ILV	+1
	Aliphatic	-	FHWY	-1
	Neither	.	ACDEGKMNPQRST	0
Size	Small	.	AGPS	
	Medium	o	DNT	
	Large	O	CEFHIKLMNQRVWY	
Electronic Property	Strong donor	D	ADEP	+2
	Weak donor	d	ILV	+1
	Neutral	-	CGHSW	0
	Weak acceptor	a	FQTY	-1
	Strong acceptor	A	KNR	-2

Table 2.1: Amino acid properties

Different types of vocabularies used are shown in column 1. For each type, all the words in the vocabulary and the amino acids mapping to these words are listed in columns 2 and 4. Column 3 lists the symbol used in place of the corresponding word.

Three amino acids, namely cysteine, proline and glycine, have very unique properties. Cysteine contains a sulphur (S) atom, and can form a disulphide covalent bond with the sulphur atom of another cysteine. The disulphide bond gives rise to tight binding between these two residues and plays an important role for the structure and stability of proteins. Similarly, proline has a special role because its backbone is a part of its side chain structure. This restricts the orientation of the peptide around a proline, and usually gives rise to a turn or kink in protein structures. Glycine has an opposite effect in a peptide, since it has a side chain that consists only of one hydrogen atom (H). Since H is very small, glycine imposes much less restriction on the polypeptide chain than any other amino acid.

2.2 Secondary structure

Inspection of the three dimensional structure of proteins reveals the presence of repeating elements of regular structure, termed *secondary structure* (compare Figures 2.3 A and B). These regular structures are stabilized by interactions between atoms within the protein,

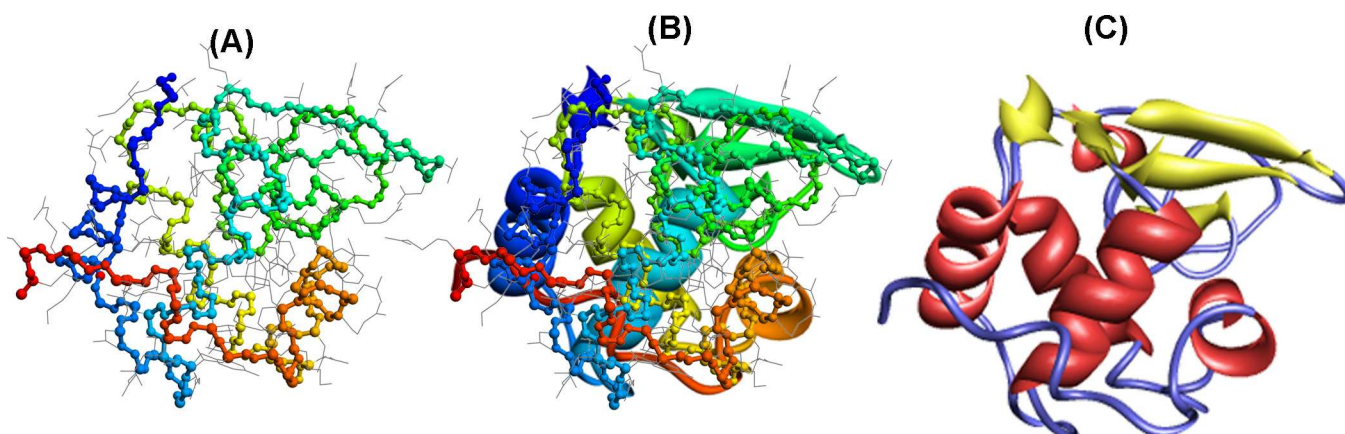


Figure 2.3: An example to demonstrate the primary, secondary and tertiary structure of proteins

(A) The structure of the protein Lysozyme (Protein Data Bank code 1HEW) is shown. The backbone is shown in ball and stick model in rainbow colors from one end to the other end; side chains are shown in grey. The sequence of amino acids that make up this protein is called its primary sequence or primary structure. (B) The backbone is superimposed with *ribbons* to highlight the folds in the protein. The overall three dimensional structure of the protein is called its tertiary structure. (C) On closer observation of the structures of proteins, three types of repetitive structures that are 'localized in 3D space' are observed, and they are: helix (red), sheet (yellow) and loop (blue). These are referred to as secondary structures because they form the intermediates between primary sequence and the final tertiary structure of the protein.

in particular the *Hydrogen Bond*. Hydrogen bonds are non-covalent bonds formed between two electronegative atoms that share one *H*. There is a convention in the nomenclature designating the common patterns of hydrogen bonds that give rise to specific secondary structure elements, the Dictionary of Secondary Structure in Proteins (DSSP) [60].

Helix, is the secondary structure formed due to hydrogen bond formation between the carbonyl group of i^{th} residue and the amino group of the $i+n^{th}$ residue, where the value of n defines whether it is a 3_{10} , α or π helix for $n = 3, 4, 5$ respectively. Therefore, the interactions between amino acids that lead to the formation of a helix are local to the residues within the helix. Sheets on the other hand, form due to long-range interactions between amino acids, that is, residues $i, i + 1, \dots, i + n$ form hydrogen bonds with the residues $i + k, i + k + 1, \dots, i + k + n$ (**parallel beta sheet**), or in the reverse order with $i + k, i + k - 1, \dots, i + k - n$ (**anti-parallel beta sheet**). A **turn** is defined as a short segment that causes the protein to bend. A **coil** is that segment of the protein that does not conform to any of the secondary structure types just described. Typically, the seven secondary structure types are reduced to three groups, *helix*, (includes types α -helix H and 3_{10} -helix G), *strand* (includes β -sheet) and *coil* (all other types). Figure 2.3C shows the secondary structure types helix, strand, turn and coil in different colors.

The linear sequence of amino acids that the protein is made up of, is referred to as

the primary sequence or **primary structure**. The description of which parts of the protein assume which secondary structure type, namely helix or sheet, is referred to as the **secondary structure** (see Figure 2.3). A complete information of the 3-dimensional positions of all atoms in the protein, or a description of how the secondary structure motifs fold to form specific domains, is referred to as **tertiary structure**. The arrangement of multiple proteins (multimers), stably associated with each other, is referred to as the **quaternary structure**. Though some proteins exist as monomers, it is very common for proteins to form multimers. Figure 2.4B is an examples of a multimers. The quaternary structure can formed from identical or nonidentical protein chains.

2.3 Tertiary structure and structure-function paradigm

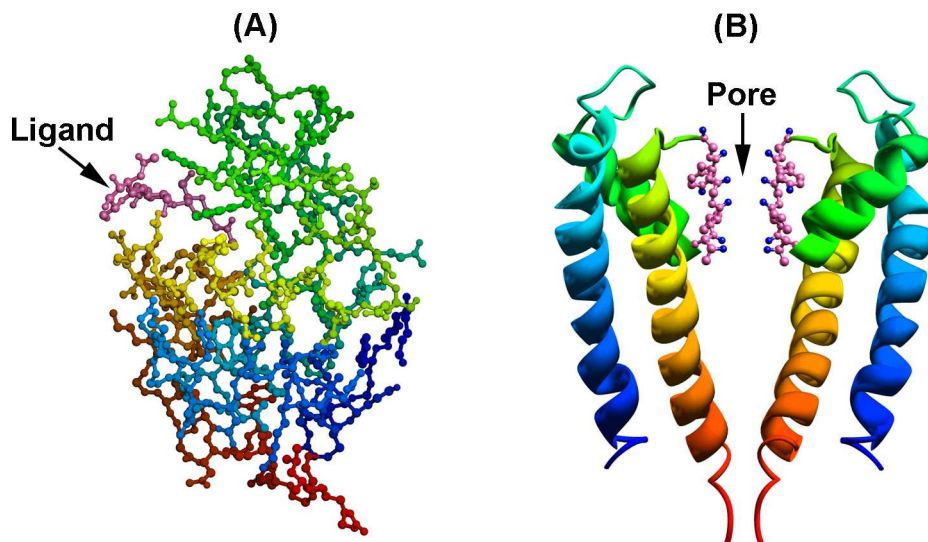


Figure 2.4: Protein function is exerted through its structure

A. Lysozyme (PDB code 1HEW). The protein is colored in rainbow color from one end to the other end. Its structure create a groove which can dock its ligand shown in magenta color. B. Potassium channel (PDB code 1BL8). The helical segments in this multimeric protein form a vertical bundle, holding loop regions that line a pore. The sidechains of the residues on the loop act as selectivity filter for potassium ions that are allowed to pass through the pore.

Proteins play functional and structural roles in living organisms. Functional roles include transduction of sensory or electrochemical signals (example G-protein coupled receptors), enzymatic action (example lysozyme), defense against foreign bodies (example antibody), transport (example hemoglobin), regulation (hormones, ion channels and transcription factors). Structural roles are played by proteins contributing to the structure or stability of a cell body (example integrins). A crucial task of a protein in the process of

exerting its function is recognizing a specific molecule out of the thousands of molecules it may come in contact with. Each protein has the ability to recognize a designated molecule, possibly another protein. This is achieved through interactions between atoms in one protein with atoms in other proteins or molecules. The molecule that a protein binds to is called a *ligand*. The three dimensional structure of the protein creates a suitable surface of potentials by which interactions with other molecules can take place; this structure is well defined for most proteins, although many proteins may possess multiple alternate structural conformations, and these may be responsible for different functional states.

Figure 2.4 shows two examples of how the three dimensional structure of a protein allows it to perform its function. Figure 2.4(A) shows the enzyme Lysozyme in rainbow color demonstrating how its three dimensional structure creates a prominent cleft between its two *domains*. The ligands that dock into this cleft are bacterial cell wall proteoglycans. Lysozyme hydrolyzes its ligands and leads to breakdown of the bacterial cell wall. Thus, the three dimensional structure of lysozyme enables it to function in self defense. Figure 2.4(B) shows an ion-channel. It has a multimeric arrangement of 4 identical protein chains (only two of which are shown in the figure for clarity). Each chain consists of two helices, and the residues on its loop create a selectivity filter allowing passage of only K^+ ions through the channel. The protein is not only selective of the specific ions it allows to pass through, but can also change between open and closed conformations of the pore [61].

2.4 Membrane and soluble proteins

Most of the proteins in an organism are present inside the cell, which is made mostly of water. Proteins that are completely in water are called *soluble proteins*. In contrast, some proteins are embedded in the membrane enveloping the cell, and these are called *membrane proteins*. The cell membrane is made up of hydrophobic fats and lipids, and provides a different environment compared to the polar aqueous (water) environment in the cell (Figure 1) than soluble proteins. Membrane proteins have a significant portion embedded in the cell membrane, and therefore experience a different environment (Figure 1B). The cell membrane is 30 Å thick, and consequently a TM helix that spans the membrane is at least 19 residues long. In cases where the TM helix is embedded obliquely in the membrane, it may be longer than 19 residues. On an average, TM helices are 22-25 residues long.

About 20-30% of genes in an organism encode membrane proteins [62, 63]. These proteins play important roles in signal reception and in physical and electrochemical interactions of cells with their environment [64, 65, 66, 67]. For example, ion channels mediate electrochemical transfer across the cell membrane by opening and closing of a pore [68]. G-protein coupled receptors (GPCRs) which form the single largest family of proteins with over 1000 genes encoding them in human genome [69] are also membrane proteins which react to a large and diverse set of ligands. Many environmental signals such as light and smell initiate signal transduction pathways through conformational changes

in GPCR structure [70]. 50% of all contemporary medicines are designed to act on this single family of membrane proteins, the GPCRs [71].

2.5 Membrane protein families and function

Many proteins are related to each other through evolution from bacterial organisms to humans. Many of the fundamental functions of cells, such as genome replication are carried out in part by proteins that are conserved in all organisms. Conservation can be detected by sequence similarity. When two proteins share the same evolutionary origin, they will likely conserve the identity or property of these amino acids crucial to protein structure and function in a given context. In some cases, however, there have been so many changes during evolution, that a common ancestry cannot be established unambiguously. In such cases it is also possible that the same structure and function has evolved independently. For example, the three dimensional structure of human rhodopsin, a protein in visual system that reacts to light, is similar to that of bacteriorhodopsin, a protein that acts as a proton pump in archaebacteria. Proteins that have similar three dimensional structure are said to come from the same *superfamily*. It is possible for proteins from the same superfamily to possess unidentifiable sequence similarity. If proteins from the same superfamily do possess sequence similarity they are said to come from the same *family*.

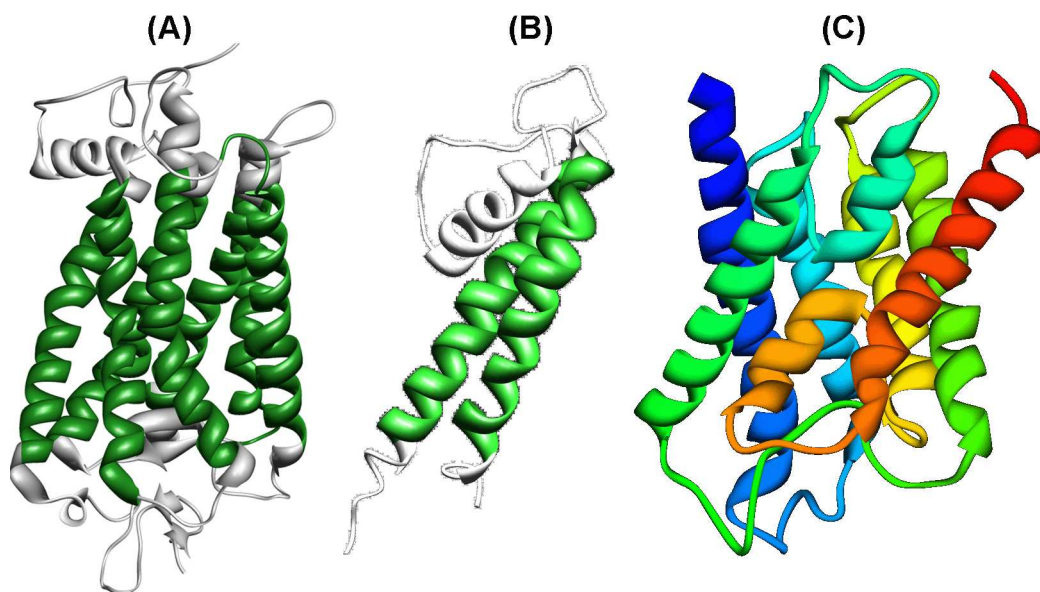


Figure 2.5: Topologies of membrane proteins

(A) Rhodopsin. Green color shows transmembrane regions. (B) KcsA potassium channel. (C) Aquaporin (shown in rainbow color to highlight two short helices, each of which has flanking loops that exit on to the same side of the membrane).

In the alpha-helical class of transmembrane proteins that is of interest in this thesis,

there are 40 known superfamilies and 52 families spanned by 123 unique protein structures known till 2006 (OPM database 1.1 release date March 2006) [72].

All helical membrane protein families contain transmembrane helices, but their numbers, lengths and orientations differ. Most membrane proteins studied to date conform to a common arrangement of each of the transmembrane segments (Figure 2.5A). First, the transmembrane segments are long enough to span the thickness of the membrane, typically longer than 19 residues. Secondly, the transmembrane helices have their two ends on two different sides of the membrane (in other words, the topology of the protein alternates as ... ec-TM-cp-TM-ec ...). This topology was believed to be typical of all transmembrane helical proteins until recently. Superfamily structures determined in recent years, like those of voltage-gated channel like proteins, chloride channel like proteins and major intrinsic proteins (aquaporin-like proteins) revealed that the transmembrane helices can be as short as 8 residues and that the flanking loops of a transmembrane segment can be located on the same side of the membrane (see Figure 2.5B and C). This paradigm shift makes a significant impact on the design of computational methods for transmembrane helix prediction. Most of the earlier methods are based on the previous model of expected transmembrane topology, and methods that take into account the new possible topologies are only beginning to emerge (see Chapter 3).

2.6 Proteomes

The collection of all the proteins *expressed* in an organism at a time is referred to as the proteome (this also captures the quantity of a given protein expressed at that time). Variations of the term are also used, for example to say membrane proteome, referring to only membrane proteins, or cellular proteome referring to proteins expressed in one cell type, and the *organism proteome*, which refers to the set of all unique proteins belonging to the organism, namely the protein equivalent of the genome of the organism. To give an estimate, the human genome for example includes about 25000 genes that encode for one million different proteins according to the Human Proteome Initiative [73]. In the work in this thesis, the terms *proteome* and *whole genome* refer to the organism proteome.

Chapter 3

Literature Review in Transmembrane Helix Prediction

A first step towards developing a transmembrane (TM) helix prediction algorithm is the understanding of the characteristics of TM helices that might help in distinguishing them from background information and specifically from non-TM helices.

The 30 Å thick hydrophobic lipid bilayer suggests that the TM helices are made up of contiguous hydrophobic residues, but exceptions exist: a long hydrophobic stretch may be a buried helix in a globular protein, or a TM segment may sometimes not be completely hydrophobic if it is shielded from the cell-membrane by interaction with other TM segments in the protein.

In this chapter we review the previous methods for transmembrane helix prediction. We describe segment-level and residue-level distinctions between transmembrane segments and soluble or nontransmembrane segments, followed by algorithms for prediction of transmembrane helices.

3.1 Segment-level distinctions between transmembrane and soluble helices

TM helices are characteristically different from helices in globular domains of soluble or membrane proteins in several aspects, summarized below.

TM helices are longer: On an average TM helices are longer compared to soluble helices — average length of TM helices is 23 residues and they are typically larger than 19 residues, while the average length of soluble helices is 9 residues [74].

Average hydrophobicity of TM helices is much higher: Average hydrophobicity of TM helices is much higher than that of soluble helices; in one study, close to half of the analyzed TM helices were more hydrophobic than any of the soluble helices analyzed

even when soluble helices of only comparable length of a minimum of 19 residues were included in the study [75]. However, about 25% of the ‘most-hydrophobic segment’s in membrane proteins had same range of hydrophobicity as that exhibited by soluble helices [75] indicating that some of the TM segments may not be distinguishable from soluble helices based on hydrophobicity alone.

Polar or charged residues are buried in TM helices: The few polar or charged residues in TM helices are usually buried in the interior of helical bundles. In contrast, polar and charged residues in soluble helical bundles usually face the outside, while hydrophobic amino acids form the buried core [76, 77]. This observation is referred to as inside-out rule. Another study showed however that the charged or polar residues Q, K and R can be lipid facing. It is assumed that the reason for this is that these residues have long side chains which can *snorkel* towards the membrane surface interact with the lipid polar head groups [74].

TM helix bundles pack more tightly with each other: TM helix bundles pack more tightly with each other than do the soluble helix bundles, based on a study of contact plots and occluded surfaces ([78, 79] and their previous work). This also means that the residues on the helix-helix interaction faces (buried faces) are small and polar contributing to the tight packing. A significant observation in this context is that glycine which is known to be a helix breaker in soluble helices is found with a higher propensity in TM helices than expected because they provide opportunities for tight packing according to the “knot- into holes” concept [80].

Proline has a high packing value in membrane proteins: Proline has a high packing value in membrane proteins but a low packing value in soluble proteins where it is known to act as a helix breaker. Kinks and bending motions are more often observed in helices which contain more than one proline PxxP or a combination of proline and glycine PxxG, spaced four residues apart [81]. Two other specific motifs are found abundantly in membrane helix bundles, giving rise to a tighter packing of the helices. One motif is the leucine zipper motif LxxLxxxLxxL which is also found in soluble helix bundles. The other motif is the glycine motif GxxxG which is common to only membrane helices [78, 82] and references therein).

3.2 Residue-level propensities of amino acids

A number of amino acid propensity scales have been calculated through statistical analysis of residues in known TM and non-TM regions. 222 published amino acid indices were compared through cluster analysis by [83], of which 88 were different hydrophobicity scales alone.

Hydrophobicity: Hydrophobicity of a residue was first defined in terms of its chemical structure. Many other scales have been computed later through statistical propensities of amino acids in transmembrane and nontransmembrane regions. The most commonly used hydrophobicity scales are those derived by Kyte and Doolittle [84], Engelman et al [85], Jones et al [86] White and Wimley [87, 88], and Deber et al [89].

White and Wimley used a thermodynamic framework to experimentally measure and model the energetics of interactions of peptide chains with the lipid bilayer. Unlike previous methods of computing hydrophobicity of amino acids which take into account only the hydrophobicity of side chains and do not include the peptide bond contributions, they compute the free energy change associated with the partitioning of peptide from water into membrane as a result of multiple processes-hydrophobic effect, electrostatic attraction between amino acid residues and anionic lipids, loss of degrees of freedom due to immobilization in the membrane and the perturbation of the lipid due to the insertion of the peptide [87, 88]. A propensity scale is derived from this analysis [90], which has shown to be better than previous methods for characterization of characterization of transmembrane segments.

A number of hydrophobicity scales have been devised:¹ A-cid and Av-cid [91], Ben-Tal et al (unpublished), Bull-Breese [92], Fauchere [93], Heijne [94], Hopp-Woods [95], KD [84], Lawson [96], Levitt, [97], Nakashima [98], Radzicka [99], Roseman [100], Sweet [101], Wolfenden [102] and WW [103].

Other Scales: A scale called the knowledge based scale for propensity of residue orientation in TM segments (kPROT) has been derived by analyzing a database of single and multi-spanning TM segments [104] for these three segments of membrane spanning helices (centre, extracellular-end and cytoplasmic-end). Jones et al observed that TM segments are often amphipathic when the protein has multiple membrane spanning segments and computed amino acid propensities separately for five classes of topogenic locations: membrane-outside, membrane-inside, membrane-middle, loop-outside and loop-inside, and also separately for single-spanning and multi-spanning proteins. The scales are computed based on a data set of 83 integral membrane proteins [86].

Charge: A lipid accessibility scale that accounts for many factors influencing the amino acid propensities in different locations in the membrane segment as opposed to water solubility alone, is derived by a careful study of membrane proteins with known structures [74]. Propensities indicated by this scale are shown to differ significantly from the usual hydrophobicity scales. This scale also takes into account multimeric nature of proteins. It also allows for charged and polar residues near the membrane edge [74].

Aromaticity: Aromatic residues exhibit distinct propensities to be facing the lipids or the phosphate head groups. When the periodicity of residues is computed in membrane

¹Names shown are how they are referred to in evaluations in later sections

segments, the period matches closely with the α -helix period of 3.6 residues. Amino acid scale derived with this analysis reflects a preference of aromatic residues to be buried in the protein core and aliphatic residues to be facing the lipids in the membrane [105]. Further analysis by separating the membrane spanning segments into middle, extracellular-end and cytoplasmic-end, and then computing the propensities in each of these segments to be membrane facing or be buried revealed a preference of aromatic residues to be facing the membrane at the edges of the segment and to be buried at the centre of the length of the membrane segment [104].

3.3 Algorithms for transmembrane helix prediction

Prediction of transmembrane segments or two-dimensional topology information of membrane proteins follows two main approaches: (i) quantifying propensities of amino acids to be membrane, cytoplasmic or extracellular or (ii) by statistical modeling of amino acid distributions, for example by using hidden Markov models or neural networks, without explicitly computing the amino acid propensity scales. Most of the early methods followed the first approach and used hydrophobicity scales. The very first method was by **Kyte and Doolittle**² [84] which used bacteriorhodopsin as a template to predict TM helices. The general approach is used by most algorithms to date. It makes progressive analysis of amino acid sequences by finding the moving average of the hydrophobicity signal followed by thresholding, filtering short segments and breaking very large segments. It is based on the expectation that most of the residues present in the non-polar bilayer environment must be non-polar. Most of the algorithms to date that use the principle of hydrophobic residues use the same approach to locate TM segments. The factors that distinguish various algorithms are (i) choice of the hydrophobicity scale or amino acid propensity scale and (ii) parameters of window (window length for analysis, minimum and maximum helix lengths, threshold on hydrophobicity and window shape). **Edelman** described an optimal choice of these parameters for accurate prediction of TM segments using standard hydropathy analysis [106].

Eisenberg et al defined hydrophobic moment of a helix which shows its amphiphilic nature [28] and later defined combinations of average hydrophobicity and hydrophobic moment over windows of residues that would be observed for TM helices and contrasted how these combinations would be different for helices in soluble proteins [29]. However, a comprehensive study of a large number of TM segments showed that there were many outliers to this boundary defined by Eisenberg et al and concluded that the hydrophobic moment and mean hydrophobicity combination cannot effectively capture all the TM helices [107].

Engelman et al showed that the choice of the window length significantly affects reliability of TM segment prediction. A small window of 7 residues as used by Kyte and

²Algorithm names are shown in bold

Doolittle, fragments the same helix into multiple peaks separated by low valleys in hydrophobicity [85]. A helix is required to be about 19 residues long to span a 30 Å bilayer region based on a helix turn length of 1.5 Å. Helices of shorter or longer lengths are also commonly seen due to non-parallel orientation of the helix with respect to the membrane-normal, and by the largely varying thickness of the bilayer. Based on this knowledge, a window length of 20 residues was proposed as an optimal length for TM helix prediction by Engelman et al and is now most frequently used. Analysis with smaller window lengths of about 5 residues is used in delineating the ends of the helices. Engelman et al also devised the **GES** hydrophobicity scale.

When the number of available crystal structures of membrane proteins increased, it became possible to analyze topogenic signals in proteins—the most important one being the positive-inside rule that states that there are positive residues located in the cytoplasmic region than in the extracellular region [108]. Jones, et al studied the amino acid propensities in relevance to such topogenic signals (loop inside, loop outside, membrane inside, membrane outside and membrane centre), and used this propensity scale for prediction, in the **MEMSAT** method [86]. They used expectation maximization in combination with a dynamic programming algorithm, very similar to that of Needleman and Wunsch [109]. For 64 out of 83 proteins, the topology was predicted correctly, 1 out of 83 membrane proteins and 5 out of 155 soluble proteins only were misclassified. Although this may be an overstated accuracy based on the fact that the threshold of classification was tuned to the dataset of membrane and soluble proteins considered, two key contributions were made by this study. One, the topology dependent scales of amino acid propensity were introduced. Two, the dataset of the 83 proteins became a gold-standard dataset for development of membrane protein structure prediction methods. Both contributions are cited extensively in literature that followed.

SOSUI is a system that achieves very high accuracy in classifying soluble and membrane proteins and also very high segment prediction accuracy [110]. The first level of classification is carried out by locating a very high hydrophobic helix. Further prediction of TM segments involves locating hydrophobic segments with amphiphilic end-segments, and distribution around a helical-wheel of polar residues at the centre of the potential helical segment. The segment accuracy quoted for SOSUI is high in their paper and in benchmark analysis [111, 110]. Another method that works on similar principles is **PRED-TMR** [112], which uses hydrophobicity analysis to locate putative TM segments and reduces false positives by detecting edge signals of TM segments. Propensities of amino acids for each position in 10-residue borders at the ends of TM segments are computed and are used to re-evaluate the predicted TM segments to reduce false positives. The filter apparently helps reduce the over prediction problem faced by simple hydrophobicity analysis methods at a small expense of accuracy.

Intrinsic helicity of amino acids in non polar environments (such as in the membrane) is another complementary feature added to hydropathy analysis to overcome the problem of false-positives. An experimental scale that captured intrinsic helicity was determined and combined with hydropathy scale for TM prediction, and was shown to have advantages

over simple hydrophobicity analysis alone [113].

Advanced statistical modeling of membrane protein topology was used for TM prediction by two methods, **HMMTOP** [114], and **TMHMM** [115]. These methods are the first methods with systematically designed statistical models to capture topogenic propensities of amino acids. Both methods use a very similar architecture of HMM modeling, characterized by separate models for extracellular loops and cytoplasmic loops, long globular regions, and membrane segments that are subject to a minimum length requirement. A consensus prediction method performed after the release of these two methods concludes them to be the best methods in TM segment prediction, being correct 75% of the time in predicting all membrane segments of a protein [116]. **TMHMM version 2.0**, was released with its models trained on a larger dataset of 160 proteins [117].

A recent method that re-explores the hydropathy signal of a protein in predicting the TM locations is **SVMtm**. It uses support vector machines for classification of feature space into TM and non TM [118]. With a stringent restriction of a minimum overlap of at least 9 residues (as opposed to only 1 or 5 residues in earlier methods, see Section 5.2.2), this method achieves about 92.5% segment accuracy.

A few algorithms exploit a signal processing framework of wavelet transform analysis to study hydropathy signals in much the same way as the early methods, except for the use of a wavelet signal in place of a simple averaging analysis over windows of residues [52, 55, 54].

A number of methods take TMHMM as a base and improve over its accuracy through modifications of the algorithm. **S-TMHMM** is the original TMHMM retrained with recent data sets. This has been performed primarily for comparison purposes with other algorithms [119]. Knowledge of functional domains of proteins and their preferential location in cytoplasmic or extracellular side is used to restrict the model in predicting these regions correctly: **AHMM** [120] and **HMM-TM** [121] retrain the models with the prior knowledge of domains.

Evolutionary profiles

Transmembrane segments in proteins contain significant information pertaining to the functional class of the membrane protein [122], which is the reason why the sequence conservation is very high in the TM domains of membrane proteins, an attribute used in TM helix prediction. In spite of a high conservation of sequence in the TM segments it is difficult to identify related proteins owing to a low overall similarity. This may be the reason why the study of evolutionary information for membrane proteins has not been very extensive, and has found only a limited application in TM structure prediction.

The first method to use evolutionary profile analyzed was **PHDhtm** [123]. It analyses profiles at each position over 13 residue-wide windows. It then uses neural networks for a two state residue level prediction. On a dataset of 69 proteins it predicts 94% of the TM segments correctly. **PRO-TMHMM** and **PRODIV-TMHMM** also incorporate evolutionary information to train the HMMs [119]. Unlike these new TMHMM based

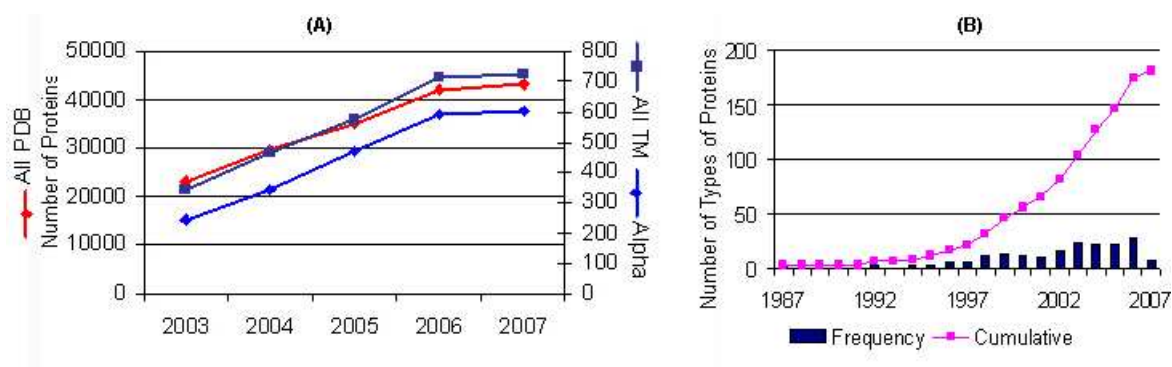


Figure 3.1: Number of experimentally solved membrane protein structures

Number of proteins whose three dimensional structure has been solved by experimental (X-ray crystallography or Nuclear magnetic resonance) methods are shown. (A) shows all the entries in the protein data bank. The y-axis for the TM-type proteins is shown on the right side of the plot. It may be seen that the structures of membrane proteins form only about 1.5% of all the structures in PDB. (B) shows only representative structures from different types of membrane proteins, as listed by Dr. Stephen White (see text for URL). Both data are up-to-date as of February 2007.

methods PHDhtm does not restrict the “allowed” topology of the protein stringently, and is likely to perform comparable to these new methods.

Comparison of prediction algorithms

Table 3.1 shows a comparison of the performance of most methods published before 2002 reproduced from [111]. In addition to the prediction algorithms described in this section, hydrophobicity scales have also been evaluated with respect to their suitability in use for TM prediction. In this analysis, new hydrophobicity scales replaced the original WW scale in the Wimley and White algorithm [103]. Evaluation metrics shown in table are described in Section 5.2.2.

3.4 State-of-the-art and open questions

Too few structures determined experimentally. There is a large gap between the number of available sequences and the number of known structures. However, there has also been significant progress in the experimental determination of membrane protein structure. Figure 3.1A shows the number of all the PDB entries for soluble proteins, membrane proteins and alpha-helical membrane proteins as observed during the last 4 years (2003 to early 2007), obtained from the PDB-TM website [1]. The y-axis for soluble proteins is shown on the left, and that for membrane proteins on the right. Although membrane proteins are found abundantly in an organism (25-30% of the total unique proteins), the trend in the last few years shows that their fraction in the solved structures

is only about 1.5%. Of these, alpha helical transmembrane proteins comprise about 85% of the 1.5%.

Novel topologies likely to exist. It is likely that more and more novel types of transmembrane structure will be discovered, and that the non-redundant sequence data available for training and especially for evaluation is not adequate to assume that the current prediction accuracies reflect the capabilities of algorithms to predict all possible types of membrane proteins.

Figure 3.1B shows the number of *types* of membrane protein structures experimentally solved by year. This figure has been generated from the list of different types of proteins at http://blanco.biomol.uci.edu/Membrane_Proteins_xtal.html maintained by Prof. Stephen White's group. The list only includes representative structures of different types of membrane proteins, but contains duplicate entries for the same protein coming from different organisms, resulting in 181 structures compared to a total of 600 structures listed in PDB-TM currently. This figure gives an idea of the rate of discovery of different types of proteins. Upon analyzing the total alpha helical transmembrane proteins (in February 2007), only 57 of them were found to be non-redundant (< 30% homology).

Reduction in error rate desirable. A comparison of established methods of membrane structure prediction is reproduced here in Table 3.1 from [111]. It shows benchmark results of all methods until the time this thesis was undertaken (2003), on a data set with 36 high resolution structures. Many hydrophobicity scales (listed in Section 3.2) were tested with White and Wimley algorithm [88], replacing their hydrophobicity scale with the scale being studied. The following observations can be made from these results, about the drawbacks of these methods:

- The fraction of proteins for which all the transmembrane segments are predicted correctly (Q_{ok}), is at most 84%. This percentage is also an overestimate, since in some cases the training data of some methods (HMMTOP2) already contains the high resolution proteins (see original paper for details), or in other cases the computational models are very large and use evolutionary information of proteins, which is not always available. Hydrophobicity analysis methods that do not use training data, on the other hand, have a much lower Q_{ok} accuracy.
- Among the methods that do not use evolutionary information, Q_{ok} is around 75% and segment accuracy is found to be at a maximum of 90% corresponding to an error rate of more than 10% in segment F-score, indicating a possibility in improving the methods for prediction.
- The theoretical models on which these methods are based and also the evaluation datasets available at the time largely did not include novel membrane protein topologies that have been discovered recently. It is likely that the above percentage accuracies over estimate the actual capabilities of existing methods.

Method	Per-segment accuracy				Per-residue accuracy				
	Qok	Qhtm % obs	Qhtm % prd	TOPO	Q2	Q2T % obs	Q2T % prd	Q2N % obs	Q2N % prd
ERROR	10	8	10	9	3	7	8	6	6
DAS	79	99	96		72	48	94	96	62
HMMTOP2	83	99	99	61	80	69	89	88	71
PHDhtm08	64	77	76	54	78	76	82	84	79
PHDhtm07	69	83	81	50	78	76	82	84	79
PHDpsihtm08	84	99	98	66	80	76	83	86	80
PRED-TMR	61	84	90		76	58	85	94	66
SOSUI	71	88	86		75	66	74	80	69
TMHMM1	71	90	90	45	80	68	81	89	72
TopPred2	75	90	90	54	77	64	83	90	69
KD	65	94	89		67	79	66	52	67
GES	64	97	90		71	74	72	66	69
Ben-Tal	60	79	89		72	53	80	95	63
Eisenberg	58	95	89		69	77	68	57	68
Hopp-Woods	56	93	86		62	80	61	43	67
WW	54	95	91		71	71	72	67	67
Av-Cid	52	93	83		60	83	58	39	72
Roseman	52	94	83		58	83	58	34	66
Levitt	48	91	84		59	80	58	38	67
A-Cid	47	95	83		58	80	56	37	66
Heijne	45	93	82		61	85	58	34	64
Bull-Breese	45	92	82		55	85	55	27	66
Sweet	43	90	83		63	83	60	43	69
Radzicka	40	93	79		56	85	55	26	63
Nakashima	39	88	83		60	84	58	36	63
Fauchere	36	92	80		56	84	56	31	65
Lawson	33	86	79		55	84	54	27	63
EM	31	92	77		57	85	55	28	64
Wolfenden	28	43	62		62	28	56	97	56

Table 3.1: Transmembrane predictions by other methods on high resolution set.

(Table is reproduced here from [135] by permission of Oxford University Press under Creative Commons License). % obs is the Recall and % pred is the Precision. A definition of these metrics may be found in the Chapter 5). It is to be noted that HMMTOP2 is trained on all of the data used for testing, and its performance would be an over estimate of its true performance.

Previous ‘good’ methods cannot adapt to novel protein types. The top ranking algorithms have very complicated statistical models requiring a large number of training parameters and typically employ hidden Markov models with a very rigid expected topology of membrane proteins. These naturally fail to recognize new topologies for proteins from unseen families or with unexpected architecture.

Most of the early analyses of membrane proteins used the photosynthesis reaction center structure solved in 1985 as a model. This same model was used as a basis for designing general computational models of membrane protein structures. Since then K^+ channel structure has been solved experimentally in 1998, showing membrane structures that do not conform to the rules derived from the analysis of the photosynthetic reaction center. Recent structures solved in 2003-2007 support the idea that we are only beginning to scratch the surface of the membrane protein structural universe.

Chapter 4

Models and Methods: Biological Language Modeling

This chapter describes the details of our methods of adapting language processing algorithms to protein sequences. Introductions to the algorithms with respect to text processing are presented in previous chapters: n-grams (Section 1.3.1), Yule values (Section 1.3.2) and latent semantic analysis (Section 1.3.3).

4.1 Biological language modeling toolkit

Computing n-gram counts of text data or protein sequence data requires efficient methods for processing when the data is very large. We developed the Biological Language Modeling Toolkit (BLMT) that consists of efficient data preprocessing and statistical analysis tools for n-gram analysis of protein sequence data. The construction of this toolkit and other post-processing methods of the output data are described here.

4.1.1 Data structures used for efficient processing

For efficient n-gram computation and searching, the data is preprocessed into *suffix arrays*, which are data structures for string processing developed for computer science. Let the string be denoted by $A = a_0a_1a_2 \dots a_{N-1}$. A suffix S_i of A is the substring from i^{th} position to the end of string A . Let S denote all the suffixes of A beginning at each of its letters $a_0, a_1, a_2, \dots, a_{N-1}$, namely, $S = \{S_0, S_1, \dots, S_{N-1}\}$, where $S_0 = a_0a_1a_2 \dots a_{N-1}$, $S_1 = a_1a_2 \dots a_{N-1}$ and $S_{N-1} = a_{N-1}$.

Suffix array: Suffix array (SA) of A is the arrangement of the suffixes S_0, S_1, \dots, S_{N-1} in lexicographical order. For example, if the string A is `abaabcb`, then $S = \{abaabcb, baabcb, aabcb, abcb, bcb, cb, b\}$, and the suffix array would be as shown Table 4.1. This lexicographic ordering is advantageous when identifying patterns of letter repeats at multiple positions in an input string. In such a case, the suffixes beginning at these

Position	Suffix array of abaabcb							LCP array
0	a	a	b	c	b			0
1	a	b	a	a	b	c	b	1
2	a	b	c	b				2
3	b							0
4	b	a	a	b	c	b		1
5	b	c	b					1
6	c	B						0

Table 4.1: Suffix array and longest common prefix array of the string abaabcb

Position	0	1	2	3	4	5	6
String	a	b	a	a	b	c	b
Pos Array (P)	2	0	3	6	1	4	5
LCP Array	0	1	2	0	1	1	0
Rank Array	1	4	0	2	5	6	3

Table 4.2: Data Structure consisting of Suffix array, longest common prefix array and the rank array

positions will all appear consecutively in the suffix array since they all begin with that same pattern.

Longest common prefix array: The longest common prefix (LCP) array is defined for a suffix array as an integer array of N elements $l_0l_1l_2 \dots l_{N-1}$, where l_n is the length of the longest common prefix between suffix S_n and S_{n-1} . In Table 4.1 for example, the suffix **abcb** and its preceding suffix **abaabcb** have the longest common prefix **ab**. Hence LCP at position 2 is 2 (the length of **ab**). LCP of the first suffix in the suffix array would be set to be 0.

Rank array: The rank array is another integer array of N elements $r_0r_1r_2 \dots r_{N-1}$, and the element r_n contains the rank (position) of suffix S_n in the lexicographically sorted suffix array. In Table 4.1 suffix S_3 is at position 2, hence $r_3 = 2$.

Construction of suffix array

Owing to the large length of any genome string, which ranges about 1-3 megabytes for each archaeal and bacterial organism and over 18 megabytes for human genome (see Table

5.1), sorting of all its suffixes is a computationally expensive task. Manber and Myers presented an efficient sorting method in their paper introducing suffix arrays [124] and the suffix array in the BLM toolkit is constructed by that algorithm.

Only the position of the first character of a suffix in the genome string is used to refer to the suffix, instead of copying the entire suffix into a new location. In other words, the set S of suffixes described in 4.1.1 would now be stored in the computer as $S = \{0, 1, \dots, N - 1\}$, and the sorted suffixes would be stored as $[2, 0, 3, 6, 1, 4, 5]$, as shown in Table 4.2. Thus the suffix array described in Table 4.1 would now be stored as a combination of a character array of the genome-string followed by an integer array P of the positions of the sorted suffixes. LCPs are stored in an integer array as described before.

In this implementation, the LCP array has been constructed separately after the construction of suffix arrays, using the linear time algorithm presented [125]. The rank array is also constructed as a by-product during the construction of LCP array.

Processing protein sequences

One suffix array is constructed for the genome sequence of one organism or for one data set of proteins. The input format of the genome sequence or any protein data has to be in multiple-sequence FASTA format.

The above description is illustrated for the case of a sample genome-like-string, in Table 4.3 and Figure 4.1. The genome sequence consisting of all its constituent proteins

```
>gi|5103389|dbj|BAA78910.1| 241aa long hypothetical protein
MVDILSSLLL
>gi|5103390|dbj|BAA78911.1| 112aa long hypothetical protein
MDPADKLMK
>gi|5103391|dbj|BAA78912.1| 100aa long hypothetical protein
MQA
```

Table 4.3: Example of a genome sequence to demonstrate Suffix array construction

is considered as a string of amino acids. This string will henceforth be referred to as the ‘*superstring*’ or ‘*genome string*’. A single blank space is introduced between every two proteins, to ensure that the join of the trailing edge of one protein and the leading edge of the next protein does not lead to incorrect frequency counts. The blank space is represented by a ‘#’ in this description.

The alphabet size of this string will hence be 22, corresponding to the 20 amino acids and the blank space and the character X for “unknown” amino acid. Care is taken to not

count X and ‘#’ among the n -grams. The headers of each protein are read into another data structure in the same order as in the genome string.

0	1	2	3	4	5	6	7	8	9	10	11	12	13	14	15	16	17	18	19	20	21	22	23	24
M	V	D	I	L	S	S	L	L	L	#	M	D	P	A	D	K	L	M	K	#	M	Q	A	#
19	24	5	8	15	23	22	13	12	11	1	16	7	20	4	6	10	14	17	9	2	18	21	3	0
24	10	20	23	14	2	15	12	3	19	16	9	8	7	17	4	11	18	21	0	13	22	6	5	1
0	1	1	0	1	0	1	1	0	0	1	0	1	1	1	1	0	1	1	1	0	0	0	1	0

- Genome String**
- Suffix (Pos) Array** Lexicographical ordering of suffixes: Position 0 is # (24 in original string), Position 1 is #MD... (10 in original string), Position 2 is #MQ... (20 in original string), Position 3 is A# (23 in original string) etc.
- Rank Array** The suffix A#... takes position 3 in the suffix array, hence its rank is 3.
- LCP Array** The number of common leading symbols.

Figure 4.1: Demonstration of suffix array and rank array

The data structure consisting of the genome-string, position array (which together are referred to as suffix array), LCP array and the rank array for each organism are stored as binary files on disk for all further processing. The file formats are as follows:

SA: unsigned int numElements= N ; unsigned char genome[N]; unsigned int Pos[N]

LCP: unsigned int LCP[N]

RA: unsigned int Rank[N]

4.1.2 Tools created

Once the basic data structures (suffix array, LCP array and rank array) are constructed, computing N -grams is fairly straightforward.

Protein number and length

The genome sequence is read into an array in the form of a genome string with a space between two proteins during suffix array construction. To compute lengths of all the proteins and their total number, the distance between consecutive spaces in the genome string is determined in linear time.

N-gram count

If $LCP(i) < n$, it corresponds to the first n letters between S_i and S_{i-1} are different, and hence give rise to two different n -grams. On the other hand, if $LCP(i) \geq n$, it means

that the two suffixes have at least the first n letters in common. The n -gram remains the same, but its count can be incremented by 1 from position $i - 1$ to i .

The n -grams (for a given n) occurring in the genome, and their counts can be computed in linear time by parsing the LCP array. Set the list of n -grams to be empty. Parse LCP array from beginning to end. At every position the LCP is less than n , the starting n letters of the suffix at that position are appended to the list of n -gram, and its count is set to 1. The parsing of LCP array is resumed from the next position and the count of the latest n -gram is incremented by one until LCP values falls to $< n$ again. The procedure is repeated until reaching the end of the LCP array. Thus, given the LCP array and suffix array, the n -gram counts can be computed in linear time.

When n -grams occurring in the genome and their respective counts are computed this way, the ordering of the n -grams is in lexicographic order. To compute top most frequencies n -grams, they are reordered by the counts using standard binary search sort.

Longest repeating sequences

The LCP array is parsed from beginning to end. If LCP at any position is $>$ a given length L , it means that there is a sequence longer than L residues that repeats in the genome.

If S_j and S_k have LCP say 100, then S_{j+1} and S_{k+1} have LCP 99. Care is to be taken to not count these two as two different repeating strings. This is achieved by parsing the rank array from beginning to end instead of parsing LCP array. For position j , the LCP at position Rank[j] is found to be 100, then it is noted, and the position is skipped to $j + 99$ to resume counting other repeating strings.

Localization of n -grams

The boundaries of beginning and end positions of individual proteins is computed as mentioned earlier. The positions of occurrences of one or more n -grams are directly read out of suffix array and are sorted into ascending order. The sorted order of n -gram positions are compared with protein end positions to find whether localization of these specific n -grams occurs in any of the proteins.

N-gram neighbours and Yule value computation

This is done as a post processing step after n -gram computation. n -gram computation reduces the size of parsing from the size of a genome to the size of 20^n . For example, say we are interested in computing the preference exhibited by amino acid pairs separated by any 2 residues between them, of the form $X**Y$. To compute these preferences for all pairs of amino acids X and Y , the list of n -grams with their counts is parsed. For a specific n -gram $XxxY$ whose count is say c , the value of count of (X,Y) is incremented by c . Thus, when the n -grams AAAA, AABA, ABBA are encountered, the count of (A,A) is incremented

by the counts of these three n-grams. By the time the list of n-grams is parsed completely, we are left with the positive preferences of amino acid pairs. The counts are normalized by $|X| \cdot |Y|$ where $|X|$ is the unigram count of amino acid X in the genome.

Computing Yule’s q-statistic. The Yule value $Y_d(x, y)$, for a pair of words x and y within the same sentence (or in a window of length d) is given as

$$Y_d(x, y) = \frac{N_{00}N_{11} - N_{01}N_{10}}{N_{00}N_{11} + N_{01}N_{10}} \quad (4.1)$$

where, for all the occurrences of amino acid pairs a_1 and a_2 appearing with a distance of d between them,

N_{11} is the number of times $a_1 = x$ and $a_2 = y$

N_{00} is the number of times $a_1 \neq x$ and $a_2 \neq y$

N_{10} is the number of times $a_1 = x$ but $a_2 \neq y$

N_{01} is the number of times $a_1 \neq x$ but $a_2 = y$

To compute Yule values, not only the count (A, A) is required, but so is the count of (A, \hat{A}) . Counts of $XxxY$ are obtained as described earlier. To obtain the counts of $Xxx\hat{Y}$, e.g. for (A, \hat{A}) the counts of (A, C) , (A, D) , (A, E) ... are computed. Yule value for $XxxY$ is computed as given in equation 4.1. Yule values are stored in plain text files with 400 rows (corresponding to 20x20 amino acid combinations). The desired distance between the two residues is given as an input parameter. For example, distances 0, 1 and 2 compute Yule values between residues of the pattern XY , $X*Y$, $X**Y$ respectively.

4.2 Adapting latent semantic analysis for secondary structure classification

Latent semantic analysis in the context of text documents has been described in Section 1.3.3. This chapter describes details of methods for adapting latent semantic analysis to protein sequences. Proteins with known secondary structures (helix, sheet and coil) were considered (see data description in Section 5.1.2), and segmentation was done at the boundary of between these three types of structure. In other words, each protein segment possesses one of the three secondary structure types. The tasks of constructing property-segment matrix, LSA and the kNN classification were performed for each vocabulary separately. An example protein is shown in Figure 4.2. It yields 9 segments, where it is segmented at the boundaries between helix (red), sheet (blue) and coil (green).

Recall that latent semantic analysis is performed over a collection of documents that are represented as vectors of word counts from a vocabulary and that these vectors are placed adjacent to each other to form a word-document matrix (Section 1.3.3).

Residues: PKPPVKFNRRIFLLNTQNVINGYVKWAINDVSLALPPTPYLGAMKYNLLH
Structures: _____SS_SEEEEEEEEEEEEEETEEEEETTEE_____SS_HHHHHHTT__TT

Figure 4.2: Secondary structure annotation of a sample protein sequence

4.2.1 Words and documents in proteins

The equivalent of a document for protein sequence analysis is a protein segment. Three separate vocabularies were considered separately here — (i) amino acids, (ii) chemical groups and (iii) amino acid types based on their electronic properties (refer to Section 2.1 for details). For example, when the property `electronic property` is considered as the vocabulary, the possible words are `strong donor`, `weak donor`, `neutral`, `weak acceptor` and `strong acceptor`. Unique words appearing in the property vocabulary and the amino acids that possess each of these property values are shown in Table 2.1.

4.2.2 Property-segment matrix

The amino acid property-segment matrix is computed analogous to the word-document matrix of text documents. The number of residues possessing each of the above property-values (words) are counted and filled in the cell C_{ij} corresponding to the row of that word and column of that segment. After all the segments arising from one protein are accounted for, segments from the next protein are computed and concatenated to the right of the columns of the first protein in the matrix. One large property-segment matrix is thus constructed from the segments of all the proteins in the datasets. The property-segment matrix is shown in Table 4.4 for the same protein segment shown in Figure 4.2 and the vocabulary of “amino acids” .

4.2.3 Feature construction and classification

Once the word-document matrix, or here, property-segment matrix is computed, the remaining procedures of matrix normalization and singular value decomposition are carried out as per established procedure for latent semantic analysis described in Section 1.3.3 (see Equation 1.4), yielding *features* corresponding to protein segments.

In direct analogy to classification of a new text document (Equation 1.6) , the goal here is to assign segments from a new protein to one of these three classes (helix, sheet and coil), given some reference protein segments whose topology is known. The classification is done as follows: The segment vectors for which secondary structure is already known are treated as reference vectors R_j , $1 \leq j \leq N$. The protein segments from test set of proteins are classified as follows:

1. Compute the document vector d as given in equation 1.2, using the same word counts that were used to normalize the property-segment matrix W .

Vocabulary	Protein Segment Number								
	1	2	3	4	5	6	7	8	9
A	0	0	0	1	0	0	1	1	0
C	0	0	0	0	0	0	0	0	0
D	0	0	0	0	1	0	0	0	0
E	0	0	0	0	0	0	0	0	0
F	1	1	0	0	0	0	0	0	0
G	0	0	1	0	0	0	0	1	0
H	0	0	0	0	0	0	0	0	1
I	0	2	0	1	0	0	0	0	0
K	2	0	0	1	0	0	0	1	0
L	0	2	0	0	0	1	1	1	1
M	0	0	0	0	0	0	0	1	0
N	1	2	1	0	1	0	0	0	2
P	3	0	0	0	0	0	3	0	0
Q	0	1	0	0	0	0	0	0	0
R	0	2	0	0	0	0	0	0	0
S	0	0	0	0	0	1	0	0	0
T	0	1	0	0	0	0	1	0	0
V	1	1	0	1	0	1	0	0	0
W	0	0	0	1	0	0	0	0	0
Y	0	0	0	1	0	0	0	1	1

Table 4.4: An example word-document matrix

2. Transform the document vector d into the reduced dimensional space as given in equation 4.2

$$T = \tilde{d}U \quad (4.2)$$

3. For a pre-chosen number K , perform K -nearest neighbor classification: compute the similarity between the test segment T and each of the reference segments R_j . Pick K most similar segments out of all the N segments. Find the label that majority of these K segments out of the K segments belong to, and assign this label to the test segment T . For example, let K be 5. If the 5 most similar segments have the labels “helix, helix helix, sheet and helix”, then the test segments is assigned the label “helix”. Similarity measure between segments used here is the *cosine similarity*, described below. The value of K used in this analysis is 5.

Classification accuracy was measured by comparing the predicted labels with the known labels for the protein segments.

4.3 Transmembrane helix feature extraction and prediction methods

In this chapter we describe how we directed the exploratory work with language and signal processing analogies towards the specific problem of transmembrane helix prediction. The chapter covers methods for feature extraction using Yule values (Section 1.3.2), latent semantic analysis (Section 1.3.3) and wavelet transform (Section 1.3.4). Implementation details of classification / statistical modeling methods used in this thesis for transmembrane helix prediction are provided.

4.3.1 Wavelet transform of a protein sequence

To apply signal processing techniques to protein sequences, the protein sequence must first be converted into a meaningful numeric signal before any signal analysis may be performed. The goal is to capture the distribution of amino acid properties in different topological locations of the TM proteins. The analysis in this work is focused on one specific amino acid property, the polarity of the amino acids. Let $R = r_1, r_2, \dots, r_N$ be the residues in the protein sequence, where $r_i \in A, C, \dots, Y$, the set of 20 amino acids. The protein sequence is mapped to a binary scale of polarity to obtain a numeric representation $p(n)$ corresponding to Equation 4.3. The definition of polar and non-polar residues follows that of [126].

$$p(n) = \begin{cases} 1 & \text{if } r_i \text{ is polar, i.e. } r_i \in \{C, D, E, H, K, N, Q, R, S, T, Y\} \\ -1 & \text{if } r_i \text{ is non-polar, i.e. } r_i \in \{A, F, G, I, L, M, P, V, W\} \end{cases} \quad (4.3)$$

$p(n)$ is a time-series representation of the protein sequence. Other possible representations for a protein signal are discrete values of charge, electronic property, size and aromaticity (see Table 2.1) and also numerous other continuous valued properties such as hydrophobicity (Section 3.2).

Figure 4.3A shows how a protein may be represented as numerical signal in terms of polarity. A protein is represented in physical dimension from one end to the other end of the amino acid chain.

Wavelet transform is applied over the binary signal of polarity. The wavelet analysis function used here is the Mexican hat function given in equation 1.7 and is computed using MATLAB wavelet toolbox. Wavelet coefficients are computed for the scales from 1 to 32. The shift parameter used is 1 residue, which yields a set of coefficients for every position in the protein sequence signal. Since $p(n)$ is a discrete signal, a piecewise constant interpolation of $p(n)$ along the length of the protein signal is used for continuous wavelet transform (MATLAB Wavelet Toolbox Release 3.0.2).

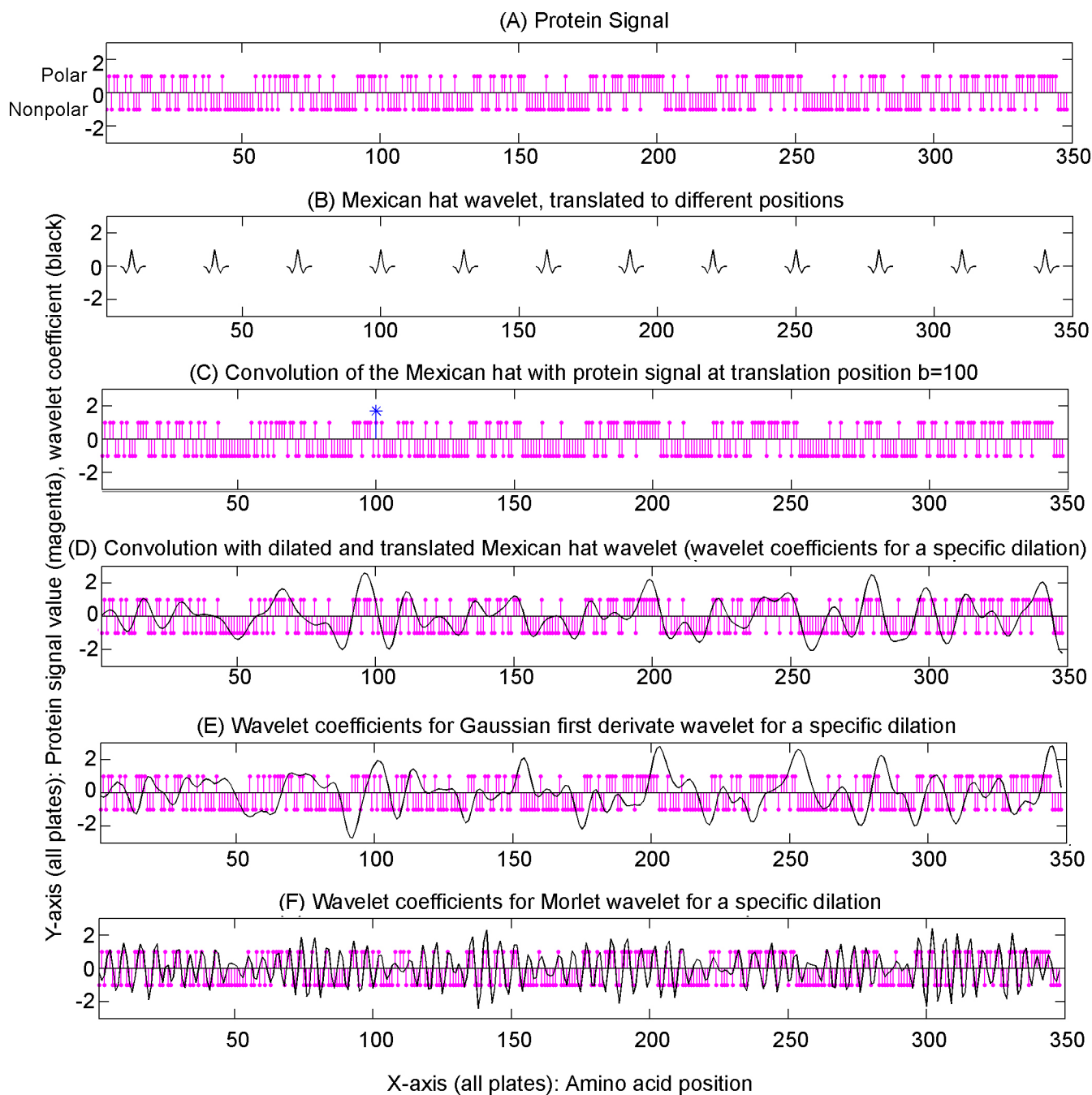


Figure 4.3: Wavelet analysis of *rhodopsin* protein signal

(A) Signal representation of the protein rhodopsin (SWISSPROT 0PSD_BOVIN) in terms of polarity of its residues (polar =1, nonpolar = -1). (B) Mexican hat wavelet, translated to different positions. For clarity, translations are shown separated by 30 positions. In actual computation such as in (D), the wavelet is translated to every position in the signal. (C) Product of the protein signal with the wavelet signal when the latter is translated to position = 100. (D) Wavelet coefficients computed with the Mexican hat wavelet at a specific dilation. (E) Same analysis as in D, but for the Gaussian 1st derivative wavelet. (F) Same analysis as in D, but for the Morlet wavelet.

Wavelet coefficients of the membrane protein rhodopsin

The transformation of the time-series representation outlined above in general for protein sequences $p(n)$ using wavelets is described below for a specific protein sequence, that of rhodopsin. Rhodopsin is a prototypical member of the G protein coupled receptor family. This example illustrates the properties of the functions that were chosen.

Choosing the mother wavelet: Which of the commonly used wavelet functions (some examples of which are shown in Figure 1.3) is suitable for the analysis of TM features in membrane proteins such as rhodopsin? The choice depends on the features of the signal that are desired to be captured. Analyzing protein signals for TM segment prediction requires locating long stretches of non-polar (hydrophobic) signals together with polar spurts symmetrically at both left and right edges of the hydrophobic segments. Therefore, the Mexican hat is expected to be a suitable analysis function for the TM segment prediction task. The symmetrical nature of the Mexican hat wavelet function (Figure 1.3B) in conjunction with the pronunciation of opposite properties (positive values) at the edges with respect to the non-polar values of the TM regions (negative values) in the center make this function an ideal choice for this analysis. Further, at a smaller dilation factor, the Mexican hat can also capture the polar head at the edges of the TM segment. The other two commonly used shapes are less suitable than the Mexican hat function: the Gaussian wavelet is anti-symmetric with respect to the center (Figure 1.3A), and the Morlet wavelet has multiple peaks (Figure 1.3C) and are therefore not expected to capture the predominantly symmetrical nature of TM segments. These characteristics are illustrated for the example protein rhodopsin, whose wavelet features have been computed using all three functions (Mexican hat, Gaussian and Morlet), as described step by step in the following paragraph and illustrated in Figures 4.3 and 4.4.

Figure 4.3 shows the steps involved in computation of wavelet features. Figure 4.3A shows the time series representation $p(n)$ of the amino acid sequence of rhodopsin (using the bovine rhodopsin sequence, SWISSPROT ID OPSD_BOVIN). A value of 1 indicates the presence of a polar and a value of -1 indicates the presence of a non-polar residue, according to Equation 4.3. The first step in analysis of this time signal $p(n)$ is convolution with the wavelet function, here shown using the Mexican hat function (Equation 1.7). Convolution is carried out for every amino acid position b along the protein sequence. To illustrate this process, Figure 4.3B displays the Mexican hat function applied to different values of b , i.e. as example at amino acid positions $b = 40, 70, 100, 130 \dots$). At each position, the protein signal is transformed according to Equation 1.9 where the wavelet function $\psi(t)$ is the Mexican hat function (Equation 1.7). This is shown as an example in Figure 4.3C for one combination of $T(a, b)$ at a single position ($b = 100$). When this transformation is carried out for a single value of a across all positions b , the wavelet transformation of $p(n)$ looks like the one shown in Figure 4.3D when using the Mexican hat function, like Figure 4.3E when using the Gaussian 1st derivative wavelet and Figure 4.3F when using the Morlet wavelet. This process is repeated for different values of dilation factor $a = 1, 2, \dots, 30$

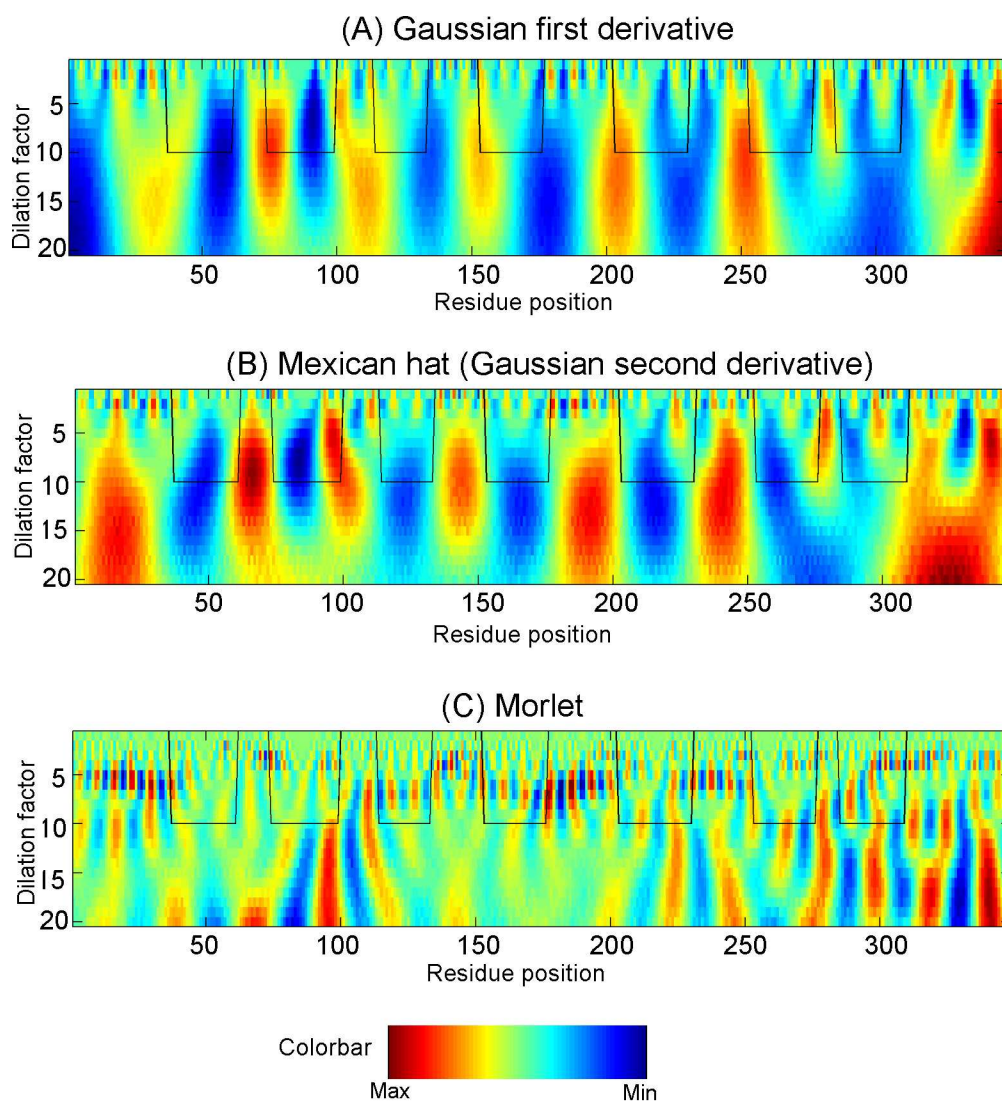


Figure 4.4: Wavelet coefficients for three different wavelet functions for *rhodopsin* Superimposed on the wavelet coefficient images are locations of TM helices (solid line value=0 corresponds to non TM region and value = 10 corresponds to TM region). The dimension along the horizontal axis in the images corresponds to the position of the residue in the protein. The vertical dimension corresponds to the different dilation factors at which wavelet coefficients are computed. By visual inspection, the Mexican hat is found to correspond better with TM locations than do the other two wavelet analysis functions.

(the “scales”). The result is shown in Figure 4.4 for each of the three mother wavelets. Here, the x-axis represents the residue number in the protein and the y-axis represents the scale at which wavelet transform is computed. The color gradient for at position (x, y) represents the wavelet coefficient for translation = x and scale = y . Thus, for the convolution with the Mexican hat wavelet, Figure 4.3D is one slice of the representation shown in Figure 4.4B; for the convolution with the Gaussian 1st derivative, Figure 4.3E is one slice of the representation shown in Figure 4.4A, and for the convolution with the Morlet wavelet function, Figure 4.3F is one slice of the representation shown in Figure 4.4C. The CWT function of MATLAB Wavelet toolbox has been used to transform $p(n)$ to its wavelet transform.

As one can see qualitatively from Figure 4.4, there are very clear color pattern obtained when using the Mexican hat function, and these correlate visually with the positions of known TM segments (indicated by thin black blocks in Figure 4.4).

The shape of the Mexican hat function is well suited because it confines the non-polar, hydrophobic amino acids by clear boundaries marked by the polar regions in contact with the phospholipids head groups. Note, that the Gaussian function, while also resulting in regular color patterns, is not able to confine the segments to those given by the known TM segments. Instead, the color patterns actually cross the center of the hydrophobic TM segment, therefore not bearing any relationship to the actual boundaries. Worse even is the Morlet function (Figure 4.4C), which does not show any discernable correlation with the known TM segments. In contrast, the Mexican hat nicely reproduces the physical reality of TM proteins: the polar heads at the ends of the TM helices result in positive peaks at smaller scales in the Mexican hat wavelet coefficients (Figure 4.4B), whereas the non-polar central stretches in the TM segments result in minimum values in wavelet coefficients at scales around 10. This observation is corroborated by the color markings observed in the rhodopsin three-dimensional structure shown in Figure 9. Here, the wavelet coefficients at dilation factor $a = 9$ are mapped using a rainbow color code. The dark blue color clearly identifies the central regions of the most hydrophobic portions of the protein, embedded in the membrane.

4.3.2 Rule-based method for transmembrane prediction

In this analysis, the primary sequence of proteins is represented in terms of the properties of amino acids. The properties considered in the rule-based method are charge, aromaticity, polarity, size and electronic properties. In Table 2.1 we already showed the 1-letter symbols used to represent each of the property values. Repeated below are the vocabularies used in this work for convenience.

- Charge: 3 possible values: positive (H, K, R), negative (D, E), neutral (A, C, F, G, I, L, M, N, P, Q, S, T, V, W, Y)
- Polarity: 2 possible values: polar (C, D, E, H, K, N, Q, R, S, T, Y), nonpolar (A, F, G, I, L, M, P, V, W)

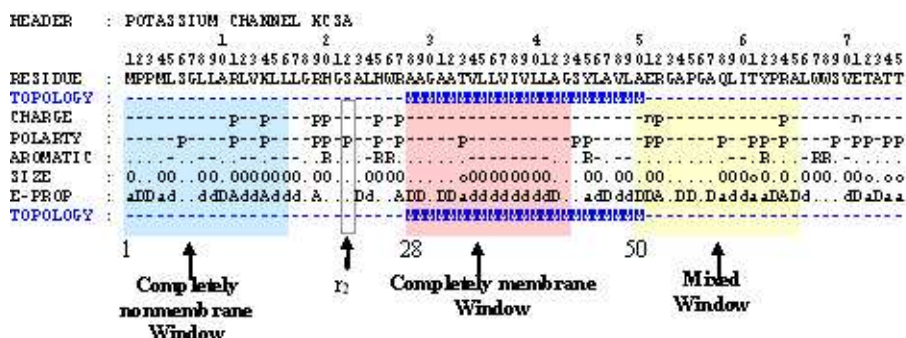


Figure 4.5: Data preprocessing and feature extraction

A sample sequence is shown with its property annotations. Line (1) header of the protein (potassium channel Kcsa). Line (2) primary amino acid sequence. Line (3) Topology: nonmembrane ‘-’ and membrane ‘M’. Line (4) Charge: positive ‘p’, negative ‘n’ and neutral ‘-’. Line (5) Polarity: polar ‘p’ and nonpolar ‘-’. Line (6) Aromaticity: aromatic ‘R’, aliphatic ‘-’ and neutral ‘.’. Line (7) Size: small ‘.’, medium ‘o’ and large ‘O’. Line (8) Electronic property: strong acceptor ‘A’, weak acceptor ‘a’, neutral ‘.’, weak donor ‘d’ and strong donor ‘D’. Line (9): topology again. A window of width 16 residues is moved across the sequence from left to right, one residue at a time. At each position the different property-feature combinations (such as “charge-negative”, size “medium”) in the window are counted. The collection of these counts in a vector forms the feature at that position. In the example shown above, the window width is shown as 16 residues. In the analyses, the width used for HMM modeling is 6 residues and that for NN modeling is 16 residues. If the length of the protein is L residues, and window length is l residues, the number of feature vectors obtained is: $L-l+1$. The three shaded windows at positions 1, 28 and 50 have labels “completely non-TM”, “completely TM” and “mixed” correspondingly.

- Aromaticity: 3 possible values: aliphatic (I, L, V), aromatic (F, H, W, Y), neutral (A, C, D, E, G, K, M, N, P, Q, R, S, T)
- Size: 3 possible values: small (A, G, P, S), medium (D, N, T), large (C, E, F, H, I, K, L, M, Q, R, V, W, Y)
- Electronic property: 5 possible values: strong donor (A, D, E, P), weak donor (I, L, V), neutral (C, G, H, S, W), weak acceptor (F, M, Q, T, Y), strong acceptor (K, N, R)

Visual Analysis: The primary sequence of each protein is decomposed into five different sequences by replacing each amino acid with its property (see Figure 4.5) using the above property-based vocabularies using one property at a time, so that five new sequences are generated.

For each protein, the following information is printed one per line in order to visually infer the property distribution in membrane and non-membrane regions: (i) header information (ii) primary sequence (iii) topology of the protein: M (membrane), i (inside) and o

(outside) (iv) charge (v) aromaticity (vi) polarity (vii) size (viii) electronic property (ix) topology annotation again. A snapshot of properties for an example protein is shown in Figure 4.5.

Quantitative analysis: Sequence properties are analyzed in windows of length 16 residues at a time. The window is placed at the left end of the sequence and then moved one residue at a time to the right. For each window of the sequence, and for each property under consideration, the number of occurrences of each of the values of the property is computed. Let $C(P, v)$ be such count for a property P and value v pair. For example, $C(\text{Charge}, \text{positive})$ for the first window of sequence shown in Figure 4.5 is 2, $C(\text{Charge}, \text{negative})$ is 0, and $C(\text{Charge}, \text{neutral})$ is 14. The windows are classified into membrane and nonmembrane types, based on topology as follows:

- Completely-membrane if $C(\text{topology}, M) = 16$
- Completely-nonmembrane if $C(\text{topology}, i) = 16$ or $C(\text{topology}, o) = 16$
- Mixed otherwise

In order to analyze the distribution of these properties in the windows, histograms of number of windows with respect to $C(P, v)$ are constructed for each P and v pair, separately for completely-membrane and completely-nonmembrane windows.

Prediction: Based on visual and quantitative analysis of the $C(P, v)$ values, expert rules are created to describe transmembrane helices. Four rules have been compiled:

```
RB1: {POSITIVE < 1 && ALIPHATIC > 6}
RB2: {POSITIVE < 1 && ALIPHATIC > 6}
      OR {POSITIVE < 1 && ALI < 1 && ALIPHATIC > 4}
RB3: {POSITIVE < 1 && ALIPHATIC > 6}
      OR {POSITIVE < 1 && ALI < 1 && ALIPHATIC > 4}
      OR {POSITIVE < 2 && ALIPHATIC > 6 && LARGE > 8}
RB4: {POSITIVE < 1 && ALIPHATIC > 6}
      OR {POSITIVE < 2 && ALIPHATIC > 6 && LARGE > 8}
```

The rules are applied in the following way to predict transmembrane helices in protein sequences with unknown topology:

1. Assign all residues to be of nonmembrane type
2. Start with a window of the sequence from N-terminus.
3. Compute $C(P, v)$ values for all (P, v) pairs.

4. If a window satisfies a rule R, then assign all the residues in the window to be of membrane type. The rule R is predefined, and is a combination of thresholds on $C(P, v)$ for specific (P, v) pairs.
5. Slide the window to the right by 1 residue. If the window covers the last residue, stop. Otherwise repeat (iii) and (iv)

4.3.3 Transmembrane helix prediction with latent semantic analysis features

Step1: Protein sequence representation. This is done as described in Section 4.3.2 visual analysis.

The protein sequence representation at this stage has 5 rows of length L, where L is the length of the protein (Fig. 4.5). In other words, the residue r_i at position i , is represented by its properties

$$r_i = [C_i \ P_i \ A_i \ S_i \ E_i] \quad (4.4)$$

where C_i , P_i , A_i , S_i and E_i are the charge, polarity, aromaticity, size and electronic-property of the residue r_i .

Step 2: Neighborhood analysis through a window. The protein sequence is analyzed with a moving window of length l ; the window is moved along the sequence one residue at a time, each position of the window yielding a feature vector. The feature vector at position i , represented by R_i is derived from the window beginning at the i^{th} residue and extending l residues to its right. It is given as

$$R_i = [C_{ij}]_{1 \times 10} \quad (4.5)$$

where, C_{ij} is the count of property-value j in window i. The specific property-values counted by C_{ij} 's are as follows:

C_{i1} count of "charge-positive"

C_{i2} count of "polarity-polar"

C_{i3} count of "polarity-nonpolar"

C_{i4} count of "aromaticity-aromatic"

C_{i5} count of "aromaticity-aliphatic"

C_{i6} count of "electronic property-strong acceptor"

C_{i7} count of "electronic property-strong donor"

C_{i8} count of "electronic property-acceptor"

		Window position											
		1	2	...	13	14	15	...	28	29	...	50	51
Property-value number	1	2	2		5	5	4		0	0		2	2
	2	3	3		6	6	5		1	2		6	6
	3	13	13		10	10	11		15	14		10	10
	4	0	0		3	3	3		0	0		1	1
	5	7	8		5	4	4		8	8		2	3
	6	2	2		3	3	2		0	0		2	2
	7	3	3		2	3	3		5	4		7	6
	8	2	1		0	0	0		1	1		3	3
	9	7	8		5	4	4		8	8		2	3
	10	0	0		0	0	0		1	1		1	1
Class label		-1	-1		0	0	0		1	1		0	-1

Figure 4.6: Feature vectors

Feature vectors of the sequence corresponding to each of the window positions are shown. The 10 rows of property number correspond to the C_{ij} list of Equation 2. The window position refers to the residue number of the first residue in the window. Feature vectors corresponding to the blue, red and yellow windows in (A) are shown in their corresponding color in the table. The class label of the feature vector is shown in the last row: completely nonmembrane -1, membrane 1.

C_{i9} count of “electronic property-donor”

C_{i10} count of “size-medium”

The choice of the above 10 properties is arrived at by studying histograms of the number of segments versus percentage of residues of a given property in segments of length l , and identifying the properties that showed distinct peaks in the histogram for TM and non-TM segments (data not shown). While r_i is the vector of properties of the amino acid at position i , R_i is the number of times a residue with a specific property value occurs in a window of length l starting at position i and extending to its right.

Step 3: Data annotation. Window size (l) used for feature construction is 16. Training data described in Section 5.1.4 is used to model neural networks/hidden Markov models. For each window in the sequence, a class label is assigned as **completely-membrane**, **completely-nonmembrane** or **mixed** in a similar way as described in Section 4.3.2.

Step 4: Protein segment matrix. When feature vectors R_i are computed for every position of the window, moving to the right one residue at a time, the entire protein will have a matrix representation P (Equation 4.6), whose columns are the feature vectors

$$P = [R_1^T \ R_2^T \ \dots \ R_{L-l+1}^T]_{10 \times L-l+1} \quad (4.6)$$

This matrix is referred to as protein-segment matrix. R_i^T is the transpose of vector R_i . The number of rows in matrix P is 10, same as the length of the residue feature

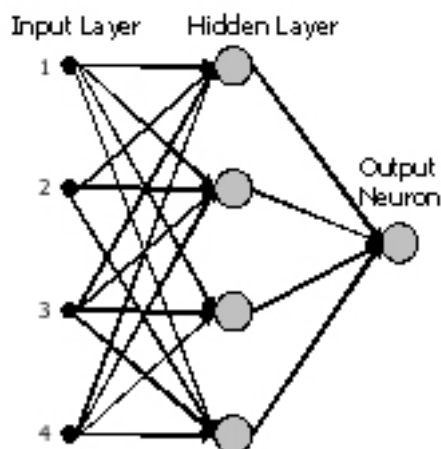


Figure 4.7: TMpro neural network architecture

The neural network has an input layer with 4 nodes that take each of the 4 dimensions of the feature vectors as input. The output layer has 1 tansig neuron that fires a value between -1 and +1 corresponding to nontransmembrane and transmembrane respectively. There is a hidden layer between input and output layers consisting of 4 neurons. The network is connected fully in the forward direction.

vector (Equation 4.5). Number of columns is $L - l + 1$, where L is the length of the protein sequence and l is the window length. The columns contain the feature vectors corresponding to their positions in the protein sequence. The matrix P is referred to as the protein feature matrix. In Figure 4.6, the columns excluding the class labels correspond to R_i 's. The entire matrix excluding the class labels corresponds to P . A protein feature matrix is created for each of the proteins in the dataset, both for training and testing purposes.

Step 4: LSA features. The protein segment matrix is subjected to singular value decomposition to obtain LSA features (Equation 1.4). *SVDS* tool has been used to compute this step. Estimated value of features of a test vector are computed as described previously in the context of LSA for secondary structure classification (Section 4.2.3). The number of dimensions retained for further analysis was chosen to be 4 (see Equation 1.5).

Step 5: Classification/Prediction. Feature classification or prediction is carried out using neural networks and hidden Markov models as described below.

Neural networks for feature classification

Model architecture: The number of input nodes of the NN is 4 and the number of output neurons is 1 (Figure 4.7). One hidden layer of 4 nodes is placed in between input and output layers (the choice of 4 units in the hidden layer is based on maximum accuracy in 10-fold cross validation of the training data). The model is fully connected in

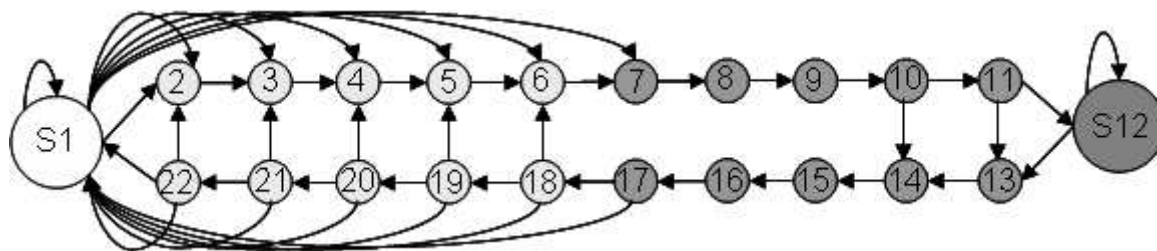


Figure 4.8: TMpro hidden Markov model architecture

The architecture models cytoplasmic and extracellular regions in a single state (S1) by 26 cluster Gaussian mixture model. The interior membrane region, that is the TM segment excluding 5 residue positions each at both ends, is modeled by a single state S12 with 12 feature clusters as a Gaussian mixture model. The transition from non-TM to TM segment is modeled with 5 sequential states on the non-TM side and 5 sequential states on the TM side. States S18-S22 are connected to states S6-S2 respectively as shown, to accommodate short loops between two TM segments. States S11 is connected to S13 to allow accommodation of short TM helices. All the transition states, S2-S11 and S13-S22 are modeled with a single Gaussian feature cluster.

the forward direction. Each of the hidden and output neurons is a tansig classifier [127]. Each input dimension is normalized such that the range of all the dimensions is the same.

Model training: The network is trained using back-propagation procedure [127], by presenting it with feature vectors and their corresponding target output class labels. MATLAB neural network toolbox has been used in this work. Mixed label feature vectors are not presented for training, since they arise from both TM and non-TM residues and hence are expected to lie in the “confusable” region in the features space. The output neuron learns to fire -1 for non-TM features and +1 for TM features. For feature vectors that are ambiguous, the output lies in the range of -1 to +1. A threshold of 0.4 is chosen based on maximum accuracy in 10-fold cross validation of the training set to be used for automatic classification of the feature into its class.

Feature vector classification with NN: Each input feature vector causes the output neuron to fire an analog value ranging from -1 to +1. The 0.4 threshold is used to label the residue at the first position in the window to be TM or non-TM. Since the feature is derived over a window of length 16, and threshold of 0.4 is more “confident” towards the TM label (in the possible range of -1 to +1), the 8 residues starting from the first position of the window are all set to be of TM type. The process is repeated for the next feature vector, and so on, and a TM label is assigned to 8 residues at a time every time the output neuron fires a value greater than the threshold.

Hidden Markov modeling

The architecture used for hidden Markov modeling (HMM) is shown in Figure 4.8. It models the cytoplasmic loops, extracellular loops and membrane regions separately. The membrane spanning region is modeled by 5 states on either ends. The internal core is modeled by one recursive state. A path through the HMM forces the membrane regions to cross all of the edge states once and only once. The internal core state accounts for variable lengths of the transmembrane segments, since this state can be transitioned to any number of times. The path when going from ec to cp is kept separate from the path the other way. That is, although the statistical features of the corresponding states are likely to be similar, the restriction makes sure that the path of traverses the membrane completely without making a wrong transition (on account of statistical similarity of mirror-states). On existing from the membrane region the path of a protein traverses through 5 loop states. The loop states are distinct for ec and cp sides as shown in Figure. States that are similar to each other biologically, such as states B and K are tied to each other. This means that the observation probabilities are same for these two states and only their transition and prior probabilities are different. The HMM is modeled with the LSA representations of the 15-window segments described in earlier Section 4.2.3. Thus 15-residue window at each position generates an observation of the HMM. The model parameters are computed as described below.

Data labeling: Labeling of training data relies upon the accuracy of the topology annotation given for the dataset. Since the states around the boundary of the loops and membranes are restricted to be traversed only once, and the self-transitioning states for membrane, ec and cp states are well defined, the path taken by a protein sequence through the HMM is well defined when the topology is known, that is, for a given topology, the sequence can be labeled with the states it transitions through in the HMM. An example of a training sequence and its labels are shown in Figure. As a first step, HMM state labels are computed for all the training sequences.

Model parameters:

Prior probabilities: Prior probability π_q for a particular state Q is defined as the probability that a sequence starts in this state. This can be computed by counting the number of training sequences that start with the label of this state and then dividing by total number of training sequences.

$$\pi_q = \frac{\text{No. of sequences starting with label } q}{\text{total number of training sequences}} \quad (4.7)$$

Q is computed for all the states in the HMM.

Transition probabilities: The HMM transitions from one state to another (possibly itself) after every observation. Transition probability is defined from one state Q_i , to another Q_j , and is the number of times the model transitions from state Q_i to state Q_j . The transition probabilities can be computed from the labeled sequences of the training data by counting the number of times label Q_i is followed by label Q_j and dividing it by the total count of label Q_i in the data.

$$T_{ij} = \frac{\text{No. of times label } i \text{ is followed by label } j}{\text{total count of label } i} \quad (4.8)$$

Observation probabilities: If the features modeled by HMM are discrete symbols, such as amino acids, the observation probabilities for each state Q , and symbol V combination are defined as the probability of seeing V when the model is in state Q . However in the analysis presented here, the HMM models the lsa feature vectors, which take continuous values as opposed to discrete symbols. For example, the LSA features for a sample protein are shown as an image in Figure. The feature vectors are scaled such that all the values in these vectors take values between 0 and 1, and are then plotted as intensity values in a two dimensional image. The feature vectors corresponding to each state are clustered using Gaussian mixture modeling (GMM). For the two self transitioning loop states, the features are modeled with 5 mixtures. For self-transitioning membrane state, the features are modeled with 4 mixtures. For all the other states, the features are modeled with 2 mixture Gaussians. GMM is a standard method for clustering, the description of which may be seen for example in (reference). The observations for a state then are described with the GMM corresponding to the features of that state. The GMM defines the prior probabilities for observing a feature from each of the mixtures, and then the Gaussian probability of the feature to belong to that cluster.

4.3.4 Decision trees

Protein sequences are analyzed in windows of 16 residues each. A protein segment matrix is constructed similarly as described in Steps 1 to 4 in previous section. Only the protein segments with labels “completely membrane” or “completely non-membrane” are used to construct the decision tree. Each protein segment serves as a data point, and each of the property counts as a feature.

The decision tree has been implemented using MATLAB wrapper software called `MATLAB arsenal` developed by Rong Yan over `weka-classifier` available at: <http://finalfantasyxi.inf.cs.cmu.edu/MATLABArsenal/MATLABArsenal.htm>.

Default parameters (trees.J48, -n=0, NoWrapper) have been used. Data set used to construct the decision tree is the training data described in Section 5.1.4. For classification of evaluation sequences, all the windows in the protein sequence are classified with the decision tree (again using the `MATLAB arsenal`).

Chapter 5

Datasets and Evaluations Metrics

5.1 Datasets

5.1.1 Dataset for n-gram analysis

Whole genome sequences: Whole genome sequences available in 2001 December were downloaded from the NCBI website [128]. Table 5.1 lists 44 organisms (bacterial, archaeal and human) that have been studied, the number of proteins in the whole genome and total length of the genome-string. These and other genomic and proteomic datasets are also stored at <http://flan.blm.cs.cmu.edu>.

Proteins: Individual proteins studied in the n-gram analysis (Chapter 6) are: lysozyme PDB ID 1HEJ, Rhodopsin PDB ID 1U19 and Swissprot ID OPSD_BOVIN and the viral sequences Swissprot IDs VGL2_CVH22 and VGL2_CVMA5.

5.1.2 Dataset for secondary structure classification

The Jpred benchmark dataset has been used for secondary structure analysis [129]. The dataset consists of 513 proteins that are pairwise non-redundant. For each sequence, the secondary structure assignment is provided according to the Dictionary of Secondary Structure Prediction (see Section 2.2). The Jpred data also contains definitions by DEFINE and STRIDE methods, and multiple sequence alignments, which are not used in this analysis. The data has been obtained from [129].

5.1.3 Dataset to compare soluble and transmembrane helices

A list of membrane proteins with known 3-dimensional structure was obtained from Stephen White's homepage [130]. Corresponding sequences were extracted from the protein data bank [131]. Sequences were used to retrieve family members of a given membrane protein from the Pfam database [132]. The G-protein Coupled Receptor (GPCR) unit

Organism	Family	Proteins	Amino acids
<i>Mycoplasma genitalium</i>	Bacteriae	484	175928
<i>Blucher</i> sp APS	Bacteriae	564	185170
<i>Ureaplasma unrealistic</i>	Bacteriae	613	228190
<i>Mycoplasma pneumonia</i>	Bacteriae	689	239745
<i>Borrelia bulldozers</i>	Bacteriae	787	149265
<i>Rickettsia prowazekii</i> strain Madrid E	Bacteriae	834	279079
<i>Chlamydia trachomatis</i>	Bacteriae	894	312176
<i>Chlamydia muridarum</i>	Bacteriae	909	322446
<i>Treponema pallidum</i>	Bacteriae	1031	350675
<i>Chlamydosporic pneumoniae</i> CWL029	Bacteriae	1052	361693
<i>Chlamydosporic pneumoniae</i> J138	Bacteriae	1070	366604
<i>Chlamydosporic pneumoniae</i> AR39	Bacteriae	1110	363837
<i>Thermoplasma acidophilum</i>	Archaea	1478	453103
<i>Helicobacter pylori</i> strain J99	Bacteriae	1491	493979
<i>Thermoplasma volcanium</i>	Archaea	1499	450114
<i>Aquifex aeolicus</i>	Bacteriae	1522	482509
<i>Helicobacter pylori</i> 26695	Bacteriae	1553	491575
<i>Mycobacterium leprae</i> strain TN	Bacteriae	1605	538772
<i>Campylobacter jejuni</i>	Bacteriae	1634	508836
<i>Haemophilus influenzae</i> Rd	Bacteriae	1709	521076
<i>Methanococcus jannaschii</i>	Archaea	1715	483561
<i>thermotoga maritima</i>	Bacteriae	1846	581825
<i>M. thermoautotrophicum</i> delta H	Archaea	1869	525506
<i>Pasteurella multocida</i>	Bacteriae	2014	668036
<i>N. meningitidis</i> serogroup B strainMC58	Bacteriae	2025	587019
<i>Halobacterium</i> spec. NRC1	Archaea	2058	586960
<i>Pyrococcus horikoshii</i> OT3	Bacteriae	2064	568543
<i>N. meningitidis</i> serogroup A strainZ2491	Bacteriae	2065	585986
<i>Lactococcus lactis</i> subsp. <i>lactis</i>	Bacteriae	2266	665344
<i>Archaeoglobus fulgidus</i>	Archaea	2420	669574
<i>Deinococcus radiodurans</i> R1 chr1	Bacteriae	2579	777108
<i>Aeropyrum pernix</i>	Archaea	2694	638683
<i>Vibrio cholerae</i> chr1	Bacteriae	2736	860189
<i>Xylella fastidiosa</i>	Bacteriae	2766	742362
<i>Synechocystis</i> spec. PCC6803	Bacteriae	3169	1033204
<i>Mycobacterium tuberculosis</i> H37Rv	Bacteriae	3918	1329250
<i>Bacillus halodurans</i> C125	Bacteriae	4066	1188109
<i>Bacillus subtilis</i>	Bacteriae	4100	1216999
<i>Escherichia coli</i> K12	Bacteriae	4289	1358989
<i>Escherichia coli</i> O157H7EDL933	Bacteriae	5349	1608700
<i>Escherichia coli</i> O157H7	Bacteriae	5361	1609187
<i>Pseudomonas aeruginosa</i> PA01	Bacteriae	5565	1859530
<i>Mesorhizobium loti</i>	Bacteriae	6752	2033374
<i>Homo sapiens</i>		25612	18283879

Table 5.1: List of organisms for which whole genome sequences have been analyzed

input data was taken from the Swissprot [133] and GPCR database [134]. Segments based on secondary structure (helices, transmembrane helices, loops) were extracted from the swissprot FEATURE entries.

5.1.4 Dataset for transmembrane segment prediction

Standard datasets

Training: Data used for training is the set of 160 proteins compiled by Sonnhammer et al [115]. This is the same dataset used to train TMHMM version 2.0.

Evaluations: Evaluations here are performed on these data sets:

1. Benchmark evaluations data is provided by the benchmark web server TMH-BM maintained by Kernytsky et al [135]. This data set includes high-resolution data set of 36 proteins, low resolution data set of 165 proteins and 616 soluble proteins and 1418 signal peptides.
2. TM proteins with recent high resolution information from the MPtopo data set consisting of 443 TM segments in 101 proteins [103].
3. A PDB_TM dataset downloaded in April 2006 which contains all transmembrane proteins with 3D structures from the PDB determined to that date [1]. PDB_TM provides a list of non-redundant subset of the set of alpha-helical TM proteins. Non-redundant is defined as having sequence identity less than 40% [1]. Chains corresponding to this non-redundant list were extracted from the complete set, resulting in 191 proteins consisting of 789 TM segments.
4. TM proteins from the alpha-helical transmembrane class of the Orientation of Proteins in the Membrane (OPM) dataset, version 1.1 downloaded in March 2007 [72]. It contains 1869 TM segments in 522 proteins with PDB structures.

Other data

NR_TM data: A data set of non-redundant proteins with high resolution 3D structure referred to as NR_TM has been compiled by Tastan and Klein-Seetharaman as follows: proteins from the 4.00 resolution list of PDB_TM have been taken. All chains have been clustered with `blastclust` with a threshold of 30% sequence identity. From each cluster, was based on literature constraints. The list of chains included in the data set are shown in Table 5.2. TM labels for this dataset have been assigned by setting all residues with Z coordinates of C_α atoms between -15Å and +15Å to be of TM type. The resulting labels have been manually corrected to remove horizontal helices and other scattered individual or pairs of residues.

PDB id	Chain	PDB id	Chain	PDB id	Chain	PDB id	Chain
2axt	C	1ar1	B	1ldf	A	1su4	A
2axt	D	1bcc	E	1lgh	A	1v55	D
2axt	E	1bcc	G	1lgh	B	1v55	G
2axt	F	1bcc	J	1lnq	A	1v55	I
2axt	H	1c3w	A	1m56	D	1v55	J
2axt	I	1ehk	A	1okc	A	1v55	K
2axt	J	1ehk	B	1ors	C	1v55	L
2axt	K	1ehk	C	1ots	A	1v55	M
2axt	L	1ijd	A	1p49	A	1vf5	D
2axt	M	1iwg	A	1pp9	D	1vf5	E
2axt	T	1jb0	A	1pw4	A	1vf5	F
2axt	Z	1jb0	F	1q16	C	1vf5	G
2b2f	A	1jb0	I	1q90	A	1xfh	A
2bhw	A	1jb0	J	1q90	B	1xl4	A
2b12	A	1jb0	K	1q90	D	1yce	A
2bs2	C	1jb0	L	1q90	G	1yew	A
2f2b	A	1jb0	M	1q90	L	1yew	B
2fyn	B	1jb0	X	1q90	N	1yew	C
2gfp	A	1kb9	H	1q90	R	1yq3	C
2hyd	A	1kb9	I	1q1e	D	1zcd	A
2ic8	A	1kqf	B	1r3j	C	2a65	A
2iub	A	1kqf	C	1rh5	A	2ahy	A
2j58	A	1l0v	C	1rh5	B	2axt	A
2oar	A	1l0v	D	1rh5	C	2axt	B

Table 5.2: List of chains included in NR_TM dataset

Table shows the PDB ID and the chain ID of the 96 sequences of the NR_TM dataset.

Specific proteins: TMpro predictions were made and analyzed in detail for these specific proteins: KcsA potassium channel: PDB ID: 1BL8, Chain D. Aquaporin: PDB ID: 1FQY, Chain A, Swissprot ID: AQP1_HUMAN. The sequences of PalH and GP160 (of which GP41 is the c-terminal side section) used in our analysis is given below:

PALH sequence

```
MDPRQLINNLKPSSTSAAATATHPHCTPFTLPSNGVISLGASEYFTLTTNAIFNPECTGTADIVLT
GAGTPTSFVDLRDPFYASTIPACYALAATTVIAYMLVIMLLITPRTFLVQGAVVLGRRRGFTNGPS
GSDAGIGIGGRPWLQKVAALTVAISLTIATADTFRVAEQQYELGLMNASALQEEVEGGMELKIIR
IISDTFLWLAQAQTLIRLFRQREKIIKWTGFALISLDVLFSLNLFVYNGNSRPRLFTDAVPA
LAYLFQLALSLLYCAWVIYYAISKKRYAFYHPKMRNIFLVAILLSVSVLVPVFFVLDISKPALA
AWGDYVRWVGAAAASVVVWEWVERIEALERDEKDKDGLGREVFDGDEMDEVPTSDWTKRFRKDN
DDKGGTATGSTWPAMSGLANRYRSHATNDLETGSVPGQRTGRHLLAVRPLWPTRPQPAATPINR
ADTASAESTAYTVRYHPISEATPPIISGDTTLRSNSEAISRSISNEEVSDSKPVLLEQTNQA
AAVAAGLHNWQNSLNPFKHRVQGPPEVSLHTAKPPTPFSSHESSNKWDVRARIEGFAATQAER
FREKTRPTVDTDPLPLTVIPAPSRRAVATESEESDTSISPTPDESSHIEVTTSRDRPARTTD
PYTPDSLQHSITHRGSISFATAVQPELDQRVENATASPTLVGSRQTPFSSSRSSPITVRSPTV
PSLPPIIDGLPVTTIPAPRRRPRVENP
```

ID gp160 of H standard; PRT; 856 AA.

AC - DT 07-JUL-2004

```
MRVKEKYQHL WRWGWRWGTM LLGMLMICA TEKLWVTVYY GVPVWKEATT TLFCASDAKA
YDTEVHNVWA THACVPTDPN PQEVVLVNVV ENFNMWKNDM VEQMHEDIIS LWDQSLKPCV
KLTPLCVSLK CTDLKNDTNT NSSSGRMIME KGEIKNCSFN ISTSIRGKVQ KEYAFFYKLD
IIPIDNDTTS YKLTSCNTSV ITQACPKVSF EPIPIHYCAP AGFAILKCNN KTFNGTGPCT
NVSTVQCTHG IRPVVSTQLL LNGSLAEDEV VIRSVNFTDN AKTIIVQLNT SVEINTRPN
NNTRKRIRIQ RGPGRAVFTI GKIGNMRQAH CNISRAKWN TLKQIASKLR EQFGNNKTII
FKQSSGGDPE IVTHSFNCGG EFFYCNSTQL FNSTWFNSTW STEGSNNTG SDTITLPCRI
KQIINMWQKV GKAMYAPPIS GQIRCSSNIT GLLLTRDGGN SNESEIFRP GGGDMRDNR
SELYKYKVVK IEPLGVAPTK AKRRVVQREK RAVGIGALFL GFLGAAGSTM GAASMTLTVQ
ARQLLSGIVQ QQNNLLRAIE AQQHLLQLTV WGIKQLQARI LAVERYLKDQ QLLGIWGCSSG
KLICTTAVPW NASWSNKSLE QIWNHTTWME WDREINNYTS LIHSLIEESQ NQKEKNEQEL
LELDKWASLW NWFNITNWLW YIKLFIMIVG GLVGLRIVFA VLSIVNRVRQ GYSPLSFQTH
LPTPRGPDRP EGIEEEGGER DRDRSIRLVN GSLALIWDDL RSLCLFSYHR LRDLLLIVTR
IVELLGRRGW EALKYWNLL QYWSQELKNS AVSLLNATAI AVAEGTDRVI EVVQGACRAI
RHIPRRIRQG LERILL
```

5.2 Evaluation metrics

5.2.1 Metrics for secondary structure prediction

The metrics for evaluation of secondary structure prediction are similar to those defined above. The contingency table (Table 5.3) defines the cells for transmembrane and

nontransmembrane. In case of secondary structure prediction the contingency table is constructed thrice for (i) helix and non-helix, (ii) sheet and non-sheet and (iii) coil and non-coil. Precision and recall are calculated for helix, sheet and coil separately using Equations 5.4 and 5.5. Overall precision and recall are computed as given below:

$$P = \frac{1}{N} \sum_t P_t * Size_t, t \text{ in } \{\text{helix, sheet, coil}\} \quad (5.1)$$

$$R = \frac{1}{N} \sum_t R_t * Size_t, t \text{ in } \{\text{helix, sheet, coil}\} \quad (5.2)$$

where $Size_t$ is the number of residues of that type (helix, sheet or coil), N is the total number of residues.

Q₃: The average precision computed as given in Equation 5.1 is also called Q₃, the average 3-class accuracy.

5.2.2 Metrics for transmembrane helix prediction

The metrics used here to evaluate TM prediction are those commonly used in the TM helix prediction literature. The different metrics used may be calculated from the elements in the contingency table shown in Table 5.3.

Actual \ Predicted	transmembrane (TM)	nontransmembrane (NTM)	
TM	A	B	Q
NTM	C	D	R
	S	T	N

Table 5.3: Contingency table for evaluation metrics

Elements of the contingency table for the 2-class (TM, NTM) prediction of residues. Metrics such as Q_2 , precision and recall are defined in terms of the elements of the contingency table. The cell A contains the number of residues that are actually TM and are also predicted to be TM. B contains number of residues that are actually NTM but are predicted to be TM. C contains the number of residues actually TM and predicted to be NTM. D contains the number of residues actually NTM and also predicted to be NTM. $Q=A+B$. $R=C+D$. $S=A+C$. $T=B+D$. $N=A+B+C+D=Q+R=S+T$.

Residue level accuracy

Q₂: The accuracy of prediction of the residues into the two classes, membrane or non-membrane. Q_2 is also the average precision of both the classes computed per residue.

The accuracy is given per-residue and is computed as follows:

$$Q_2 = 100 * \frac{\text{number of correctly predicted residues}}{\text{total number of residues}} = 100 * \frac{A+D}{N} \quad (5.3)$$

Precision: Precision is computed for the transmembrane and nontransmembrane classes separately. It is defined as the percentage of the residues correctly predicted to be of one class of the total residues predicted to be of that class. Precision is computed as:

$$\begin{aligned} Q_{2T}^{pred} &= 100 * \frac{\text{number of residues predicted correctly as TM}}{\text{total number of residues predicted as TM}} = \frac{A}{Q} \\ Q_{2N}^{pred} &= 100 * \frac{\text{number of residues predicted correctly as NTM}}{\text{total number of residues predicted as NTM}} = \frac{D}{R} \end{aligned} \quad (5.4)$$

Recall: Recall is also computed separately for the transmembrane and nontransmembrane classes. It is defined as the percentage of the residues that belong to a class that are predicted to be of that class. Recall is computed as:

$$\begin{aligned} Q_{2T}^{obs} &= 100 * \frac{\text{number of residues predicted correctly as TM}}{\text{total number of residues that are actually TM}} = \frac{A}{S} \\ Q_{2N}^{obs} &= 100 * \frac{\text{number of residues predicted correctly as NTM}}{\text{total number of residues that are actually NTM}} = \frac{D}{T} \end{aligned} \quad (5.5)$$

Segment level accuracy

Segment level precision and recall are also important metrics in evaluating TM predictions. These metrics have a wide range of definitions—in the number of residues required to overlap between predicted and observed segments to be considered a correct prediction, in whether to count a predicted (observed) segment twice when it overlaps with two observed (predicted) segments. These issues were addressed by Chen et al in the benchmark comparisons of most of the TM prediction algorithms, and the metrics used in this work are the same as defined there [111].

- A predicted segment is treated as a correct prediction if it overlaps with an observed (actual) TM segment by at least 3 residues.
- If two observed segments overlap with one predicted segment, only one of the observed segments is treated as “predicted correctly”. The other segment is treated as a “miss” or a false-negative.
- If two predicted segments overlap with one observed segment, only one of the predicted segments is treated as “predicted correctly”. The other segment is treated as a false-positive.

Segment accuracies are computed per protein and averaged over the total proteins in the dataset.

Segment recall

$$Q_{htm}^{obs} = 100 * \frac{\text{Number of correctly predicted segments}}{\text{Number of all the TM segments observed in the dataset}} \quad (5.6)$$

Segment precision

$$Q_{htm}^{pred} = 100 * \frac{\text{Number of correctly predicted segments}}{\text{Number of all the TM segments predicted in the dataset}} \quad (5.7)$$

Chapter 6

Biological Feature Development and Analysis

6.1 N-gram analysis

N-grams have proven useful in statistical natural language processing, particularly to infer topic or information from a natural language text document (Section 1.3.1). In our approach of drawing parallels between natural language text and speech and biological sequences (see Chapter 1), we studied n-gram distributions across proteomes. In analogy to the question “What kind of things do people say?” we ask the question “What kind of amino acid sequences occur in the proteins of an organism?”. After statistical distribution of n-grams in organisms, we studied the biological significance of these statistical distributions of n-grams for protein structure and function. This is analogous to the question “what do the things people say mean?”. An understanding of the sequence space occupied by proteins in different organisms would have important applications for “translation” of proteins from the language of one organism into that of another, and design of drugs that target sequences that might be unique or preferred by pathogenic organisms over those in human hosts.

6.1.1 Biological language modeling toolkit

The proposed statistical analysis of biological sequences with n-grams requires string matching and string searches. Due to the large size of genomic data, the search for subsequences becomes computationally intensive. Searching for a substring from large text data is a well-studied problem in computer science, with applications to diverse areas including data compression, network intrusion detection, information retrieval and word processing [136]. Data structures such as suffix trees [137] and suffix arrays [124] have been used as preferred data structures for text processing applications [138, 139, 124] and also for biological data [140]. Suffix arrays permit search of a sub-string of length P in a string of length N in $O(P+\log N)$ time, and requires $O(N)$ space for construction,

which is competitive with those of suffix trees [124]. Preprocessed suffix arrays can be used to efficiently extract global n-gram statistics and compare them amongst genomes. When suffix arrays are complemented with other data arrays, e.g. the Longest Common Prefix (LCP) array [124] and/or Rank array [125], they provide additional functionality at reduced computational cost.

We developed a toolkit, the Biological Language Modeling Toolkit (BLMT), that combines the following functions:

1. Data preprocessing

- Construction of suffix array
- Construction of LCP array and rank array

2. Tools

- Computing protein number and length
- N-gram count and most frequent n-gram counts for any N
- Relative frequencies of specific n-grams across organisms
- Longest repeating sequences
- Localization and co-localization of n-grams for grouping proteins
- N-gram neighbor (left and right) preferences
- Yule value computation
- Annotation of a protein sequence with n-gram characteristics from global statistics

Availability: Web interface is available at <http://flan.blm.cs.cmu.edu/>. Source code is also available, at: <http://www.cs.cmu.edu/~blmt/source/>. Details of the download, installation and usage are given in Appendix A.

Data preprocessing into suffix array

The suffix array structure originally described by Manber and Myers [124] is constructed for whole-genome proteomic data of an organism. The efficiency of the suffix array is further improved by accompanying data structures including the longest common prefix (LCP) and the rank array described in ref. [125]. The toolkit allows processing of genome sequences upto 25MB data sizes. Sequences of the order of the size of human proteome have been tested.

Position	0	1	2	3	4	5	6	7	8	9	10	11	12	13	14	15	16	17	18	19	20	21	22	23	24
Rank Array	19	24	5	8	15	23	22	13	12	11	1	16	7	20	4	6	10	14	17	9	2	18	21	3	0
Sequence	M	V	D	I	L	S	S	L	L	L	#	M	D	P	A	D	K	L	M	K	#	M	Q	A	#
Suffix Array	24	10	20	23	14	2	15	12	3	19	16	9	8	7	17	4	11	18	21	0	13	22	6	5	1
LCP array	0	1	2	0	1	0	1	1	0	0	1	0	1	2	1	1	0	1	1	1	0	0	0	1	0
Suffixes sorted in lexicographic order	#	#	#	A	A	D	D	D	I	K	K	L	L	L	L	L	M	M	M	M	P	Q	S	S	V
	M	M	#	D	I	K	P	L	#	L	#	L	L	M	S	D	K	Q	V	A	A	L	S	D	
	D	Q		K	L	L	A	S	M	M	M	#	L	K	S	P	#	A	D	D	#	L	L	I	
	P	A		L	S	M	D	S	Q	K	D	M	#	#	L	A	M	#	I	K		L	L	L	
	...	#	

Figure 6.1: Example of a suffix array and its longest common prefix array and rank array, for the sequence

MVDILSSLL#MDPADKLMK#MQA#. An example suffix S5 (row 3, shown in pink) is the suffix beginning at position-5 (S5). This suffix appears as the 23rd suffix in SA. Rank of S5 is 23. Similarly, suffix array carries the value ‘5’ at position 23, indicating that the 23rd suffix is S5. Longest common prefixes between adjacent suffixes are shown in same color. LCP array contains the lengths of these longest common prefixes. For example, at position 13, the LCP with previous suffix is “LL”, and its length is 2: $LCP(13) = 2$.

Example of a suffix array data structure for protein sequences: The suffix array and its construction have been presented in Chapter 4.1. For a given sequence, a suffix at position i is the substring beginning at position i and extending to the end of the string. In Figure 6.1, the suffix at position 5 is shown in pink color. A suffix array is the arrangement of all the possible suffixes of the input string in lexicographical order. To store the sorted order of the suffixes, only their beginning positions are entered in the suffix array data structure, as shown in the 4th row in Figure 6.1. The longest common prefix (LCP) array stores the length of common prefix substring between a suffix and its preceding entry in the sorted suffix array. The rank array stores for each position in the input string, the position of its suffix in the suffix array. That is, if a suffix S_n appears at the i^{th} position in the lexicographical order of the suffix array, then $rank[i] = j$.

Tools

All tools can be applied to protein or nucleic acid sequences, except the statistical correlations tool to compute Yule values. This tool can be applied to only protein sequences.

N-gram counts: The functionality of the toolkit includes n-gram counts from protein or nucleic acid sequences, where n is an arbitrary integer or range of integers. Locating sequence repeats becomes computationally expensive when the search is to be performed on a database of the size of multiple genomes or when n is large. BLMT uses the underlying suffix array structure to retrieve repeating sequences of any length greater than a threshold set by the user or the longest repeating sequences efficiently. BLMT also computes the co-occurrence counts of specific n-grams in subsets of the data, e.g. within individual

proteins, and supports identification of n-gram neighbors (left and right). BLMT allows retrieval of proteins that contain common sequences longer than a threshold and annotation of n-gram counts along proteins. The n-gram counts can be sorted in ascending or descending order of their counts, or in lexicographic ordering of the n-grams.

Motif	patterns that match motif			
Aab?baA	AAA?AAA	ACA?ACA	AGA?AGA	ATA?ATA
	AAC?CAA	ACC?CCA	AGC?CGA	ATC?CTA
	AAG?GAA	ACG?GCA	AGG?GGA	ATG?GTA
	AAT?TAA	ACT?TCA	AGT?TGA	ATT?TTA
Cab?CaA	CAA?AAC	CCA?ACC	CGA?AGC	CTA?ATC
	CAC?CAC	CCC?CCC	CGC?CGC	CTC?CTC
	CAG?GAC	CCG?GCC	CGG?GGC	CTG?GTC
	CAT?TAC	CCT?TCC	CGT?TGC	CTT?TTC
Gab?baG	GAA?AAG	GCA?ACG	GGA?AGG	GTA?ATG
	GAC?CAG	GCC?CCG	GGC?CGG	GTC?CTG
	GAG?GAG	GCG?GCG	GGG?GGG	GTG?GTG
	GAT?TAG	GCT?TCG	GGT?TGG	GTT?TTG
Tab?baT	TAA?AAT	TCA?ACT	TGA?AGT	TTA?ATT
	TAC?CAT	TCC?CCT	TGC?CGT	TTC?CTT
	TAG?GAT	TCG?GCT	TGG?GGT	TTG?GTT
	TAT?TAT	TCT?TCT	TGT?TGT	TTT?TTT

Table 6.1: Motif search in biological language modeling toolkit

Column 1 shows patterns that match the regular expression $Xab?baX$. N-grams that match each of the generated motifs are shown in the remaining columns.

N-gram colocation: Co-location of two or more specific n-grams in individual proteins may be determined.

Motif recognition: A tool that computes the number of occurrences of specific motifs or regular expressions is built into the toolkit. The tool allows enumeration of n-grams that conform to a specific pattern, such as $XYabc??cbaXY$, where X and Y are specific amino acids, a to z are wildcards that allow describing a pattern, and a general wild card ? that matches with any of the 20 amino acids. For example, the pattern $Xab?baX$ retrieves the counts of each of the patterns shown in column 1 of Table 6.1.

Reduced alphabet n-grams: Amino acids may be mapped to a reduced vocabulary based on their properties prior to searching and enumeration of patterns.

Statistical correlations: N-gram counts are used to compute statistical correlations between them using Yule's q-statistic [141]. Yule values range from -1 and +1 reflecting negative or positive influence of the occurrence of two amino acids on each other. This tool computes Yule value between two amino acids separated by a specific distance (such as A**C).

Annotation of a protein: The toolkit also allows reading in Yule or other correlation values pre-computed with other tools. A protein sequence can be annotated with the statistical values (Yule value/n-gram frequency/any other statistics read-in from a file) for the amino acids found along the protein sequence.

Language models: Perplexity of N-gram language model is computed as

$$Pr(W_i|W_i, \dots, W_{i-1}) = Pr(W_i|W_{i-N+1}, \dots, W_{i-1}) \quad (6.1)$$

where W_i are the probabilities of observing the word i . After computing the language model for an organism (or such data set of protein sequences), the likelihood of observing a new sequence in comparison to a reference language model is reported.

6.1.2 Distribution across organisms

Probabilistic models can distinguish organisms

A simple Markovian unigram (context independent amino acid) model from the proteins of *Aeropyrum pernix* was trained. When training and test set were from the same organism, a perplexity (a variation on cross-entropy) of 16.6 was observed, whereas data from other organisms varied from 16.8 to 21.9. Thus the differences between the 'sub-languages' of the different organisms are automatically detectable with even the simplest language model. This observation is purely based on the large differences in unigram distributions and is independent of the organism that is used to train the model.

Genome signatures

We developed a modification of Zipf-like analysis that can reveal differences between word-usage in different organisms. First, the amino acid n-grams of a given length are sorted in descending order by frequency for the organism of choice. Two examples using the simplest case, $n=1$, are shown in Figure 6.2 for *Aeropyrum pernix* and *Neisseria meningitidis* to illustrate the principle. The frequencies of the sorted n-grams are shown in bold red. Thin lines indicate the respective frequencies of n-grams in all the other organisms studied. The same plots for the other 42 organisms studied for $n=1$ and also for other n ($n < 5$) can be viewed at www.cs.cmu.edu/~blmt. While there is striking variation in rank of certain n-grams in different organisms, the most rare n-grams in one

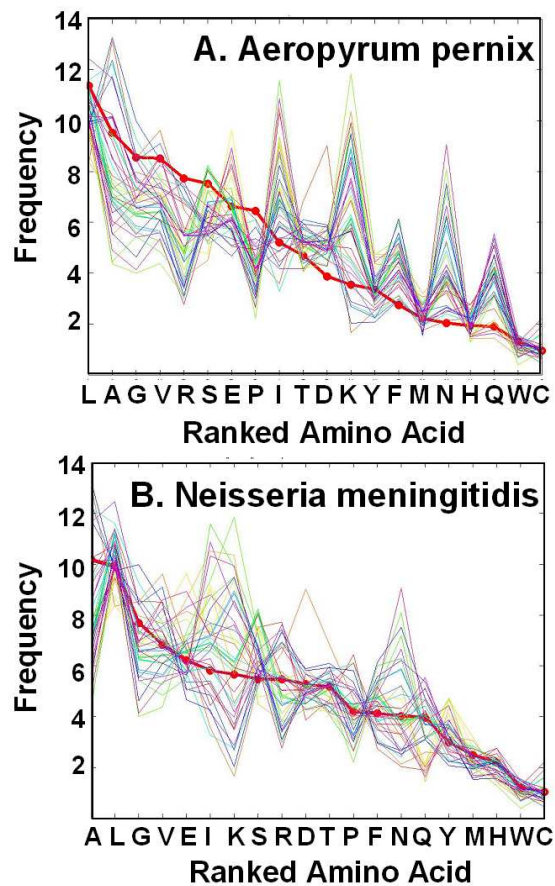


Figure 6.2: Top 20 unigrams in Aeropyrum pernix and Neisseria meningitidis

Distribution of amino acid n-grams with $n=1$ in *Neisseria meningitidis* in comparison to the distribution of the corresponding amino acids in 44 other organisms. N-grams of the reference organism are plotted in descending order of their frequency in the genome (in bold red). X-axis shows labels of the n-grams. Frequencies of corresponding n-grams from genomes of various other organisms are also shown (thin lines).

Aeropyrum pernix4		Methano bacterium		Methano coccus jannas		Thermoplasma acidophilum		Thermoplasma volcanium		Escherichia coli O157H7		Neisseria meningitidis		Human Human	
AAAA	215	AAAA	83	EILK	144	LISA	40	EIAK	43	ALAA	269	AAAA	184	EEEE	4724
LAAA	158	LEEL	81	KLKE	131	SSIL	39	GIIS	43	LAAL	254	AAAL	144	PPPP	4114
LALA	158	EALE	81	EKLK	130	DLIR	39	LSSI	43	LLAL	245	SDGI	141	SSSS	4047
AALA	152	LREL	77	EKIK	129	LAIL	39	LALL	41	AALA	241	LAAA	128	AAAA	4000
AAAL	152	ELLE	74	EEIK	127	ISAI	38	EIEK	40	LAAA	240	MPSE	123	LLLL	3536
LEEA	150	RALE	68	LKKL	125	ISDL	38	LGLI	40	LLLL	234	ALAA	121	GGGG	2857
ALAA	149	EALK	66	IKEI	121	ISGL	38	IGII	40	ALLA	230	LAAL	110	QQQQ	2342
LAAL	136	LLEL	60	EELK	120	IGSG	38	LSIL	39	LLLA	225	AALA	106	GPPG	2124
LLAS	126	EEAL	60	ELKK	120	IGLI	37	IEKL	39	LAAA	216	AVAA	104	HTGE	2035
ALAL	123	EVLE	59	EIIK	118	SAIL	37	GISV	39	LALL	216	AALL	102	GEKP	1841

Table 6.2: Counts of top 10 4-grams in whole-genomes of some of the organisms studied

organism are overall rare in all organisms. Specific differences in n-grams other than unigrams are explored in detail below.

Organism-specific usage of “phrases” in protein sequences

The Zipf-like analysis described above (Section 6.1.2) allows us to quantify the differences in specific n-gram frequencies across organisms. In such comparisons, we identified n-grams that are frequent in some organisms while simultaneously being rare (or completely absent in some cases) in others. Examples are shown for *Aeropyrum pernix*, *Neisseria meningitidis* and *Homo sapiens* in Figure 6.3. In *A. pernix*, the *LEEA* frequency is strikingly high. In *N. meningitidis*, *MPSE*, *SDGI* and *GRLK* are amongst the top 20 most frequently used 4-grams, but are used in no other organism with such high frequencies. Human n-gram frequencies in particular differ from those found in bacteria and archaea, presumably due to the evolutionary distance to the unicellular organisms.

These highly idiosyncratic n-grams can be viewed as “phrases” that are preferably used in the particular organism. The observation of organism-specific phrases is not unique to extremophile or other specialized organisms. Instead, idiosyncratic phrases appear in all the organisms (see Section 6.1.2), and the results for other organisms (including very common and ubiquitous bacteria such as *Escherichia coli*) can be viewed at www.cs.cmu.edu/~blmt.

Phrases are not due to random variation

To test if the observation of idiosyncratic n-grams could be explained by chance sampling, we generated two sets of 20 artificial genomes by Monte Carlo simulation using the unigram frequencies of *Neisseria meningitidis* and *Aeropyrum pernix*, respectively. Figure 6.4 shows a Zipf-like comparison as described above for the natural genomes, for *Neisseria meningitidis* in comparison to the random genomes in (A), for *Aeropyrum pernix* in comparison to the random genomes in (B), and for one of the random genomes in comparison to the other random genomes and the *Neisseria* and *Aeropyrum* genomes in (C). As one

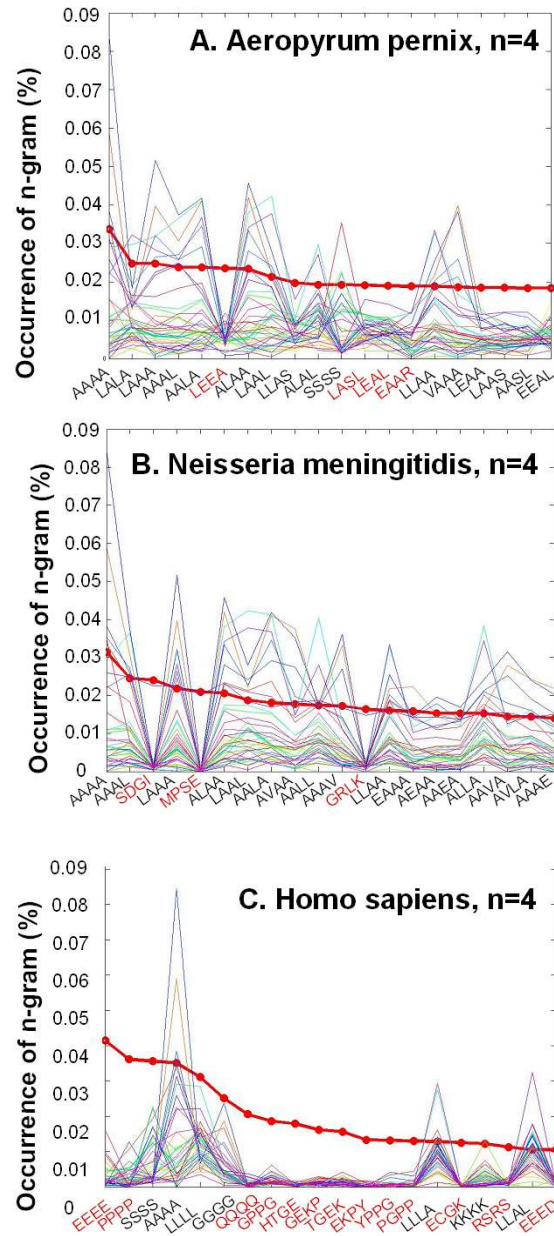


Figure 6.3: N-gram genome signatures

Distribution of amino acid n-grams with $n=4$ in *A. pernix*, *N. meningitidis* and *Homo sapiens*, in comparison to the distribution of the corresponding amino acids in 44 other organisms.

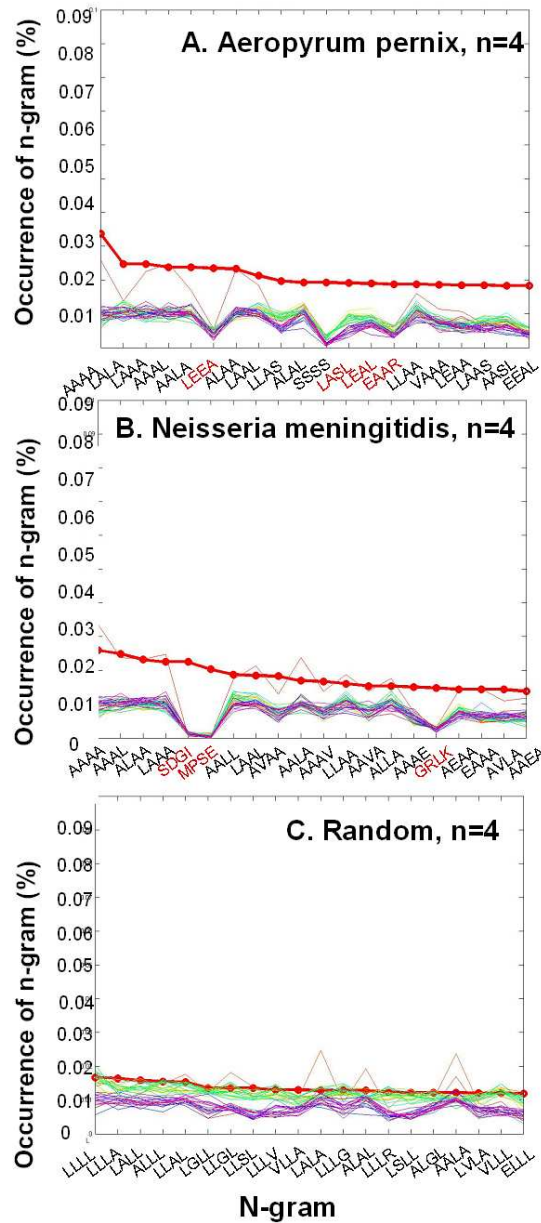


Figure 6.4: Random genomes versus natural genomes

Top 20 most frequently used 4-grams in (A) *Aeropyrum pernix*, (B) *Neisseria meningitidis* and (C) random genome. Line colours are as in Figure 6.2. Note that both natural genomes strike out, not only the one according to which the n-grams were ranked.

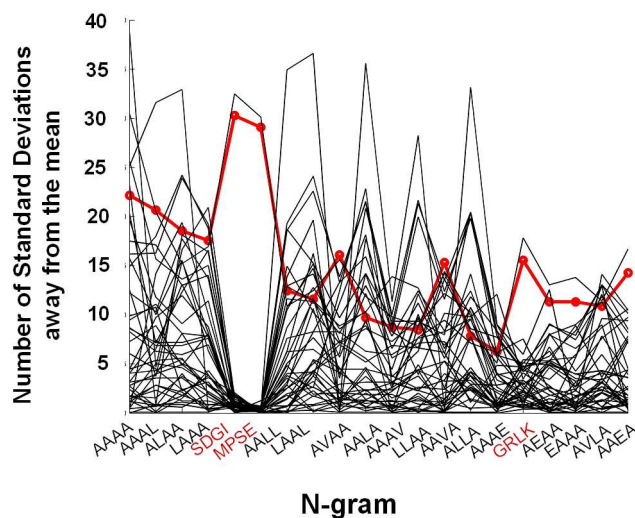


Figure 6.5: Genome signatures standard deviations

Distance from mean values based on unigram distributions in *N. Meningitidis*. Values are plotted as multiples of standard deviation. The unigram distribution was as in Figure 6.2. This figure has been generated by a colleague Dr. Deborah Weisser.

can see, in both natural genomes the frequencies are well above the baseline variation due to chance sampling.

Phrase frequencies can be very distant from mean values

To further strengthen the notion that the phrases are not due to random variation, we calculated the distance of 4-gram frequencies in multiples of standard deviations for the top 20 4-grams in *Neisseria meningitidis*. The result is shown in Figure 6.5. The phrases SDGI and MPSE are approximately 30 standard deviations away from the means based on unigram distributions. In contrast, all of the other organism, except for a different strain of *Neisseria meningitidis*, show only very small standard deviations from mean values based on their own unigram frequencies. GRLK is also more frequent than would be expected based on independent unigram probabilities, although not to the same degree as SDGI and MPSE. The large deviation from mean values clearly shows that phrases are not only organism-specific in absolute terms but are also quantifiably distant from the values predicted by independent unigram frequencies of the same organism.

6.1.3 Distribution across functions

We explored if the statistical n-gram distributions correlate with structural and functional properties of proteins.

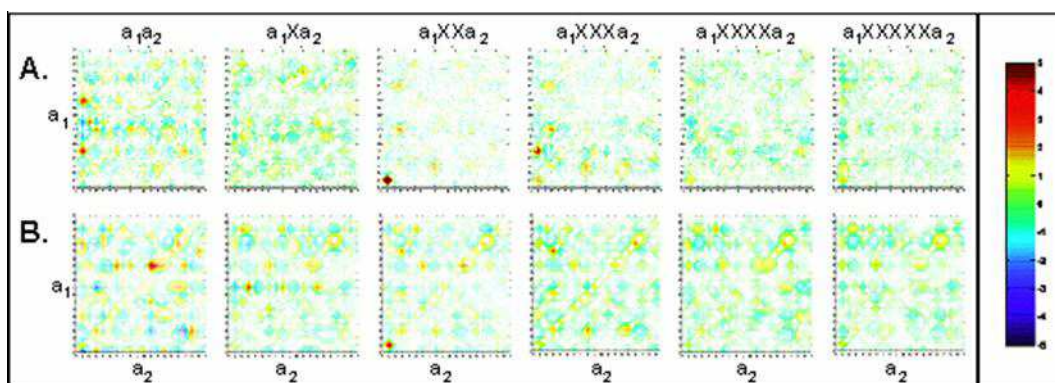


Figure 6.6: Preferences between neighboring amino acids in whole genomes

Positive and negative preferences between neighboring amino acids, separated by a distance of 0 to 5 residues are shown for *Aeropyrum pernix* (A) and *Thermoplasma acidophilum* (B). Red corresponds to positive preference and blue corresponds to negative preference (see color bar).

Folding

In natural language, while frequent words are often dispensable, rare words convey the meaning of a text. To test the hypothesis that rare amino acid n-grams are particularly important for protein structure and function, we investigated if inverse frequencies correlate with experimentally determined folding initiation sites in the protein folding model system, lysozyme. We observed a correlation between the locations of rare trigrams and the location of residual structure in the unfolded protein as evidenced by maxima in relaxation rates measured in NMR spectroscopic experiments (Figure 6.7). Although this was a very interesting observation, lack of experimental information about folding initiation sites for other proteins prevented us from inferring statistical significance.

Misfolding and stability

Experimental data is available for bacteriorhodopsin and rhodopsin, two membrane proteins enumerating which mutations cause an increase or decrease in the stability of the folded protein and also which mutations cause the protein to misfold. Inverse 4-gram frequencies were computed for these two proteins to infer the locations important to the folding and stability of the proteins. In Figure 6.8 the inverse 4-gram frequencies ($1/f$) are shown for rhodopsin for the original protein sequence (blue) and for mutated sequences (magenta). Note that, the mutations are point mutations, which means only one mutation is considered at one time. In the figure however, the $1/f$ of mutated data is superimposed for all the mutations of interest. Where mutations of interest were close and fall into the same 4-gram, only one of the mutation with higher destabilization according to experimental data, is considered. For experimental data see supplementary information in

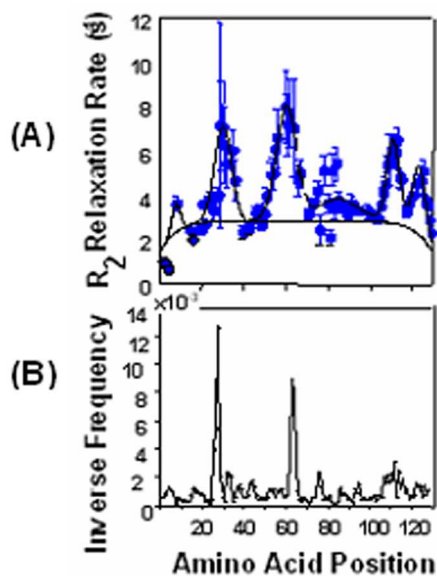


Figure 6.7: Rare trigrams in lysozyme coincide with folding initiation sites

A. Transverse relaxation rates (from Klein-Seetharaman et al., *Science* 295:1719 (3/1/2002) [5]. Reprinted with permission from AAAS). Large values above the black line indicate the presence of residual structure. B. Inverse trigram frequency in human lysozyme.

Publication 6 listed in 119. Inspection of Figure 6.8 reveals that some of the point mutations cause differences in inverse n-gram frequencies and cause misfolding in rhodopsin. However, mutations in rare amino acids such as cysteine (example shown is at position 140) also cause changes in inverse frequencies without affecting folding of the protein. We therefore conclude that inverse frequencies alone are not sufficient to differentiate between mutations that cause misfolding from those that do not.

Host-specificity of viruses

We studied one retrovirus that infects human and one that infects mouse. See Section 5.1.1 for sequence information. We compared the occurrence of n-grams in human, mouse and the two virus species. The number of unique n-grams found in the virus but not found in the host/non-host organism are shown in Table 6.3. The number of 5-grams from virus that are “not found” in host organism are fewer for both human and mouse viruses. It remains to be tested whether this hypothesis is true for other viral organisms and if these observations are biologically significant.

Negative charges in calcium sequestering proteins

Calcium (Ca^{2+}) plays an important role in many of the signaling pathways in the cells of living organisms, and is referred to as the “life and d death signal”. Homeostasis of Ca^{2+}

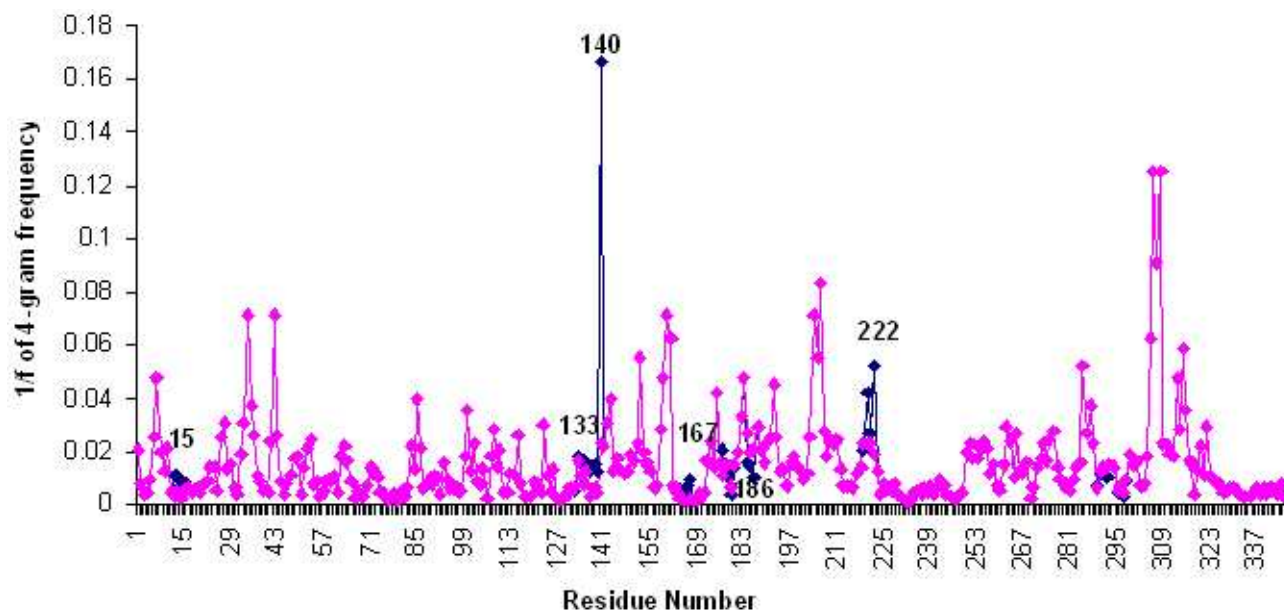


Figure 6.8: Changes in 1/f of 4-grams in mammalian rhodopsin upon mutations

For mammalian rhodopsin (PDB ID 1U19, 1/f of 4-grams in human are plotted in blue along the x-axis. On this, the same plot but for a sequence with mutations in some positions is shown in magenta. The labeled positions are those where the mutation causes a decrease in the Meta stability of rhodopsin.

	Human genome	Mouse genome
Human virus	2039	2077
Mouse virus	2462	1130

Table 6.3: 5 grams that occur in virus but not in host genome

is known to be achieved by way of calcium binding and buffering proteins, and through channels that allow a flux of the ions into and out of the cell. Many Ca^{2+} binding and buffering proteins are known that exist in the endoplasmic reticulum and the sarcoplasmic reticulum of the muscle cells. For example, calcium ions play a role in the adaptation of photoreceptor to the intensity of light. Drop in Ca^{2+} activates guanylate-cyclase through GC activating proteins (GCAP is an EF-hand motif calcium binding protein). Possibly it shortens the lifetime of activated-rhodopsin, by interfering with rhodopsin-kinase through S-modulin.

Two types of Ca^{2+} binding proteins have been identified. One type includes members of the large EF-hand protein family, which binds Ca^{2+} with high affinity and specificity. The other group of proteins contains domains of high negative charge density that binds Ca^{2+} with high capacity and low affinity. Both types of Ca^{2+} binding proteins are usually

involved in Ca^{2+} regulation. To help identify candidates of proteins that may contribute to Ca^{2+} regulation in retina, we investigated the occurrence of n-grams with high preponderance of the negatively charged amino acids E and D. We found a large number of proteins in human genome that contain long stretches of negative charges and may therefore bind Ca^{2+} .

6.1.4 Conclusions

Using n-gram statistical analysis of whole-genome protein sequences we have shown that there are organism-specific phrases in direct analogy to human languages. We developed a biological language modeling toolkit (freely accessible at www.cs.cmu.edu/~blmt) for genome-wide statistical amino acid n-gram analysis and comparison across organisms. Its functions were applied to 44 different bacterial, archaeal and the human genome. Amino acid n-gram distribution was found to be characteristic of organisms, as evidenced by (1) the ability of simple Markovian unigram models to distinguish organisms, (2) the marked variation in n-gram distributions across organisms above random variation, and (3) identification of organism-specific phrases in protein sequences that are greater than an order of magnitude standard deviations away from the mean. These lines of evidence suggested that different organisms utilize different “vocabularies” and “phrases”, an observation that may provide novel approaches to drug development by specifically targeting these phrases.

We explored to see if the n-gram idiosyncrasies coincide with any structurally or functionally relevant locations in proteins. In some cases, the rare n-grams point to structural information, but the available experimental data was not sufficient to confirm this. In other cases, n-gram frequencies did not provide clues to their relation to functional aspects.

It is concluded that n-grams may serve as useful features but require additional information to generate strong hypothesis in the context of protein structure or function.

6.2 Latent semantic analysis for secondary structure classification

In the previous chapter we described n-gram analysis as the first approach in exploring the analogy between biology and language. Next we applied a *bag of words* model to biological sequences, referred to as latent semantic analysis (LSA). See Section 1.3.3 for an introduction to the LSA algorithm. We used LSA to examine alternate choices for word equivalents in biological sequences. To achieve this, we studied the well-established problem of *secondary structure classification* (classification into helix, sheet and coil types) with LSA, using alternate vocabulary representations of protein sequences.

The LSA model was trained on a subset of the data; secondary structure of each segment in test data was predicted based on the model. See Chapter 4.2 for details of

implementation. This study was first performed using the amino acids as features, and was then repeated using chemical groups and electronic properties of amino acid groups as features. Data processing and the algorithm are described in Section 5.1.2 and 4.2.3.

In order to establish the use of a Singular Value Decomposition (SVD) component in the LSA model, we also performed the same secondary structure classification using simple Vector Space Model (VSM) features which does not employ the SVD. See Section 1.3.3 for the relation between VSM and LSA.

The results of the classification of the segments are given in Tables 6.4 and 6.5 for VSM and in Tables 6.6 and 6.7 for LSA, and are discussed below. For a description of the performance measures precision and recall, see Section 5.2.

Amino acids. The precision of both helix and sheet are higher with LSA than with VSM: 69.1 and 52.3%, in comparison to 42.7 and 30.1%, respectively. Only coil is predicted more accurately with VSM. The recall values drop when going from VSM to LSA but yield better confidence in secondary structure assignment. The average performance over the three classes (helix, strand, and coil), of both precision and recall, is significantly better with the combination of LSA with amino acids as vocabulary.

Chemical groups. Next, we studied the effect of increasing the detail in description of the amino acids by rewriting the sequence using chemical groups as vocabulary and explored the performance of the two models using this vocabulary. The basic chemical groups that form the building blocks in the 20 amino acids that were treated as *words* are shown in Figure 2.2. The chemical groups represent the amino acids in greater detail, namely in terms of their chemical composition. Thus, overlap in chemical properties because of the same chemical group being a component of the amino acid side chain is accounted for, in vocabulary. For VSM, the choice of the chemical composition as vocabulary as opposed to the amino acids is advantageous. The increases in precision for helix and strand are comparable to those seen when comparing VSM and LSA in the case of amino acids. The precision of coil prediction is similar for both amino acid and chemical group vocabularies. For the prediction of helix, VSM as compared to LSA gives even better results. However, the strand and coil predictions are comparable or lower in LSA than in VSM. Thus, for the chemical vocabulary, the combination of VSM with chemical groups gives the best Q_3 performance in precision. One might argue that LSA is already capable of extracting synonymous words; and hence that it would be able to identify similarities between amino acids. However similarity of amino acids arises due to similarity in chemical composition whereas, LSA determines synonymy based on context; hence it might give additional advantage to give explicit indication of amino acid similarity.

Amino acid types. Finally, we investigated the effect of decreasing the detail in the description of the amino acid sequence. While the chemical vocabulary, is more detailed than the amino acid vocabulary, the amino acid type vocabulary is less detailed than the

Vocabulary	Data	Precision				
		Helix	Strand	Coil	m	M
Amino Acids	Training data	97.8	56.7	91.4	82.7	81.9
	Test data	42.7	30.1	83.3	62	52
Chemical Groups	Training data	96.7	58.9	92.9	83.6	82.6
	Test data	64.6	53.9	78.4	69.5	65.5
Amino acid Types	Training data	77.1	57	81.7	72	NA
	Test data	72.5	48.4	77.4	66.1	NA

Table 6.4: Precision of secondary structure classification using vector space model

Precision of protein segment classification into the three secondary structure classes (helix, strand, coil) using vector space model and different choices of vocabulary.

Vocabulary	Data	Recall				
		Helix	Strand	Coil	m	M
Amino Acids	Training data	99.6	87.6	65.9	77.5	84.3
	Test data	65.8	67.3	20	40.6	51
Chemical Groups	Training data	99.6	88.3	68.4	79	85.4
	Test data	55.3	48.7	85.7	69.7	63
Amino acid Types	Training data	95.5	80.3	28.8	68.1	NA
	Test data	84.9	71.1	27	61.1	NA

Table 6.5: Recall of secondary structure classification using vector space model

Legend as in Table 6.4.

Vocabulary	Data	Precision				
		Helix	Strand	Coil	m	M
Amino Acids	Training Data	98.9	60.1	94.9	85.8	84.6
	Testing Data	69.1	52.3	73.6	67.1	67.7
Chemical Groups	Training Data	99.6	66.2	82.7	82.6	80.9
	Test Data	80	50	50	55.7	59.7
Amino acid Types	Training Data	82.7	53.3	75.6	70.6	70.6
	Test Data	90	70	30	60.5	60.5

Table 6.6: Precision of secondary structure classification using latent semantic analysis model

Legend as in Table 6.4.

Vocabulary	Data	Recall				
		Helix	Strand	Coil	m	M
Amino Acids	Training Data	99.6	92.1	69.4	80.6	87.1
	Testing Data	42.8	49.6	84.4	67.6	58.9
Chemical Groups	Training Data	99.6	89	54.2	81	80.9
	Testing Data	40	40	80	64.4	55.1
Amino acid Types	Training Data	96.2	81.4	23.5	67	67
	Testing Data	70	50	70	63.5	63.5

Table 6.7: Recall of secondary structure classification using latent semantic analysis
Legend as in Table 6.4.

amino acid vocabulary. Amino acid types represent a reduced set of amino acids in which they were mapped into different classes. Words are viewed as “classes of amino acids”. Since there is significant overlap in chemical properties of the 20 different amino acid side chains, many different reduced vocabularies have been proposed. The grouping of amino acids that is used in this work is based on electronic properties, and is shown in Table 2.1. Using amino acid types slightly improved classification accuracy of helix in comparison to using chemical groups, but did not have significant effect on strand and coil when using the VSM model. However, when the LSA model was applied, the combination of the LSA model with this vocabulary yielded by far the best prediction accuracy for helix and strand types, also while the recall value was also high. Helix was predicted with 90% and strand with 70% precision in comparison to 80% and 53.9%, the best results with any of the other combinations of models and vocabularies. The prediction of coil using LSA and amino acid type was very poor. In this case, VSM using amino acids as vocabulary was best, most likely due to the highly predictive nature of proline for coil due to its disruptive nature for regular secondary structure.

6.2.1 Conclusions

While the average three-class precision (Q_3) was best using chemical groups as vocabulary and using VSM analysis, classification accuracy in individual classes was not the best with this model. Helices and sheets were best classified using LSA with amino acid types as vocabulary, with 90% and 70% precision, 70% and 50% recall. Coils are characterized with higher precision using amino acids as vocabulary and VSM for analysis.

The results demonstrate that VSM and LSA capture sequence preferences in structural types. Protein sequences represented in terms of chemical groups and amino acid types provide more clues on structure than the classically used amino acids as functional building blocks. Significantly, comparing results within the same analysis model (VSM or LSA), the precision in classifying helix and strand increases when going from amino acids to

chemical groups or amino acid types for unseen data. Furthermore, it does not show a corresponding drop in recall. This result suggests that different alphabets differ in the amount of information they carry for a specific prediction task within a given prediction method.

6.3 Transmembrane helix prediction

6.3.1 Features to characterize transmembrane segments

Results presented in previous chapters have shown that the application of a biology-language analogy is suitable to infer protein structural characteristics: n-grams, latent semantic analysis and alternate vocabulary representation can distinguish the nuances of sequence characteristics between secondary structure elements. Here, we applied these methods to identify useful features that can distinguish transmembrane (TM) segments from non-transmembrane segments and to distinguish membrane and globular proteins.

Three different approaches were taken:

1. Propensities of amino acids in TM segments have been studied earlier (Section 3.2). Here we investigated if the propensities of *pairs* of amino acids vary between TM and non TM segments? This addresses the question if there is a positional preference of one amino acid with respect to another within the TM segment which is different when the pair is present in a nonmembrane segment. The results are presented in Section 6.3.2 below.
2. It is known that it is not only hydrophobicity but also aromaticity and charge properties that are different between TM and non TM helices. Is it useful to represent the primary sequence of protein with a reduced vocabulary that accounts for the similarities between amino acids? This question is addressed in Section 6.3.3.
3. In Section 6.3.4 we describe the ability of signal processing methods such as time-to-frequency transforms to extract features specific to membrane helices and non-membrane segments.

6.3.2 Comparison of soluble and transmembrane proteins

It is known that buried helices in globular proteins and transmembrane helices in multi-spanning or multimeric membrane proteins are amphipathic, where one of the helix is hydrophobic and while the opposite face is hydrophilic. In order to study this amphipathic property quantitatively, we analyzed the positional preferences of amino acid pairs with respect to each other, using Yule's q-statistic. See Section 1.3.2 for introduction. This measure is commonly used in natural language processing to quantify word preferences on each other as a measure of coherence of text [35].

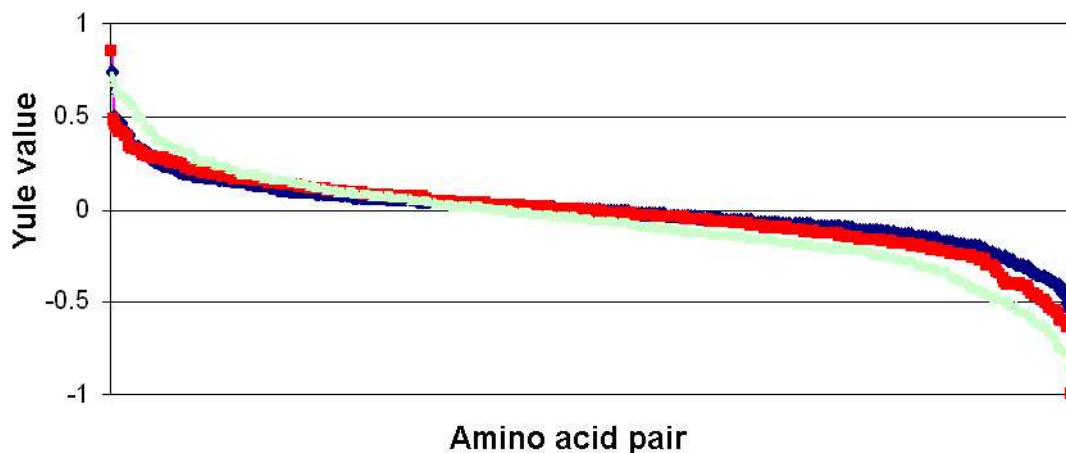


Figure 6.9: Yule values in soluble and transmembrane helices

Comparison of transmembrane (blue), soluble (red) and GPCR (green) helices.

In analogy to using Yule's q -statistic to quantify the preference of two words to appear in each other's neighborhood in texts, the biological language modeling toolkit extends this concept to be applied to biological sequences (Section 4.1.2). We computed Yule value associations between amino acid pairs in helices of transmembrane and non transmembrane types using the BLM toolkit.

In a regular helical arrangement a given helical residue is a direct neighbor of its 3rd and 4th residues because the period of a helix is 3.6 residues [142]. The i_{th} residue has $(i + 4)_{th}$ residue on the same face of the helix, while $(i + 1)_{th}$, $(i + 2)_{nd}$ and $(i + 3)_{rd}$ residues are on different faces of the helix. In the study of amphipathicity of a helix, it is more meaningful to restrict the allowed distance between the two amino acids, or *words*. We studied amino acid preferences for distances of 0, 1, 2 and 3 between them. In other words, for every pair of amino acids x and y , Yule values are computed separately for occurrences of xy , $x * y$, $x ** y$ and $x *** y$, where $*$ is any amino acid. Since the above described period of a helix is 3.6 residues, there is no need to study Yule values for larger distances separating amino acids, because the residues are no longer close in 3-dimensional space.

Yule values are computed separately for datasets of transmembrane helices and soluble helices. The description of datasets is given in Section 5.1.3.

Yule values differ for soluble and TM helices: We found that the preferences of neighboring amino acids are distinct for soluble and transmembrane helices (Figure 6.9). Furthermore, the preferences become even stronger when the transmembrane helical data is restricted to a specific family, such as G-protein coupled receptors (GPCR). The Yule values for the 20x20 pairs of amino acids separated by a distance of 2 residues ($x ** y$) are shown in Figure 6.9 for the datasets of soluble helices, transmembrane helices and

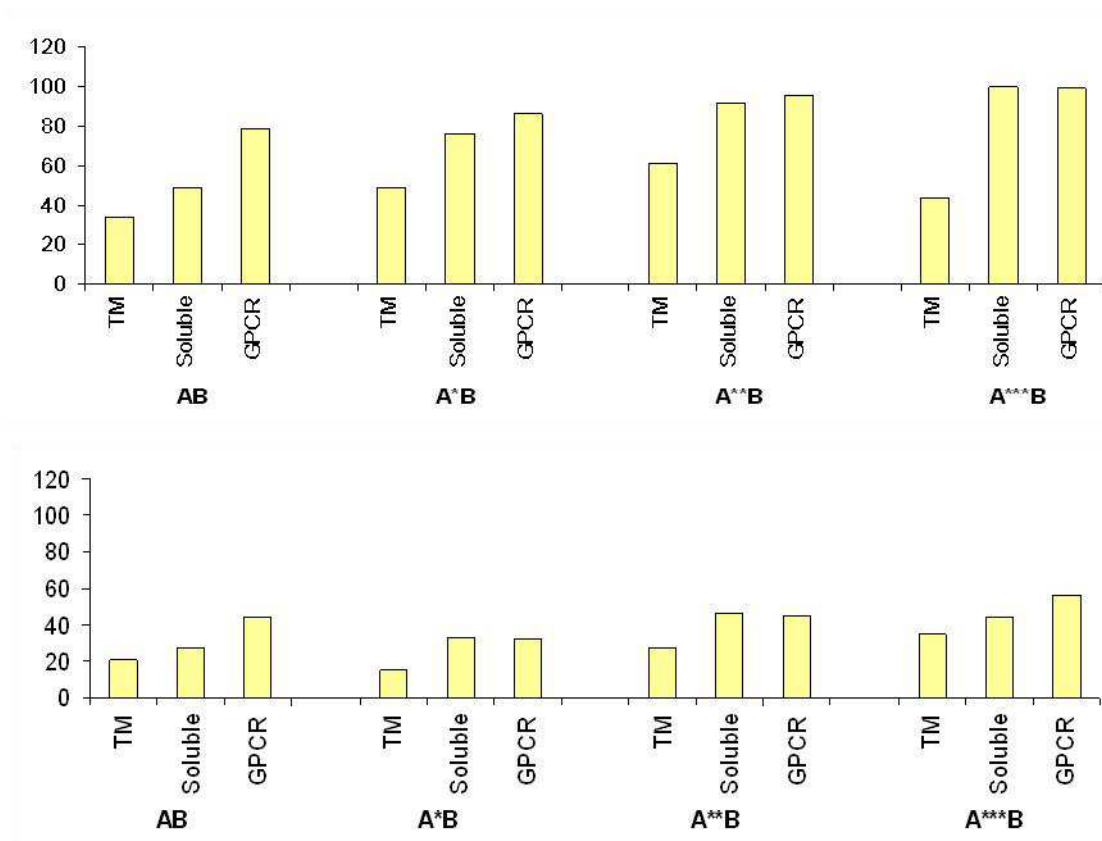


Figure 6.10: Fraction of amino acid pairs possessing strong preferences with each other

(A) Top panel shows the fraction of amino acid pairs that have Yule values < -0.25 , meaning that these pairs rarely occur with each other. (B) Bottom panel shows fraction of amino acid pairs with Yule value > 0.25 , meaning that these pairs show a tendency to occur with each other at different distances labeled on the x-axis. The dataset type, and the distance between the two residues in the amino acid pair are marked on the x-axis.

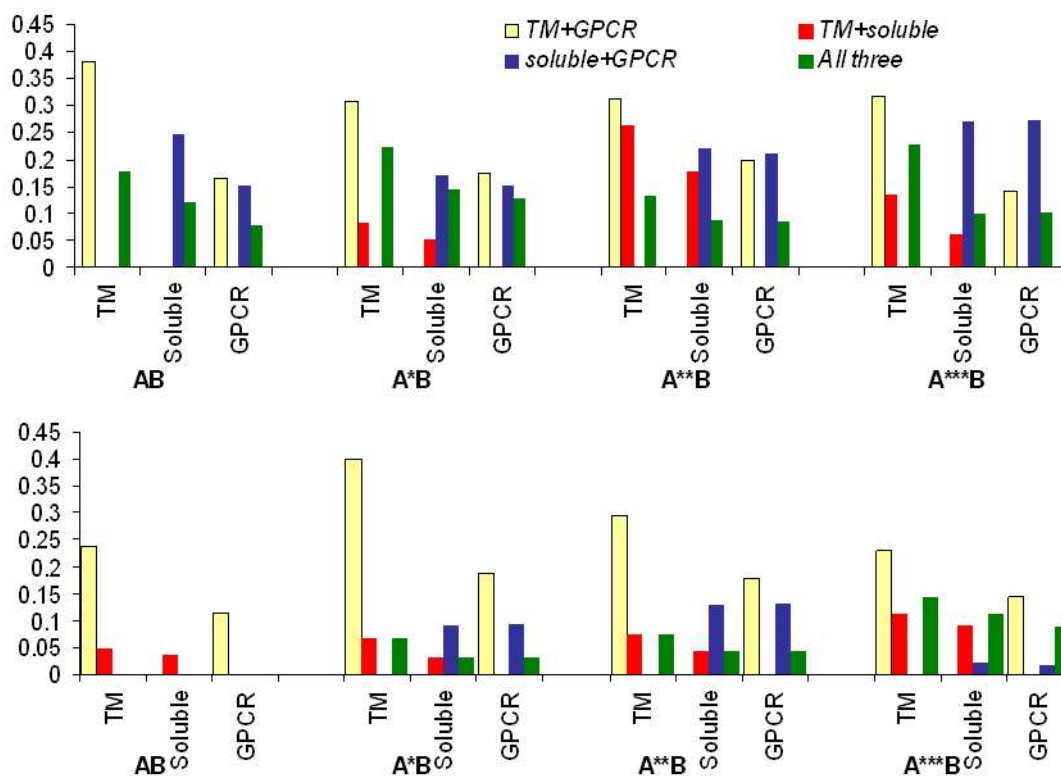


Figure 6.11: Fraction of amino acid pairs possessing similar Yule values in soluble and transmembrane datasets

Overlap between the helices datasets. For each highly over- or under-represented pair from Figure 6.10, the degree of overlap between transmembrane and GPCR helices (yellow), between transmembrane and soluble helices (red) between soluble and GPCR helices (orange) and between all three datasets (green) are indicated.

GPCR helices. Each of the three plots shows the Yule values in descending order from the highest value for that dataset, therefore the x-axis is not the same for each of the plots in the graph. For a random distribution of amino acids the Yule values would be expected to be 0. The figure demonstrates how strong the preferences are in each of the datasets and shows that the total number of residues showing non-random preferences (non zero Yule values) is similarly high between soluble and transmembrane helices, and highest for GPCR helices.

To analyze whether the Yule values deviating most from 0 are for the same or different specific pairs in the three datasets, we analyzed what fraction of the 20x20 pairs show a strong positive or negative preference. Figure 6.10 shows for each dataset and for a given distance, what fraction of the amino acid pairs have a Yule value lesser than -0.25 (top panel in figure) and greater than 0.25 (bottom panel). The most striking observation from this figure is that all datasets rule out a larger number of amino acid pairs (negative Yule value); the number of pairs for which they show positive preference is a smaller fraction.

Next, we compared how many amino acid pairs show the same preference in these different datasets. Pairs corresponding to each of the bars in Figure 6.10 are taken, and checked whether they belong to the same bar in a different dataset. As an example, consider Figure 6.10A AB transmembrane < -0.25 . About 30% of the total pairs belong to this categories in the transmembrane dataset. Of these, the pairs that also belong to the category AB soluble < -0.25 are counted, and shown as a percentage in Figure 6.11 with a red bar. Similarly those that also occur in AB GPCR < -0.25 are shown with a yellow bar. This comparison is repeated for each of the categories in Figure 6.10 and shown in Figure 6.11. This figure shows that the preferred pairs of amino acids are distinct between soluble and membrane helices. The preferences become stronger when the analysis is restricted to a specific family of proteins, because the transmembrane domains are likely to be conserved for a given family.

Amphipathic nature found in TM helices: While the objective of determining soluble and TM helix differences is met with this analysis, it also results in an additional observation that is likely to prove useful towards the broad goal of this work: amino acid pairs show different distributions for different distances separating them; that is, the pair $X*Y$ may be more likely to occur in a transmembrane helix than the pair $X***Y$ where X and Y are any two specific amino acids. Given that it takes 3.6 residues to complete a full circle in a helix, this means that X and Y are less likely to be on the same face of the helix but are more likely to appear on opposite faces (or the other way round).

Observed differences between Yule values representing amino acid neighbor preferences in soluble and transmembrane helices are highly encouraging. In particular, the preferences strongly depend on the distance separating the two amino acids in a pair. If these preferences were not there, a simple amino acid propensity scale that distinguishes between soluble and membrane helices [104, 143] would be sufficient. This is not the case as is seen from left to right in each pane in Figures 6.10 and 6.10. Amino acid neighboring preferences vary with the distance of separation between the amino acids.

6.3.3 Alternate vocabulary representation of primary sequence

In most of the work to study protein structure, the primary sequence is represented as a chain of amino acids. However, because of the common chemical groups between the side chains of different amino acids, there is an overlap in their properties, as described in Section 2.1. The natural language processing analogy of this overlap of properties is that different words can have the same meaning. Natural language processing techniques also have to address the problem of having multiple words with the same meaning, which is analogous to an n-mer of amino acids occurring with different structural conformations in proteins [144, 145]. We developed three approaches to study alternate vocabularies in analysis of membrane helices.

6.3.3.1 Rule based decision on windowed property features

To study the amino acids occurring in TM segments in terms of their properties, a method of visual analysis are described in Section 4.3.2, was developed. Inspection of the output for different membrane proteins led to the observations that most of the TM segments follow simple rules of distribution of types of amino acids. For example,

1. **There is rarely a positive charge in a TM segment.**
2. **There are large number of aromatic residues in TM segments.** Specifically, in each window of 15 residue, there are at least 6 aliphatic residues.

Applying only Rule 1 above wrongly predicts many soluble regions (possibly buried soluble regions or signal peptides) as transmembrane. However adding the additional Rule 2 filters the soluble segments, and improves the accuracy. A hierarchical analysis of this kind was adopted for predicting TM helices, and tested on benchmark data. The set of rules that have been compiled are given in Section 4.3.2.

Benchmark analysis. Chen et al [111] developed a benchmark server to allow performance comparison of different TM prediction algorithms. The results obtained with the rule based (RB) decision system on a high resolution dataset, are shown in Table 6.8, ordered by segment precision, in comparison to other published methods on this dataset. Although the metrics of evaluation adopted by us and that in the Chen et al paper [111] is the same, the quantitative results of various methods did not match. Using the prediction labels for different methods given by Chen et al, we recomputed the accuracies with our program, so that the results are directly comparable. The metrics of evaluation are described in Chapter 5. Rule based methods are shown with bold labels **RBn**, where **n** corresponds to a different rule listed in Section 4.3.2.

The parameters of the analysis of this approach are not over-specific to the sequence characteristics of the dataset. It may be seen from the tables that this method ranks highest among the simple methods (that is, those that use only hydrophobicity scale and not advanced statistical modeling). The key advantage of using this system is that the

Method	Q_{ok}	F-score	Q_{htm}^{obs}	Q_{htm}^{pred}	Q_2	Q_{2T}^{obs}	Q_{2T}^{pred}	Q_{2N}^{obs}	Q_{2N}^{pred}
hmmtop	86	94	95	94	80	72	86	90	78
DT	72	94	96	92	73	62	80	81	66
tmhmm	78	92	91	94	80	72	88	91	79
sosui	75	91	93	90	75	72	81	85	77
das	75	91	93	90	72	46	94	97	67
toppred2	83	91	87	96	77	63	87	92	74
LSA+RB2	61	89	83	96	76	66	80	85	74
predtmr	58	88	83	94	76	60	90	94	73
ww	67	86	85	87	72	75	73	75	77
ben-tal	58	86	75	98	72	50	90	95	68
ges	75	85	89	82	71	78	68	67	77
prabhakaran	75	85	89	82	71	77	68	67	77
LSA	70	85	85	85	72	52	84	91	68
RB4	39	80	68	93	70	55	77	85	67
RB3	42	79	71	89	70	57	73	82	68
eisenberg	67	75	78	73	69	81	63	57	77
RB2	25	73	55	96	67	40	79	90	62
kd	64	72	76	69	67	83	58	46	75
RB1	28	71	57	89	66	43	74	86	62
ges-simple	72	71	87	58	74	72	77	81	76
hopp-woods	64	68	72	65	62	84	55	37	72
levitt	61	67	72	63	59	85	52	31	69
a-c	64	66	72	61	58	83	53	33	68
av-cid	64	66	72	61	60	85	53	33	72
sweet	61	66	70	62	63	85	54	36	73
nakashima	58	65	68	63	60	87	53	30	72
radzicka	64	65	70	61	56	87	50	23	66
vh	64	64	69	59	61	87	53	29	72
fauchere	58	64	69	59	56	86	50	23	65
wolfenden	28	63	41	98	62	28	90	97	60
roseman	58	63	68	58	58	86	51	27	68
lawson	56	60	63	57	55	84	49	21	59
bull-breese	58	60	63	57	55	87	49	20	63
em	58	58	64	53	57	87	50	23	67
kd-simple	58	54	78	38	74	85	66	61	82

Table 6.8: Transmembrane structure prediction on high-resolution dataset

Results of TM helix prediction on high resolution data set (ordered descending by segment F-score). The results are provided by the benchmark server [135] (results of other methods reproduced by permission of Oxford University Press). RB1, RB2, RB3 and RB4 are the four rules given in Section 4.3.2. See Section 5.2.2 for details on metrics.

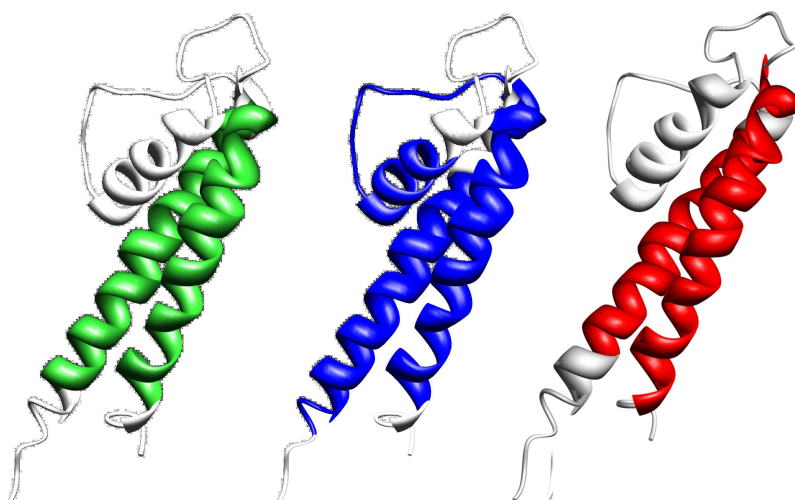


Figure 6.12: Comparison of TM prediction by rule based decision method and TMHMMv2.0

Ion channel protein K⁺csA (PDB: 1BL8). Actual TM locations (green), TM prediction by TMHMM v2.0 [117] (blue) and TM prediction by RB framework (red), and are shown.

precision of prediction of TM segments is very high, and the boundaries of prediction are very close to the observed boundaries.

The precision of TM segment location is very high with the rule-based decision system. A distinct advantage of this method is that the analysis provides an insight into the characteristics of the TM segments, without information being lost in the statistics of numerical scales. The general rules that TM segments follow, and deviations and their characteristics are visible, which might prove useful in further analysis on helix interactions or segment displacements with respect to the membrane. The drawback of this method is that it does not recognize all of the TM segments. A hierarchical decision system may however be used to yield better results with different levels of confidence. See next section for how this method may be used in conjunction with other methods.

The errors in the prediction by simple expert created rules are of two types, commonly referred to as *false positives* and *misses* or *false negatives*. Complex hierarchical rule based decision system is to be studied with the following knowledge of the distribution of amino acids:

1. **Separate potentially single spanning membrane proteins from multispanning membrane proteins (using relaxed rules).** For single spanning helices, the rules are likely to be different. For example, aromatic residues face the buried core in the middle segment of TM helices; in single spanning helices since buried core may not be present,¹ rules would be different for these helices from those in

¹Buried core may also be present in multimeric single spanning proteins

	Data	Q_{ok}	Segment F-score	Segment Recall Q_{htm}^{obs}	Segment Precision Q_{htm}^{pred}	Q_2	# of TM proteins misclassified as soluble proteins
1	MPtopo	53	86	91	81	79	6
2	PDB_TM						
3	High res	72	94	96	92	73	0

Table 6.9: Transmembrane structure prediction with decision trees

See Section 5.2.2 for details on metrics.

multispanning proteins. This would aid in recovering some of the misses (false-negatives).

2. **Compare aromatic moment of the TM helices.** Aromatic residues normally do not lie on all faces of the TM helix— they occur on the buried face only in the middle of a segment and on the outer face in each edge of a segment. A lack of aromatic moment in all subsegments in the helix, inspite of possessing many aromatic residues (which happens when the aromatic residues are evenly distributed on all sides) would indicate that the predicted TM segment is in fact a false-positive.

6.3.3.2 Decision trees

In order to capture rules that encompass all the different types of TM segments from the latest data sets, we compiled a decision tree as described in Section 4.3.4. However, for evaluation purposes, in order to not overtrain the decision tree, the training data set used is the same as for other methods and that used to train TMHMM, namely the set of 160 proteins 5.1.4. The results obtained on the benchmark server are shown in Table 6.8, in the row marked DT. The performance is far superior compared to all of the rule based methods. It is also superior compared to most other methods, with a segment F-score as high as 94%. Results obtained upon evaluation of other larger data sets with decision trees are shown in Table 6.9.

6.3.3.3 Latent semantic analysis for transmembrane structure

As described earlier in Section 1.3.3, LSA extracts the relations between different documents (here, protein segments) based on the distribution of words in the documents. Additional information on similarity of the amino acids is explicitly provided by representing amino acids in a reduced alphabet of their properties. Protein segments in moving windows of 15-residues are analyzed at a time, treating each segment as a document. Documents with known TM structure (completely TM, completely nTM or mixed) are used as reference in classifying segments of proteins with unknown TM structure. K-nearest

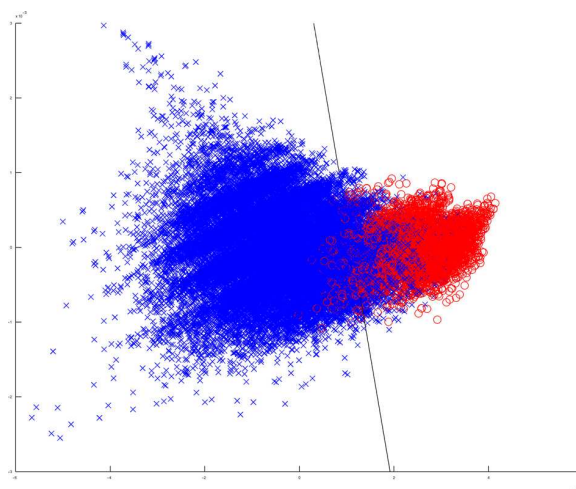


Figure 6.13: Classification of protein feature vectors of the completely-membrane or completely-nonmembrane type

Figure shows the data points of the training set, and linear classifier learnt from this data. The first two dimensions of the features after principal component analysis are shown in the scattergram. It may be seen that even a simple linear classifier can separate out a large fraction of the data points into the correct class.

neighbour classification is used for the classification of test documents with reference documents. The details of implementation are given in Section 4.3.3. First, we estimated the separability of the feature vectors derived from latent semantic reduction of amino acid property features. Figure 6.13 shows a scattergram of the first two dimensions against each other of features derived with window size 16. Data corresponding to completely non-TM type are shown with a blue '+' marker and those corresponding to completely TM type are shown with a red 'o' marker. A linear classifier learnt using Fischer's discriminant over these data points is also shown (black line). It can be seen qualitatively that although there is a region of confusability, a large number of data of either class fall in the non-confused region. We can use the linear classifier to estimate the separability of the feature sets. Of the feature vectors originating from completely-TM or completely non-TM windows of the training data, only 7% are misclassified. When all the feature vectors of the training set including those with mixed label are classified, only 15% of the features are misclassified, indicating that there is a good separability of the TM features from non-TM features. In TMpro, we used a neural network to learn the boundary between these feature vectors. When a smaller window size of only 6 residues is used, features corresponding to TM and non-TM are not separable with a boundary. We therefore used a hidden Markov model that can capture gradual variation in the features along the sequence. The TMpro feature vectors combined with the linear classifier, the HMM and the NN classifier, will be referred to in the following as TMpro LC, TMpro HMM and TMpro NN, respectively.

From the previous results of rule-based system in Table 6.8, it is seen that there are TM segments that show exceptions in their distribution of amino acids. There are occasionally charged residues in the TM segments. The LSA framework clearly accounts for complex relations in the distribution of amino acid properties that are not obvious from an independent representation in terms of these properties.

Accuracies of TM prediction obtained with LSA framework analysis are shown in Table 6.8. The added advantage of LSA over rule based method may be seen clearly from the improvement in Q_2 accuracy. The improvement is primarily by the inclusion of more TM segments (see increase in segment recall Q_{htm}^{obs}) in the prediction; there is a large increase in Q_{ok} , which is the percentage of proteins in which all predicted helices and observed helices match one to one ($Q_{htm}^{obs} = Q_{htm}^{pred} = 100\%$). this can also be seen by a large increase in columns Q_{ok} besides Q_{obs} and Q_2 . There is a corresponding increase in the segment recall (Q_{htm}^{obs}) as well.

6.3.4 Wavelet signal processing

Finally, we investigated wavelet transforms applied to binary representation of the sequence based on its **polarity** signal to locate transmembrane segment locations. It is expected that the amphipathicity nature of TM or soluble helices will be observed by comparing the wavelet coefficients at different scales of analysis.

The details of implementation are given described in Section 4.3.1.

Wavelet coefficients computed for the protein sequence of *rhodopsin* are shown as a two-dimensional image in Figure 6.14. The dimension along the horizontal axis in the image corresponds to the position of the residue in the protein. The vertical dimension corresponds to the different scales at which wavelet coefficients are computed. It can be seen that the visible patterns in the wavelet coefficients correspond to the actual locations of the TM segments. The coefficients computed at a scale of 10 are mapped onto the three dimensional structure of the protein, to clearly show how the features correspond to the actual TM locations of the protein. In preliminary analysis (using a very simple hidden Markov model architecture on a set of 83 proteins (see Chapter 5), a Q_2 accuracy of 80% was achieved.

6.3.4.1 Conclusions

While the analysis here is only preliminary at this stage, the close correspondence of the features to the actual TM locations suggests that the analysis would make a contribution towards the final goal of transmembrane segment prediction and characterization. The analysis would benefit from a choice of wavelet analyzing functions, perhaps Haar and Debauches wavelet functions that are popularly used in edge detection applications. Currently only the left half of the wavelet coefficients is analyzed. Analysis with complete wavelet packets is yet to be made that capture high frequency components in the signal.

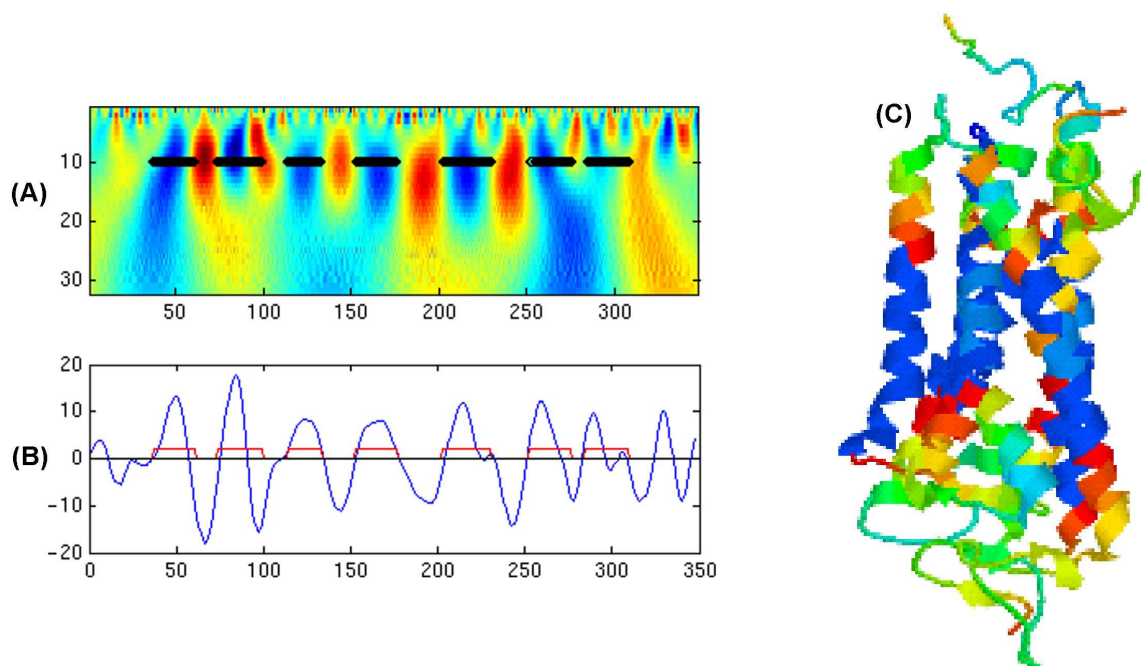


Figure 6.14: Wavelet coefficients computed for the protein sequence of *rhodopsin*

(A) Two-dimensional image of wavelet coefficients: The dimension along the horizontal axis in the image corresponds to the position of the residue in the protein. The vertical dimension corresponds to the different scales at which wavelet coefficients are computed. (B) Wavelet coefficients at scale 10 are plotted along y-axis, against the positions of the residues of the protein along x-axis. Locations of observed TM helices are shown in red. (C) The coefficients computed at a scale of 10 are mapped onto the three dimensional structure of the protein, clearly showing how the patterns in wavelet coefficients correspond to the actual TM locations of the protein. Note that the color coding in the two images are automatically generated by MATLAB and PDB-viewer programs and are different from each other.

Chapter 7

TMpro: High-Accuracy Algorithm for Transmembrane Helix Prediction

In this chapter we apply the biological feature extraction methods described in previous chapter (Chapter 6) towards the objective of high-accuracy transmembrane (TM) helix prediction. An algorithm for TM helix prediction referred to as TMpro has been developed by this approach. The workflow of the algorithm, evaluations and enhancements are presented in this chapter.

7.1 TMpro

Background. All of the previous methods in TM helix prediction conformed to two methods, that of using mean hydrophobicity in a segment or modeling statistical propensities of amino acids in each location along the TM segment. The drawback of the first approach is that the accuracy is low in predicting TM segments, and the confusion with soluble proteins is high (see Table 3.1). On the other hand, advanced methods with statistical modeling of amino acid propensities suffered from over training and restriction of permissible topologies. Typically there are at least several hundred parameters to be trained for these models. However, currently available training data is very small and does not contain representatives of all the possible membrane protein families, and not all the possible TM segment characteristics.

Amino acid propensities in TM segments correlate with not only hydrophobicity or polarity of the residue but also with its charge and aromaticity. However, instead of using this information to drive a single explicit scale of propensities that would represent an average over many TM segments and over the entire length of TM segments, we computed feature distributions in terms of these properties using latent semantic analysis (Section 6.3.3.3). This allows computing statistical models that can delineate the features derived from TM segments from those derived from non-TM segments using a classification boundary.

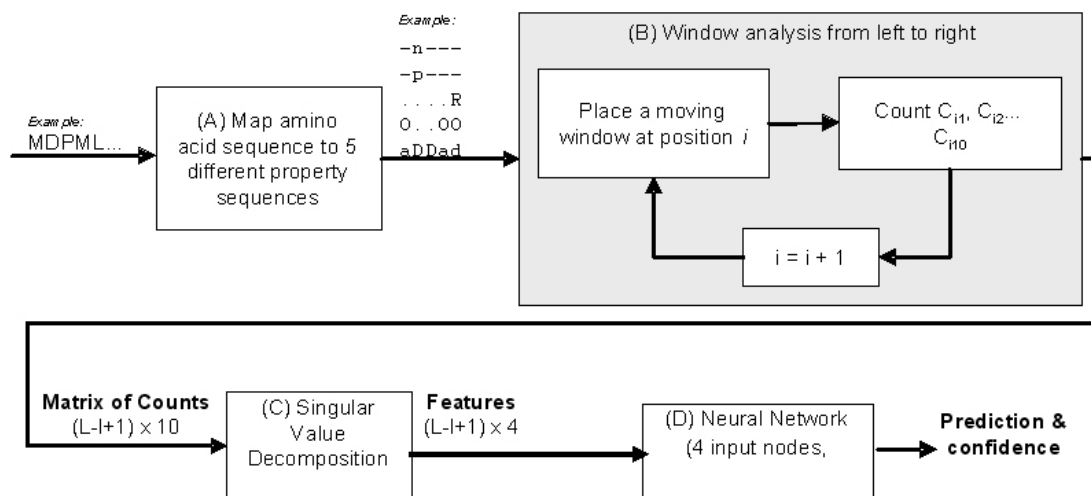


Figure 7.1: TMpro algorithm for TM helix prediction

Primary sequence of protein (amino acid sequence) is input to the system. (A) maps it to 5 amino acid property sequences. The output has size $5 \times L$ (rows x columns) where L is the length of the protein sequence. These 5 sequences form input to (B) which performs window analysis, and outputs a matrix of counts of 10 properties (C_1 to C_{10}) for each window position. This output has the size $10 \times L-l+1$, where l is the length of the window. The outputs from (B) for all proteins are collected together and singular value decomposition is performed by C. During testing phase, as SVD approximation is performed for the matrix of a single test protein. The output of this block (C) forms the final features used by the Neural Network (NN). Features are evaluated by the NN model (D) and the output is generated. The model outputs an analog output ranging from -1 to 1 that indicates the closeness of the feature to non-TM or to TM. This analog value is thresholded to get a 2-state prediction for each residue (TM, non-TM).

Algorithm. The algorithm TMpro is described below, a block diagram is shown in Figure 7.1 and the implementation details are given in Section 4.3.3. The steps are as follows:

1. The primary sequence, which is originally in terms of the 20 amino acids, is decomposed into five different primary sequences, each one representing one property of the amino acids, namely polarity, charge, aromaticity, size and electronic property.
2. These property label sequences are then studied in a moving window.
3. The feature space is reduced by singular value decomposition.
4. As opposed to a simple threshold yielding a linear boundary between TM and non-TM features, an advanced statistical model is used to separate the features in the two classes by a nonlinear boundary. A neural network (NN) is used to classify the reduced dimension features as TM and non-TM, while a hidden Markov model

7. TMpro: High-Accuracy Algorithm for Transmembrane Helix Prediction 99

(HMM) is built independently to capture the sequential nature of TM and non-TM features. The HMM architecture used here is a simpler one and therefore less restrictive compared to the models of TMHMM or HMMTOP [117].

5. The prediction labels output by NN and HMM are arrived at independently; where they disagree, a final judgment may be done manually with the aid of the analog output of NN.

Discussion Figure 6.13 in page of the previous chapter shows the distribution (only top 2 dimensions) of the LSA features for TM and non-TM segments. With a simple linear classifier, we obtained high accuracy as shown in Table 7.1.

To improve the accuracy, two options were considered: neural networks (NN) and hidden Markov models (HMM). HMMs are better suited to capture the sequential nature of the topology, namely that it transitions from non-TM to TM with varying lengths in each state. However, if the architecture of the model is made too flexible (in order to not restrict permissible topologies), HMM may not function as the best possible model. In order to test this, we modeled a HMM with a simpler architecture (compared to those found in literature such as TMHMM or HMMTOP), as described in Section 4.3.3. A smaller window size of 6 residues was used to derive features that are modeled with HMMs.

Availability: <http://flan.blm.cs.cmu.edu/tmpro/> and <http://linzer.blm.cs.cmu.edu/tmpro/>. Details of the web interface features and usage are given in Appendix B.

Acknowledgement: The code development for the web based user interface was done by Christopher Jon Jursa.

7.1.1 Benchmark analysis of TMpro

In order to compare the performance of the three different implementations of TMpro to previous work we used the TMH benchmark web server for evaluations [111]. We trained our models with the same data set as had been used for training TMHMM, namely the set of 160 proteins. The data set used for evaluation is the set of 36 proteins (called high-resolution data set) from the bench-mark analysis paper [111], referred to as data set 1, below. We performed the evaluations by submitting the predictions on the benchmark evaluation server [135]. The predictions on alpha helical membrane proteins are evaluated by the following set of metrics [111]: Q_{ok} is the percentage of proteins whose membrane segments are all predicted correctly. Segment recall (Q_{htm}^{obs} on benchmark server) is the percentage of experimentally determined (or 'observed') segments that are predicted correctly. Segment precision (Q_{htm}^{pred} on benchmark server) is the percentage of predicted segments that are correct. The residue accuracy Q_2 refers to the percentage of residues

7. TMpro: High-Accuracy Algorithm for Transmembrane Helix Prediction 100

	Method	Q_{ok}	Segment F-score	Segment Recall Q_{htm}^{obs}	Segment Precision Q_{htm}^{pred}	Q_2	# of TM proteins misclassified as soluble proteins
1a	TMHMM	71	90	90	90	80	3
1b	TMpro LC	61	94	94	94	76	0
1c	TMpro HMM	66	95	97	92	77	0
1d	TMpro NN	83	96	95	96	75	0
1f	TMpro NN without SVD	69	94	95	93	73	0

Table 7.1: Transmembrane structure prediction on high-resolution dataset

(ordered by segment precision Q_{htm}^{pred}). See Section 5.2.2 for details on metrics.

that are predicted correctly. We also computed the F-score, which is the geometric mean of segment level recall and precision (Q_{htm}^{obs} and Q_{htm}^{pred}). Recall and precision can each be increased arbitrarily at the expense of the other value, the two metrics when seen independently do not reflect the strength of the algorithm. The geometric mean of the two, (effectively the point where the two measures are expected to be equal) is used as the metric.

The evaluation of TMpro (LC), TMpro (HMM) and TMpro (NN) by the benchmark server (on data set 1) is shown in Table 7.1, in comparison to that of TMHMM [111]. All three implementations of TMpro show improvements over TMHMM results. Even the simple linear classifier yields a 4% increase in the F-score, with an “even increase” in both the segment recall and precision. The HMM model improves the Q_{ok} compared to the linear classifier. While the F-score remains the same, there is an imbalance between recall and precision. Although Q_{ok} in both TMpro (LC) and TMpro (HMM) is lower than in TMHMM, the segment level accuracies are improved in both these methods. TMpro (NN) shows the highest improvement in Q_{ok} . The results obtained with the NN method yield a Q_{ok} of 83% (a 12% increase over TMHMM). A high value of Q_{ok} , which is the most stringent metric at the segment level, indicates that the TMpro NN achieves very good prediction of TM helices. This value of Q_{ok} is higher than those achieved by any of the methods that have been evaluated by [111] excepting HMMTOP (which uses the entire test set proteins in training, as opposed to only 3 proteins of >95% similarity used in training TMpro and TMHMM), and PHDpsihtm08 [146] which uses evolutionary information and a complex model with hundreds of model parameters. The segment F-score reaches 95% with an even balance between segment recall and precision. This segment accuracy represents a 50% reduction in error rate as compared to TMHMM, which is the best method not using evolutionary information evaluated in the benchmark analysis [111]. In other words, 10% of errors in the segments missed or over-predicted by TMHMM, half of those difficult segments are correctly predicted by TMpro. TMHMM

7. TMpro: High-Accuracy Algorithm for Transmembrane Helix Prediction 101

	Method	Q_{ok}	Segment F-score	Segment Recall Q_{htm}^{obs}	Segment Precision Q_{htm}^{pred}	Q_2	# of TM proteins misclassified as soluble proteins
PDB_TM (191 proteins and 789 TM segments)							
2a	TMHMM	68	90	89	90	84	13
3b	SOSUI	60	87	86	87		14
2c	TMpro NN No SVD	57	93	93	93	81	2
2d	TMpro no SVD	57	91	93	90	81	
MPtopo (101 proteins and 443 TM segments)							
3a	TMHMM	66	91	89	94	84	5
3b	SOSUI	68	89	91	87	82	7
3c	TMpro NN	60	93	92	94	79	0

Table 7.2: Transmembrane structure prediction on recent and larger datasets
(ordered by segment precision Q_{htm}^{pred}). See Section 5.2.2 for details on metrics.

misclassifies 3 proteins as soluble proteins, in contrast to TMpro which does not misclassify any. The results of all the methods evaluated in benchmark are shown in Table 3.

7.1.2 Performance on recent data sets

The benchmark analysis described in the previous section is useful in comparing the TMpro method with other well accepted methods, but the evaluation data set does not include recently determined membrane protein structures. We therefore computed the accuracies achieved by the TMpro on two recent data sets, MPtopo and PDB_TM. In order to allow for a fair comparison with TMHMM, the training set was kept the same as that used for TMHMM 2.0, namely the set of 160 proteins. Since TMpro (NN) gave the best prediction results in the benchmark analysis, we only studied TMpro (NN) further. In this and the subsequent sections, we henceforth refer to TMpro (NN) as TMpro. In the evaluation of TMpro performance on more recent data, we also compared our predictions with two other algorithms that do not use evolutionary profile: SOSUI [110] and DAS-TMfilter [147, 148]. The results of the comparison between TMpro, TMHMM, SOSUI, DAS-TMfilter are shown in Table 7.2. As can be seen, TMpro achieves a 2-3% increase in segment F-score in comparison to TMHMM, 4-6% in comparison to SOSUI and 3-5% in comparison to DAS-TMfilter. Thus, we conclude that amino acid properties used in conjunction with latent semantic analysis and neural network classifier are highly predictive of TM segments on the two recent data sets.

7.1.3 Confusion with globular proteins

The benchmark server provides a set of 616 globular proteins also for evaluation. Classification of proteins into globular and membrane types is a problem fundamentally different from predicting the sequential positions of TM helices in membrane proteins. As a result, the use of TM helix prediction methods to differentiating between TM and non-TM proteins is an inappropriate use of these methods, but it is a useful exercise in estimating to what extent hydrophobic helices in soluble proteins are confused to be TM helices. We found that 14% of the globular proteins are confused to be that of membrane type by TMpro according to the analysis by the benchmark server. However, it is to be noted that all the methods that have lower confusion with globular proteins also miss many membrane proteins and wrongly classify them to be of globular type. TMpro misclassifies only 1 of the MPTopo proteins as soluble protein, whereas TMHMM and DAS-TMfilter misclassified 5 TM proteins and SOSUI misclassified 7 TM proteins as soluble proteins. In the PDB-TM set, TMpro misclassifies only 2 proteins as soluble proteins as compared to 13 proteins by TMHMM and 17 proteins by SOSUI and 10 proteins by DAS-TMfilter that were mis-classified (Table 7.2).

7.1.4 Error analysis

From the evaluations presented above it is clear that TMpro predicts some false positives and misses some true positives. In order to understand the cause for these errors, we made the following analyses:

Accuracy of TMpro on membrane proteins with varying number of TM segments: Figure 7.2 shows true positives, false positives and false negatives for 31 membrane proteins from the NR-TM data set. The proteins are arranged along the x-axis in descending order of number of observed TM segments. It may be seen that for proteins with fewer TM segments, TMpro is accurate in most cases. When there are more than 5 observed segments, TMpro fails to predict some of the observed segments. This however does not strongly affect the TMpro prediction accuracies, because the number of proteins with few TM segments in the current datasets is larger than those with many segments. To demonstrate this fact, we show the number of proteins as a function of TM segments in OPM dataset (see Section 5.1.4) in Figure 7.3. There is an exponential decrease as the number of membrane segments increases. The better performance of TMpro for proteins with fewer segments is complementary to that observed with TMHMM, which is more accurate for membrane proteins with larger number of TM segments but poorer for proteins with few TM segments.

Characteristics of predicted and observed segments in terms of amino acid properties: Next, we asked the question if the wrongly predicted segments violate the

7. TMpro: High-Accuracy Algorithm for Transmembrane Helix Prediction¹⁰³

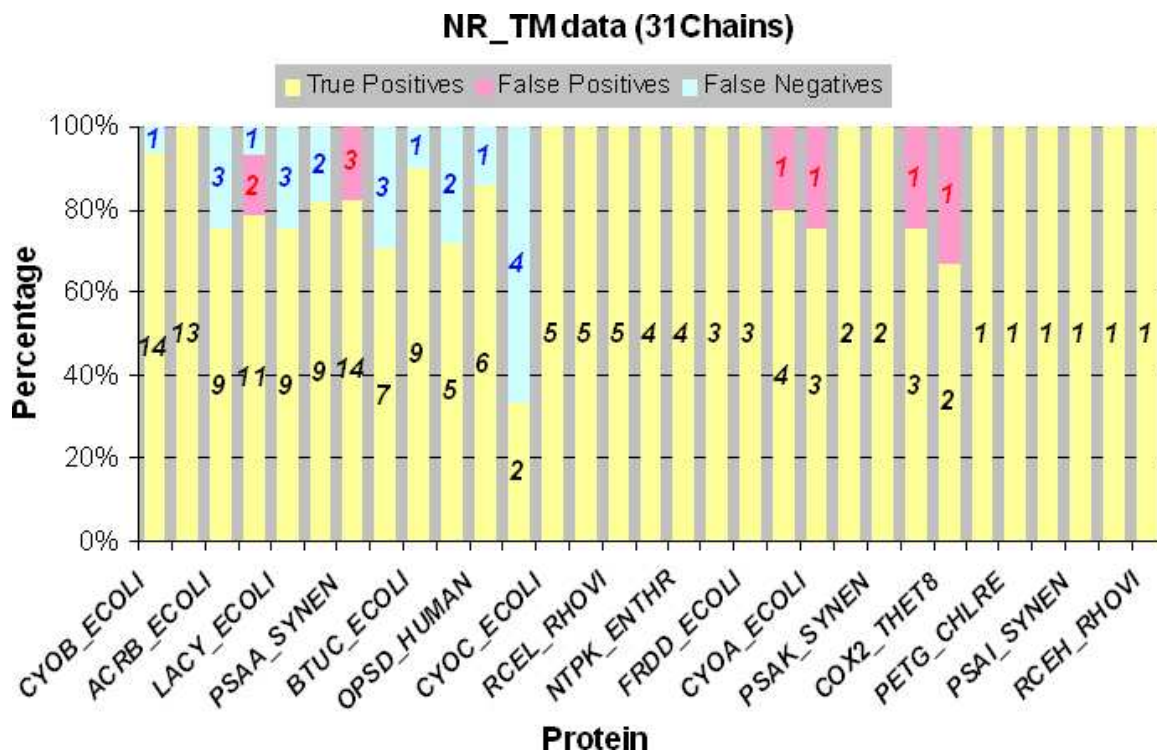


Figure 7.2: TMpro algorithm performance on a small representative data set of high resolution proteins

The data set is called NR_TM (See Section 5.1.4 for details). The 31 proteins of the data set are arranged along the x-axis, in descending order of the number of experimentally observed TM helices in the protein. For each protein, the number of (1) correctly predicted TM helices (yellow), (2) false-positives (pink) and (3) false-negatives (blue) are shown along y-axis. For each protein, the total number of true positives, false positives and false negatives has been normalized to 100%.

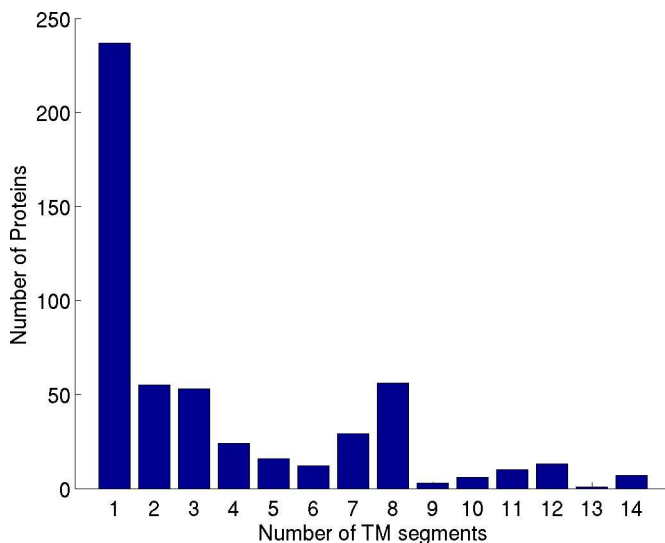


Figure 7.3: Number of proteins as a function of observed TM segments

Dataset shown is the OPM dataset with a total of 1869 TM segments in 522 proteins with PDB structures (see Section 5.1.4).

range of properties that would be observed in true segments. To this end, we analysed the distribution of amino acid properties in the observed and predicted segments.

For each of the properties, positive charge, negative charge, aromaticity and aliphaticity, we counted what percentage of the segments possessed the property. We compared this for all predicted segments in membrane and globular proteins, and observed segments in membrane proteins. The range of observed percentages are shown in figures in Appendix C. The range of properties exhibited by all wrongly and correctly predicted segments in membrane and globular proteins was within the same observed in the true segments. For example, the number of positive charges in true segments ranges from 0-6, while that in predicted segments in membrane proteins ranges from 0-5 and in globular proteins from 0-2. Thus, this error analysis does not provide avenues for error recovery.

Secondary structure characteristics of false positives from globular proteins:

PDB structures are available for the globular proteins analyzed. Figure 7.4 shows for each of the predicted segments, the fraction of each of the secondary structures in the segment. The segments are ordered ascending by helix content. As can be seen, only 15% of the segments (towards far right) contain more than 90% helix. Examples of predicted segments with each of the different constitutions of secondary structure content (namely fully helix, fully sheet, fully coil, mixed) are shown mapped onto 3D structures in Figure 7.5.

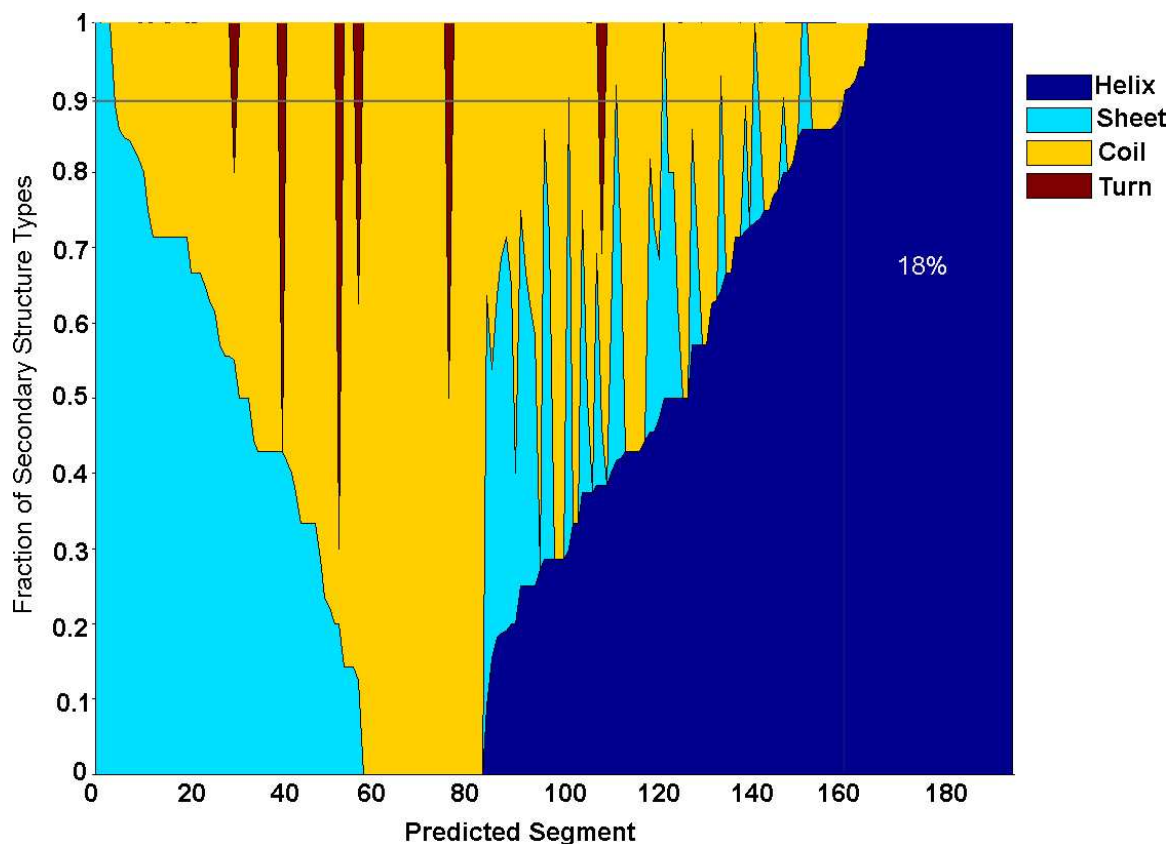


Figure 7.4: Secondary structure content in wrongly predicted segments by TMpro in globular proteins

For all the segments wrongly predicted by TMpro in globular proteins, the secondary structure content is computed from their PDB structures. X-axis shows the predicted segments. Y-axis shows the fraction of each of the secondary structure types, namely, helix, sheet and turn and coil. The color coding is shown in the legend. The segments are arranged in ascending order of their helix content.

7.1.5 Error recovery

Errors exhibited by TMpro are primarily in two cases: false positives in globular proteins and false-negatives in membrane proteins. The following procedures have been found to help in recovering from these errors.

Threshold on minimum fraction of helix secondary structure content: Based on the analysis of Figure 7.4, it has been found that setting a constraint that at least 90% of the segment is required to be a helix, has eliminated 82% of the wrongly predicted segments from globular proteins, and 95% of the soluble proteins are correctly identified as non-membrane proteins. Even for a less stringent constraint that 80% of the segment only is required to be helix, 93% of the soluble proteins are correctly classified.

Of course, the secondary structure information is not always available in practice.

7. TMpro: High-Accuracy Algorithm for Transmembrane Helix Prediction 106

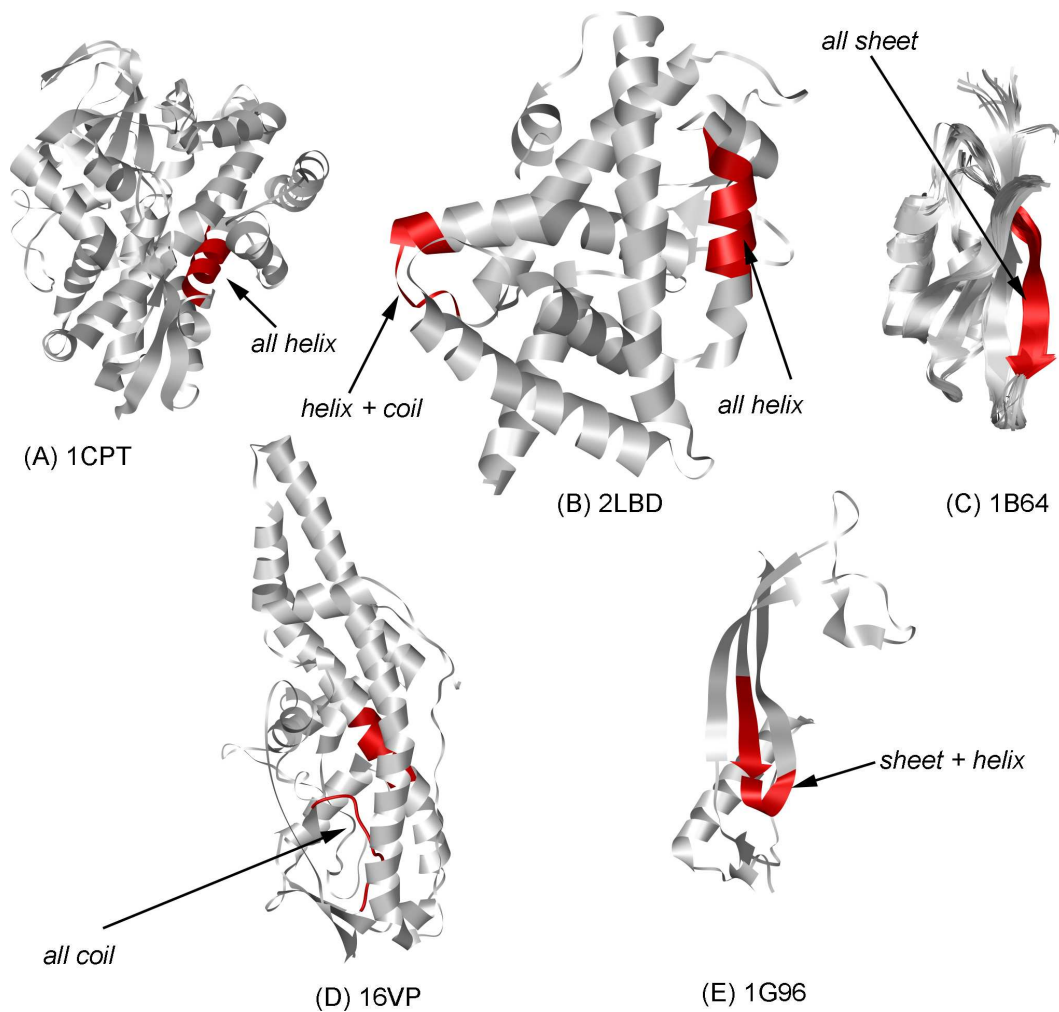


Figure 7.5: TM segments wrongly predicted by TMpro in globular proteins
Erroneously predicted segments are shown in red.

However, use of secondary structure prediction algorithms may be seen as an avenue to improve recovery from false positive globular proteins.

Merge predictions of TMpro and TMHMM: It has been found from error analysis that TMpro predicts well for the predominant class of membrane proteins, namely those with 1-6 observed TM segments. Complementary to this, TMHMM predicts well for membrane proteins with larger number of observed TM segments. In order to benefit from these two methods, we merged their predictions in this manner: If a segment that is predicted by TMHMM is completely missed by TMpro, then include that segment.

Results of merged predictions are shown in Table 7.3. It can be seen that results are superior to those by either of the two methods individually.

7. TMpro: High-Accuracy Algorithm for Transmembrane Helix Prediction¹⁰⁷

	Method	Q_{ok}	Segment F-score	Segment Recall Q_{htm}^{obs}	Segment Precision Q_{htm}^{pred}	Q_2	# of TM proteins misclassified as soluble proteins
PDB_TM (191 proteins and 789 TM segments)							
1a	TMpro	57	93	93	93	81	2
1b	TMHMM	68	90	89	90	84	13
1c	Merge	69	95	97	993	84	2
MPtopo (101 proteins and 443 TM segments)							
2a	TMpro	59	93	92	94	79	0
2b	TMHMM	66	92	89	94	84	5
2c	Merge	64	95	95	94	84	0
OPM (522 proteins and 1869 TM segments)							
3a	TMpro	55	87	85	88	81	6
3b	TMHMM	62	87	86	88	80	40
3c	Merge	65	92	93	92	80	1
NR_TM (96 proteins and 328 TM segments)							
4a	TMpro	65	94	92	96	82	0
4b	TMHMM	65	89	88	91	83	7
4c	Merge	70	95	95	95	83	0

Table 7.3: Prediction accuracies of merged predictions of TMpro and TMHMM
See Section 5.2.2 for details on metrics.

7.2 Web server

TMpro can be accessed through a traditional web interface where a user can submit one or up to 2000 protein sequences at a time and obtain the prediction of TM segments. The basic TM prediction tool does not require any software other than a web browser. To view the results with a user-interactive chart, Java Run Time Environment (JRE) is required to be present on the user's computer. JRE can be downloaded from www.java.com.

The predictions can be viewed with a user-interactive chart that is generated as a Java Applet or in a standardized TMpro format. The user-interactive chart allows visualizing the positions of the predicted TM segments along the primary sequence. If a SWISSPROT or PDB id is submitted for prediction, the "feature" or "secondary structure" information from these sources respectively is extracted automatically and is shown on the chart. Any number of sequence annotations provided by the user can be added to the plot. Information is appended to the TMpro standard format file and the applet regenerates the chart marking these values on the plot every time a new input is provided (Figure B.3). This feature allows integration of information from diverse sources by visually combining it in a chart for comprehensive analysis. This is a unique feature of our interface and

is particularly important in TM structure prediction, where user input is particularly valuable in integration of different information sources on a membrane protein of interest.

For scientists studying a single protein or a few proteins, the interaction with the TMpro tool is likely to be manual through the web interface. But often, it is also of interest to make TM predictions on larger data sets or integrated with other applications, such as other prediction methods. Interoperability with other applications is enabled through a web service, which is made adherent to current W3C standards including Extensible Markup Language (XML) based languages such as Simple Object Access Protocol (SOAP) and Web Services Description Language (WSDL).

Further details: Further details of the web interface and web service are given in Appendix B.

7.3 Application of TMpro to specific proteins

7.3.1 Proteins with unconventional topology

In Chapter 6.3.1, we have demonstrated that without using evolutionary information, without restricting the membrane topology and with only using 25 free parameters, the TMpro approach results in very high accuracies in TM structure prediction of TM proteins with known topology. We believe that these features will make TMpro particularly useful in future predictions of TM helices in proteins from novel families and with novel topologies. Although substantiating this claim quantitatively will require solving new membrane protein structures, we would like to present three specific examples to qualitatively illustrate the potential strengths and weaknesses of this method. Figure 7.6 shows the predicted TM segments of the KcsA potassium channel (PDB ID 1BL8, [61]), the aquaporins (represented by PDB ID 1FQY[149]). TMpro predictions are compared to those from TMHMM, DAS-TMfilter, SOSUI as representatives of single-sequence methods, and PRODIV-TMHMM as a representative of a multiple-sequence alignment-based method.

KcsA potassium channel

In contrast to the general topology of membrane proteins which have a membrane segment completely traversing from the cytoplasmic (cp) to extracellular (ec) side or vice versa, resulting in a cp-TM-ec-TM-cp... topology, the KcsA potassium channel has a short 11-residue pore-forming helix (ph) and an 8-residue pore-forming loop (pl) that are surrounded by TM helices of a tetrameric arrangement of 4 chains. The loops on either side of this short helix exit onto the extracellular side of the membrane, giving the protein the topology of “cp-TM-ec-ph-pl-ec-TM-cp”. The predictions of the TM segments in the KcsA potassium channel are shown in Figure 7.6A. TMHMM incorrectly predicts part of the pore-forming helix and a part of the extracellular loop together as a TM segment while

7. TMpro: High-Accuracy Algorithm for Transmembrane Helix Prediction¹⁰⁹

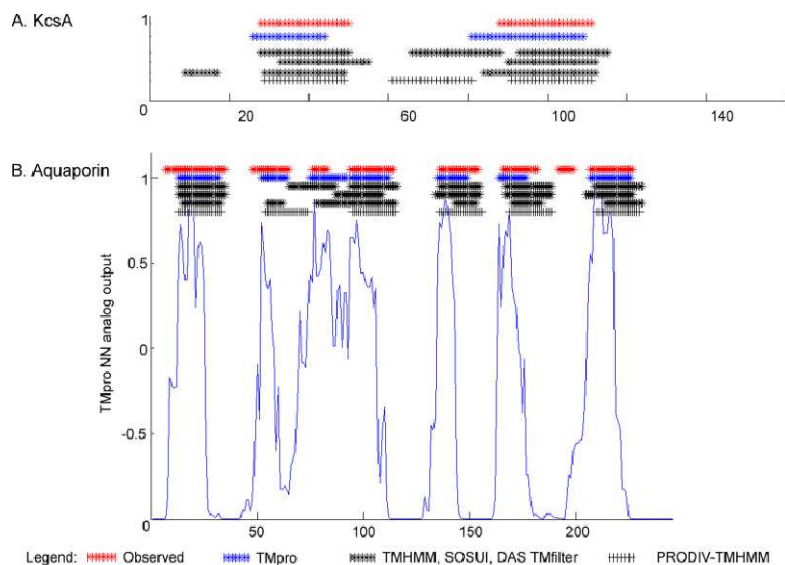


Figure 7.6: TM helix predictions on KcsA and Aquaporin by various methods

TM helix predictions of the potassium channel (KCSA_STRCO) and Aquaporin (AQP1_HUMAN) are shown. For KcsA TMpro and SOSUI predictions conform with the observed TM helices, but TMHMM, DAS-TMfilter and PRODIV-TMHMM all incorrectly predict an additional TM segment.

TMpro correctly predicts 2 TM segments, matching with the observed segments. SOSUI also correctly predicts only 2 TM segments while DAS-TMfilter predicts 3 segments. The evolutionary method PRODIV-TMHMM predicts 3 segments incorrectly.

Aquaporins

Aquaporins also deviate from the cp-TM-ec-TM-cp topology in that they have two short TM helices (about half the length of a normal TM helix) which are very distant in primary sequence but are close in the 3D structure to form what looks like a single TM helix in a back to back orientation of the two short helices. In this highly unusual topology, the two short helices are of the type cp-TM-cp and ec-TM-ec. The TM helix predictions are shown in Figure 2B. None of the methods compared can correctly predict both short TM helices, including TMpro. Of the observed eight TM helices, TMpro, TMHMM and DAS-TMfilter predict 6 while SOSUI predicts 5 (7.6B). TMpro and DAS-TMfilter both predict an unusually long helix that connects TM segments 3 and 4. Although this prediction is wrong, both the methods provide some evidence for the separation of the two TM helices: DAS-TMfilter gives a text out-put that there is a possibility of two helices; in the analog output of TMpro NN there is a minimum at the position of the loop. In contrast, PRODIV-TMHMM is not able to infer the two short helices. However, it does show a better alignment of the other predicted helices with the observed locations.

7. TMpro: High-Accuracy Algorithm for Transmembrane Helix Prediction 110

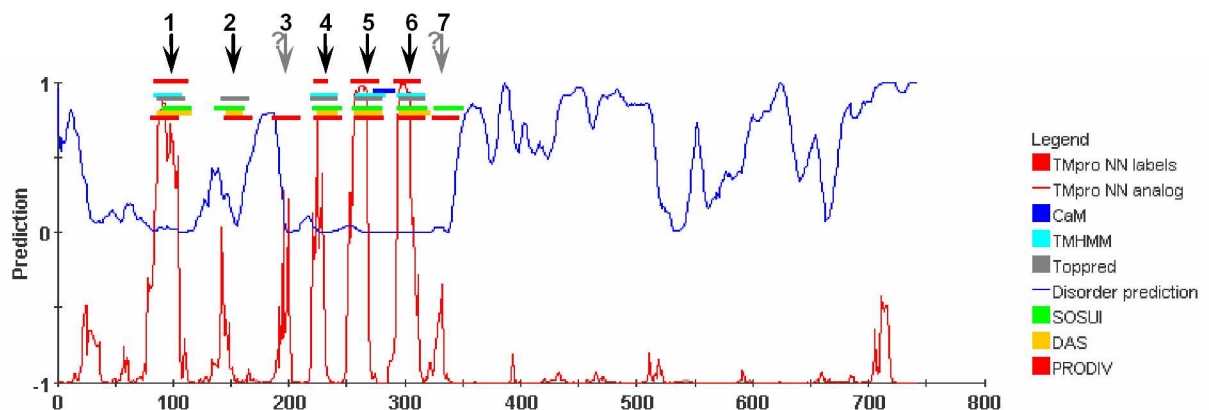


Figure 7.7: Annotation of PalH protein with prediction information from many sources

A protein sequence with not much known information (and hence unlikely to have been in training sequences of previous methods) has been taken for study. Shown here in the figure, are the TM segment prediction by various methods (TMpro, TMHMM, Toppred, SOSUI, DAS TMfilter and PRODIV-TMHMM). As can be seen the methods agree on 4 TM segments but do not agree on 3 other predicted segments. To resolve this disagreement and to arrive at a hypothesis of its membrane topology, other sources of information have been sought. Shown here are the calmodulin binding site (CaM) and protein disorder prediction. In addition, phosphorylation sites have also been predicted although not shown here. Currently, annotation of protein from sources other than TM prediction algorithms is required in order to arrive at a plausible membrane topology of a specific protein, especially when such information is not known for any of its family members. The figure is obtained through the use of TMpro web server.

7.3.2 Hypotheses of transmembrane structure for proteins with unknown transmembrane structure

PalH

Outcome of the study of different TM helix prediction algorithms for a specific protein *PalH* is shown in Figure 7.7. *PalH* protein is found in *Botrytis cinerea*. Analysis with a number of methods are shown labeled along the sequence, which shows that there are 4-7 TM segments in the protein, but offers no means of concluding exactly how many TM segments are present, and in turn about the overall topology of the protein. In such a situation a biologist has to superimpose other information on the protein and arrive at a conclusion manually. In case of this protein, additional information such as calmodulin binding site, protein disorder prediction (shown in figure), phosphorylation sites and surface prediction (not shown in figure) are utilized in arriving at the following hypothesis: *PalH* is probably a protein with an even number, and mostly likely 6 TM helices and that the N and C termini are both located in the cytoplasm. The reasoning for this hypothesis is that

7. TMpro: High-Accuracy Algorithm for Transmembrane Helix Prediction 111

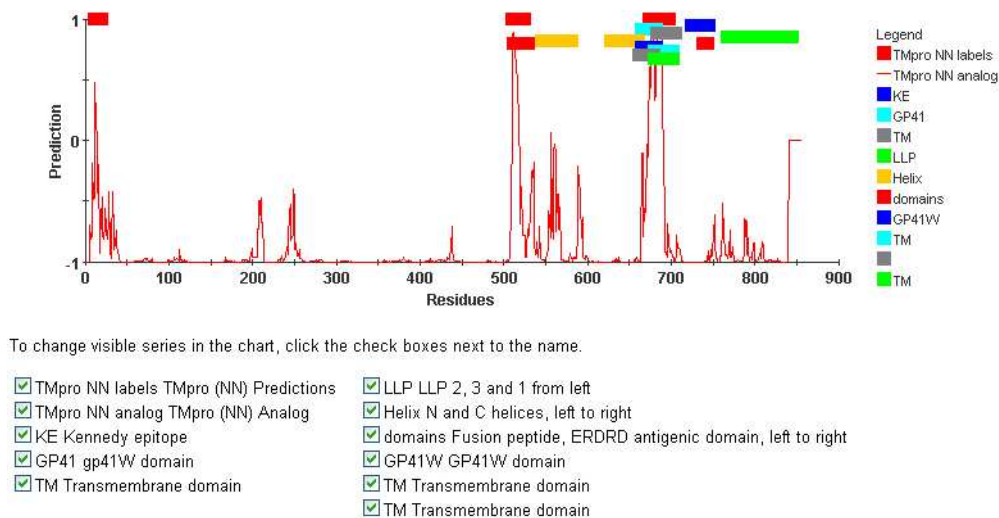


Figure 7.8: Annotation of HIV Glycoprotein gp160 with structural information

Shown here in the figure, are the TM segments predicted by TMpro and other information known or hypothesized by experimental information, as given in SWISSPROT data base. TMpro predicts two segments in the gp41 region of the glycoprotein GP160 (C-terminal side), of which one of them is known to be fusion peptide, and the other one the TM domain in the viral envelope. An additional segment is predicted in the N-terminal side, which is likely to be a signal peptide. The figure is obtained through the use of TMpro web server.

1. there are protein interaction sites (phosphorylation) in both the N and the C terminal sequence, so those can only be cytoplasmic
2. disorder prediction fits well with the positions of helices
3. surface prediction fits well with long cytoplasmic C-terminus
4. the requirement that calmodulin binding site (CaM) has to be on the cytoplasmic side rules out the possibility of 4 TM segments and also the configuration of 6 TM helices that includes segment 3.

Thus, the final hypothesis is for the protein to have 6 TM helices, numbered 1, 2, 4, 5, 6 and 7 in the figure.

HIV glycoprotein gp41

The structure and resulting topology of the gp41 portion of the Env protein of the human immunodeficiency virus (HIV) is not known. Two opposing transmembrane topologies have been proposed, a single transmembrane helix or a triple strand beta-barrel [150]. In an effort to understand which, if either, of these models is correct, we applied computational tools for visualization of amino acid properties and transmembrane segment

7. TMpro: High-Accuracy Algorithm for Transmembrane Helix Prediction¹¹²

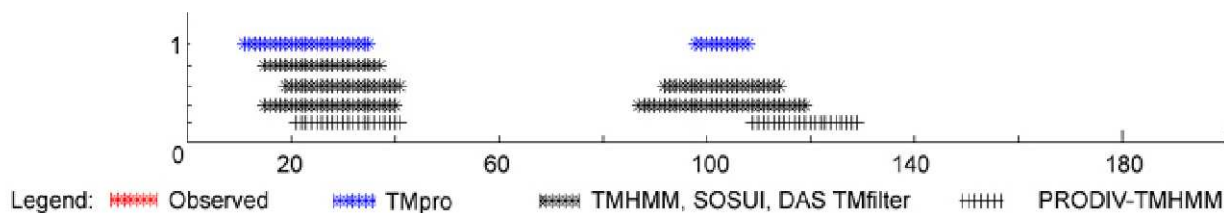


Figure 7.9: TM helix predictions on GP41 by various methods

TM helix predictions of the HIV virus envelope glycoprotein gp41 are shown. TMpro predictions conform with the current hypothesis, as do the predictions of SOSUI and DAS-TMfilter, of the presence of a fusion peptide on the N-terminal and a TM region to the right of it. TMHMM fails to predict the TM helix, while that predicted by PRODIV-TMHMM does not overlap well with the hypothesized region.

prediction to a number of Env sequences obtained from the Los Alamos HIV database [151, 152]. Many of these sequences were predicted to contain only one transmembrane domain, while some were predicted to contain two or more. Annotations of the gp160 sequence with known information and TMpro prediction is shown in Figure 7.8. TM helix predictions of gp41 are also shown in Figure 7.9. TMpro predicts two TM segments with high confidence; one of them is the known fusion peptide, which constitutes a TM helix during HIV fusion with the host cell. Of the other methods compared (TMHMM, DAS-TMfilter, SOSUI, PRED-TMR, HMMTOP), only DAS-TMfilter and SOSUI predict two TM segments - the other methods do not predict the TM helix at all and predict the fusion peptide as the only TM segment. The transmembrane beta-barrel prediction algorithm PRED-TMBB [153] found no evidence of a beta-barrel structure. Taken together, these findings support the hypothesis that gp41 has a single transmembrane domain and a well-structured cytoplasmic domain with evidence for interactions with the membrane surface, possibly in form of “dipping” helices such as found abundantly in the chloride channel structure [154]. Furthermore, we identified a highly conserved positively charged residue (698 Arginines, 12 Lysines, and no other amino acid in the HIV alignment) in the center of the predicted transmembrane helix, implying a structural and/or functional role of this residue. Experimental studies to validate these predictions are underway.

Acknowledgement: The positional conservation of properties work was done by Andrew Walsh and Judith Klein-Seetharaman.

Chapter 8

Summary of Contributions

The focus of this thesis has been development of algorithms analogous to those traditionally used for natural language processing, to the processing of biological sequences to solve specific problems in biology.

8.1 Scientific contributions

The Biological Language Modeling Toolkit (BLMT) has been developed for analysis of biological sequences in analogy to the CMU-Cambridge Statistical Language Modeling Toolkit for analysis of natural language. BLMT was used to determine frequencies of n-grams or other statistical features of word associations that are frequently used as features in analyzing texts, for genome sequences. The amino acids were defined as the words of biological sequence language. This work has shown that biological sequence language differs from organism to organism, and has resulted in identification of idiosyncratic signatures of genomes. However, we found that amino acid word n-grams usually do not allow direct inference of structural or functional properties of the proteins encoded in the genomes. Therefore, word association statistics of alternate word-equivalents instead of the amino acid vocabulary, namely chemical structures and amino acid properties was investigated as building blocks of biological sequence language. In combination with the latent semantic analysis model often used in natural language processing, these features were found highly predictive of transmembrane segments, the identification of which is a biologically important task in the analysis of a large subset of proteins encoded in genomes, the membrane proteins. The work led to the development of TMpro, an algorithm to predict transmembrane segments in proteins. TMpro has been evaluated on benchmarking and state-of-the-art membrane protein data sets and has been found to achieve a very high accuracy in TM helix prediction. The TMpro algorithm is available as a web-interface and as a web-service at <http://flan.blm.cs.cmu.edu/tmpro/>.

This work has also resulted in the following products and publications.

8.2 Biological language modeling toolkit

Biological language modeling toolkit has been developed that preprocesses genomic and proteomic data into suffix arrays and constructs longest common prefix array and rank array for efficient computation of n-grams. The toolkit also has built-in functions to compute n-gram counts, compare n-grams across multiple genome or protein data sets, compute Yule values and perform statistical language modeling of genome sequences or protein data sets.

Availability: Web interface: <http://flan.blm.cs.cmu.edu/>. Source code is also available, at: <http://www.cs.cmu.edu/~blmt/source/>. Details of the download, installation and usage are given in Appendix A.

Acknowledgement: Vijayalaxmi Manoharan developed the web interface for the biological language modeling toolkit.

8.3 TMpro web server for transmembrane helix prediction

A web server has been developed to perform transmembrane helix predictions using TMpro algorithm on single or multiple protein sequences. It also generates a multi-feature graph to aid manual analysis of specific protein predictions.

Availability: <http://flan.blm.cs.cmu.edu/tmpro/> and <http://linzer.blm.cs.cmu.edu/tmpro/>
Details of the web interface features and usage are given in Appendix B.

Acknowledgement: Code development of the web interface was carried out by Christopher Jon Jursa.

Chapter 9

Future Work

9.1 Application of the analytical framework to other areas

In approaches of protein sequence processing to infer structural or functional characteristics, amino acids, pair-wise amino acid similarity measures (e.g. BLOSUM matrix) or measures of amino acid properties (e.g. hydrophobicity scale) have been used to represent the protein sequences. Here, we represented the protein sequence in terms of five different properties of amino acids independently, and developed a method to capture all the possible property combinations a segment of protein might exhibit. It has been demonstrated in this thesis that this framework achieves significant improvement in classification of soluble helices and in prediction of transmembrane helices. This suggests that the approach may be of general utility, for example if applied to the study of other characteristics or structural features observed at segment level of proteins. Good candidates are prediction of transmembrane beta barrel structures and beta-helices.

While adapting the framework to study other problems in computational biology, the choice of the vocabulary, number of dimensions retained for further analysis after singular value decomposition, and the choice of the statistical modeling methods to be applied need to be redesigned to fit the specific biological problem and the specific characteristics that are aimed to be captured.

When experimentally determined structures become available for larger number of membrane proteins, the parameters of TMpro may need to be recomputed. The feature space spanned by transmembrane and nontransmembrane segments, and also the statistical models that differentiate between these two types of features need to be reanalyzed. Further, the appropriate choice of the number of dimensions to be retained after singular value decomposition and also the number of nodes in the neural network, will need to be re-estimated.

9.2 Enhancements to TMpro

The TMpro algorithm for transmembrane helix prediction achieves high accuracy but has still room for improvement. Below are avenues that are directly suggested by the results of this thesis.

Yule values. For each amino acid pair occurring in a predicted segment, Yule values previously computed for transmembrane helix dataset are compared with those computed for soluble helix dataset. The differences, especially for the pairs that have strong dissociation one dataset, and these can be used to infer validity of the predicted segment.

Secondary structure content. Secondary structure content has been found to be a source of error recovery (Section 7.1.5). Using a secondary structure prediction algorithm in conjunction with TMpro is another avenue for future enhancement. The predictions may be used again to filter possible false-positives from predicted segments, or may be used as input to the neural network prediction.

Modeling of extracellular and cytoplasmic loops. The latent semantic analysis model studied in this thesis was primarily aimed at recognizing transmembrane helices. The parameters chosen were optimal for this task. To recognize the topology of transmembrane proteins (namely, to predict whether the nontransmembrane segments are cytoplasmic or extracellular), a parallel set of features may be used with parameters remodeled appropriately. For example, a shorter window of 3-5 residues for analysis would be suitable to identify polar ends of transmembrane segments or positively charged cytoplasmic regions.

Merging predictions from complementary methods. Prediction algorithms in general and especially the two we studied, namely TMpro and TMHMM, have complementary capabilities. In the section on error recovery (Section 7.1.5), we have shown that merging the results of TMpro and TMHMM resulted in superior accuracy compared to either of the two methods. Characteristics of proteins, for example its length, hydrophobicity, predicted secondary structure class may be studied in relevance to the accuracy of various transmembrane helix prediction algorithms and utilized towards choosing the appropriate algorithm for the conditions observed in the protein under study. This method of combining prediction methods is analogous to multi-sensor fusion or multi-engine machine translation.

Evolutionary information. The objective of this thesis was to focus on transmembrane helix prediction from only primary sequence of the protein, without using evolutionary information because this information is not available for all proteins. However, where such information is available, it is valuable towards transmembrane helix prediction and it may be incorporated into the prediction algorithm.

9.3 Genome level predictions

Two specific proteins (palH and gp41) for which no information is available about their transmembrane structure, predictions have been made with TMpro and a final hypothesis of their transmembrane structure has been presented in Chapter 7. This can be extended for all potential membrane proteins in a genome. A compilation of predicted or hypothesized transmembrane segments may be created and released for access by other experimental biologists so that they can use the information in designing experiments to infer characteristics of these proteins or in validating the predictions.

Chapter 10

Publications resulting from the thesis work

Publications from this thesis work are listed below in the order they were presented in the Executive Summary chapter.

Journal publications

1. **Computational biology and language**, Madhavi Ganapathiraju, N. Balakrishnan, Raj Reddy and Judith Klein-Seetharaman, *Lecture Notes in Computer Science*, LNCS/LNAI 3345, 2006, pp 25-47.
2. **The challenge of transmembrane helix prediction**, Madhavi Ganapathiraju and Judith Klein-Seetharaman, *Journal of Biosciences*, in preperation, 2007.
3. **BLMT: Statistical analysis of sequences using N-grams**, Madhavi Ganapathiraju, Vijayalaxmi Manoharan and Judith Klein-Seetharaman, *Applied Bioinformatics*, October, 2004.
4. **Collaborative Discovery and Biological Language Modeling Interface**, Madhavi Ganapathiraju, Vijayalaxmi Manoharan, Raj Reddy and Judith Klein-Seetharaman, *Lecture Notes in Artificial Intelligence*, LNCS/LNAI 3864, 2006, pp 300-321.
5. **Retinitis pigmentosa associated with rhodopsin mutations: Correlation between phenotypic variability and molecular effects**, Alessandro Iannaccone, David Man, Naushin Waseemc, Barbara J. Jennings, Madhavi Ganapathiraju, Kevin Gallaher, Elisheva Reese, Shomi S. Bhattacharya, Judith Klein-Seetharaman, *Vision Research*, 46 (27), 2006, pp 4556-67.
6. **Comparison of Stability Predictions and Simulated Unfolding of Rhodopsin Structures**, Oznur Tastan, Esther Yu, Madhavi Ganapathiraju, Anes Aref, AJ

Rader and Judith Klein-Seetharaman, *Photochemistry and Photobiology*, in press, 2007.

7. **Characterization of protein secondary structure: application of latent semantic analysis using different vocabularies**, Madhavi Ganapathiraju, Judith Klein-Seetharaman, N. Balakrishnan, and Raj Reddy, *IEEE Signal Processing Magazine*, May 2004, pp 78-87.
8. **TMpro: Transmembrane helix prediction using amino acid property features and latent semantic analysis**, Madhavi Ganapathiraju, N. Balakrishnan, Raj Reddy and Judith Klein-Seetharaman, *INCOB2007 Proceedings in BMC Bioinformatics*, in press, 2007.
9. **TMpro Webserver and web service for transmembrane helix prediction**, Madhavi Ganapathiraju, Christopher Jon Jursa, Hassan Karimi and Judith Klein-Seetharaman, in preparation, 2007.

Conference publications

10. **Comparative n-gram analysis of whole-genome sequences**, Madhavi Ganapathiraju, Deborah Weisser, Judith Klein-Seetharaman, Roni Rosenfeld, Jaime Carbonell and Raj Reddy, *HLT'02: Human Language Technologies Conference*, San Diego, March, 2002.
11. **Yule value tables from protein datasets**, Madhavi Ganapathiraju, Deborah Weisser and Judith Klein-Seetharaman, *The eighth multiconference on systemics, cybernetics and informatics*, Orlando, Florida, July 2004.

Posters

12. **Rare and frequent amino acid n-grams in whole-genome protein sequences**, Madhavi Ganapathiraju, Judith Klein-Seetharaman, Roni Rosenfeld, Jaime Carbonell and Raj Reddy, *RECOMB'02: The Sixth Annual International Conference on Research in Computational Molecular Biology*, Washington DC, USA, April, 2002.
13. **High Accuracy Transmembrane Helix Prediction by Text Processing Algorithms**, Madhavi K. Ganapathiraju, and Judith Klein-Seetharaman, *Annual Meeting of the Biophysical Society*, Baltimore, USA, March 2007.
14. **The Transmembrane Topology of the HIV gp41 Protein**, Andrew S. Walsh, Madhavi Ganapathiraju, Jason Newman, Roni Rosenfeld, Ronald C. Montelaro and Judith Klein-Seetharaman, *51st Annual Meeting of the Biophysical Society*, Baltimore, USA, March 2007.

Publications in language technologies

15. **Improving Recognition Accuracy on CVSD speech in mismatched conditions**, Madhavi Ganapathiraju, N. Balakrishnan and Raj Reddy, WSEAS Transactions on Computers, 2(4), October 2003San Diego, March, 2002.
16. **Digital Library of India: a testbed for Indian language research**, N. Balakrishnan, Raj Reddy, Madhavi Ganapathiraju, Vamshi Ambati, IEEE Technical Committee on Digital Libraries (TCDL) Bulletin, 3(1), 2006.
17. **Multilingual Book Reader: Transliteration, Word-to-Word Translation and Full-text Translation**, Prashanth Balajapally, Phanindra Pydimarri, Madhavi Ganapathiraju, N. Balakrishnan, Raj Reddy, VALA 2006: 13th Biennial Conference and Exhibition Conference of Victorian Association for Library Automation, Melbourne, Australia, February 8-10, 2006.

Citations of this thesis in other work

The two concept papers on n-gram analysis and latent semantic analysis for biological sequences have already been cited by several other researchers:

N-gram analysis have been applied as features in the prediction tasks of protein family classification [17, 156, 157], transmembrane helix boundary detection [17], protein secondary structure prediction [158, 159], modeling genome evolution [160, 161, 162, 163], protein remote homology detection [164], functional proteomics [165] and analysis of known protein structures in terms of their distribution with sequences of a given length [145]. Latent semantic analysis has been applied for remote homology detection [164, 166, 167], prediction of secondary structure content in proteins [168, 169].

Appendix A

Biological Language Modeling Toolkit: Source Code

Source code is available at <http://www.cs.cmu.edu/~blmt/source/>

Download the sourcecode for version 2.0 of the toolkit. It may be installed on a unix machine or using Cygwin on windows platform. Download the sourcecode and unzip and untar the file using the following commands:

```
gunzip blmt_v1.0.tar.gz
tar -xvf blmt_v1.0.tar
cd blmt
make
```

1. Compilation of programs

There is a makefile in the Final directory.

[Tutorial help for non-computer scientists: -c creates an object file *.o are the object files -o links two or more object files to create the executable (o is output)]

The following commands will be applicable to makefile:

Global compilation of all the programs in the toolkit:

make [or make all]: removes all *.o files and compiles all programs.

make clean-all: removes all *.o files and all executables [So that you can re-compile them afresh].

make clean: removes only *.o files

Each individual program can also be compiled separately:

make faa2srt: [Compiles the faa2srt.cpp file and creates the faa2srt executable. Note that this does not remove *.o files before. *.o files need to be removed anytime there is a change to the C-code and you want that to be updated].

make srt2lcp make ngrams make proteinCount make proteinNGram make yule make map2srt make langmodel make wcngrams

Usage of the programs (input/output options etc)

./programname -help shows the different options that go with the program called programName

Example usage (see below):

```
./ngrams
  -fsrt bb.a.srt
  -flcp bb.a.lcp
  -n 5
  -printall
  -sortc
```

faa2srt: Creates a Suffix Array from a Fasta format Genome file.

```
./faa2srt -help
```

Usage: ./faa2srt

```
-ffaa <Genome (Input) filename (.faa)>
-fsrt <Output filename (default: inputfilename.srt)>
-help display this help message
```

Example usage: ./faa2srt -ffaa human.faa

Note: For long genomes, you have to adjust the maximum length of the genome to suit your file: In mylib.h find SUPERLEN 12000000, change to larger value if needed.

srt2lcp: Creates the Least Common Prefix (LCP) and Rank arrays

corresponding to a Suffix Array.

```
./srt2lcp -help
```

Usage: ./srt2lcp

```
-fsrt <Sorted-Suffix-Array of Genome (Input) filename (.faa.srt)>  
-flcp <LCP (Output) filename (default: inputfilename.lcp)>  
-frnk <Rank (Output) filename (default: inputfilename.rnk)>  
-help display this help message
```

Example: ./srt2lcp -fsrt human.faa.srt

ngrams: Finds the various n-grams occurring in a Genome and also the number of times that a particular n-gram occurs. Also computes listing the n-grams in descending order of their number of occurrences. Prints out counts of n-grams alone (without the n-gram itself), to allow the output to be used easily by other programs (plots?)

```
./ngrams -help
```

Usage: ./ngrams

```
./ngrams
```

```
-fsrt <Sorted Suffix Array (Input)filename>  
-flcp <LCP array file (Input)>  
-fngrams <Output Filename to print n-gram counts>  
-n <n-gram length: eg. "-n 4">  
-top N <print only top N n-grams: eg. "-top 20">  
    (with this option, n-grams are sorted by count)  
    (Also, if N is 0 or -top option not given all n-grams are printed)  
[-printngram] (default: OFF. Give this flag if you want n-gram  
    to be printed besides the count of n-gram)  
    (-printall was old switch for the same action. Still supported  
[-sortbycount] (default: OFF. Give this flag to sort n-grams  
    by count instead alphabetically)  
[-pzn] <Print also n-grams that do not occur in the input>  
    counts for these non-occurring ngrams would be 0  
-help display this help message
```

Example: ./ngrams -fsrt human.faa.srt -flcp human.faa.lcp -fngrams
human.4grams.txt -n 4 -top 20 -sortbycount

proteinCount:Counts the total number of proteins in a Genome and lists out the lengths and headers (optionally), for all the proteins.

```
./proteinCount -help
```

Usage: ./proteinCount

```
-ffaa <Genome (.faa) (Input) filename>  
-fsrt <Sorted Suffix Array(Input)filename>  
-fprot <Protein count (Output) filename>  
[-printall] (default: OFF. Give this flag if you want proteins  
  Headers to be printed  
[-nosort] (default: OFF. Give this flag to NOT sort proteins  
  by length  
-help display this help message
```

Example:

```
./proteinCount  
-ffaa human.faa  
-fsrt human.faa.srt  
-fprot  
human.protCount.txt  
-printall  
-nosort
```

proteinNGram:Given a protein sequence, this program lists out the frequency of occurrence of each n-gram appearing the protein when seen through a sliding window. For example, if the input sequence is ABFGMAW, the program can list out number of occurrences of ABFG, BFGM, FGMA and GMAW. This program is useful in comparing n-gram preferences across organisms.

```
./proteinNGram -help
```

Usage: ./proteinNGram

```
-fsrt <Sorted Suffix Array (Input)filename>  
-flcp <LCP filename>  
-fprot <Input Protein Sequence (for n-gram analysis)>  
-fstats <Output file to write n-gram statistics> -n  
  <n-gram length; Default: 4> -help display this help message
```

Example: `./proteinNGram`

```
-fsrt human.faa.srt
-flcp human.faa.lcp
-fprot prot0157.txt
-fstats human_prot0157.stats -n 4
```

wcngrams: Wild card matched ngrams. Input a pattern with wildcard characters `?`, `<` and `>` to match 'any amino acid/nucleotide', 'beginning' and 'end' of sequence. These wildcards may be combined with other specific amino acid/nucleotide combinations.

`./wcngrams -help`

Usage: `./wcngrams`

```
-fsrt <Sorted Suffix Array (Input)filename>
-flcp <LCP array file (Input)>
-pattern <pattern: Such as "A?C?A" or "<MA?A"> or "MA?A">
      where ? matches any-1 character, < means beginning and > means end,
      of a sequence Maximum of 999 chars;
-help display this help message
```

yule: Find Yule statistics of patterns such as `"A**B"` in a database. The computed yule are written out to text files.

Usage: `./yule`

```
-fsrt <Sorted Suffix Array (Input)filename>
-flcp <LCP filename>
-fprot <Input Protein Sequence (for n-gram analysis)>
-foutprefix <Output file to write n-gram statistics>
-nfrom ngram-lengths to be considered can be specified as a range
-nto using -nfrom to -nto. for example -nfrom 2 -nto 4 means 2 to 4.
-help display this help message
```

langmodel: N-gram language model is computed for the training set. Test set sequence perplexities are then compared with the language model.

Usage: `./langmodel`

```
-fsrt <Sorted Suffix Array (Input)filename>
-flcp <LCP filename>
-fprot <Input Protein Sequence (for n-gram analysis)>
```



```
-fpsrt <Input Protein Sorted Array filename (optional)
  ***Note that only -fprot or -psrt need to be given
  ***If the sorted array is already computed, it will be faster
  if srt file is given as input
-fplcp <Input Protein LCP Array filename (optional)
-foutprefix <Output file to write n-gram statistics>
-nfrom <n-gram from length; Default: 4>
-nto <n-gram to length; Default: 4>
-help display this help message
```

map2srt: Amino acid or Nucleotide sequences may be mapped to reduced alphabet such as electronic properties or polarity. Suffix array is then computed for the mapped sequences.

```
Usage: ./map2srt
  -ffaa <Genome (Input) filename (.faa)>
  -mtype <Matype [pnp, ep]>
  -help display this help message
```

Appendix B

TMpro Web Interface

TMpro can be accessed through a traditional web interface where a user can submit one or up to 2000 protein sequences at a time and obtain the prediction of TM segments. The basic TM prediction tool does not require any software other than a web browser. To view the results with a user-interactive chart, Java Run Time Environment (JRE) is required to be present on the user's computer. JRE can be downloaded from www.java.com.

Availability

<http://flan.blm.cs.cmu.edu/tmpro/> (web server).

<http://blm.sis.pitt.edu:8080/TMPro/> (web service).

The web interface has been designed by us, while code development for web interface and the design and development of web service have been carried out by Christopher Jon Jursa and Dr. Hassan Karimi of University of Pittsburgh School of Information Sciences.

User-interface

Input

One or more protein sequences can be input in FASTA format as text or be uploaded as a file. If only one sequence is given, it may be pasted in raw sequence format. Alternatively, the Swiss-Prot id or PDB id may also be given, for which the corresponding sequence is fetched from the Uniprot server.

Output

Plain text output: Textual output gives residue ranges of the predicted TM segments (Figure B.1). Results are also sent as an email to the user if the email address is provided in the input page. Predictions of all the submitted sequences are returned in one page:

each protein begins with the FASTA header; below which start and end positions of the predicted segments are given comma separated, one predicted segment per line.

```
TMPro v1 prediction for your submission: ID: tmpro-1170244754505
Predicted Segments:

>2a06 C 8: Number of TM segments = 8
27,50
88,98
106,140
175,195
226,244
287,303
319,333
345,366
>2a06 D 1: Number of TM segments = 1
204,216
>2a06 E 1: Number of TM segments = 2
34,42
132,141

Your Notes:
PDBTMALPHA First 3 sequences

TMpro-format output Data:

[Chart 1] [Chart 2] [Chart 3]
```

Figure B.1: TMpro web server - plain text output of predictions

On the first output page, the residue numbers of the beginning and ending of predicted segments are given, one segment per line. Predictions of a protein are preceded by the header of the protein starting with a '>', same as in FASTA format of sequences. This line also indicates how many segments have been predicted. If any notes have been submitted in the input page, the notes will be included in this output page under "Your Notes". This box can be used to keep track of what sequence(s) have been submitted. For example in this example, the notes say that the input sequences are the first 3 sequences from the PDB_TM-ALPHA data set (the data set name being some thing of relevance to the user). At the bottom of this output page are buttons to charts of individual proteins. Since three sequences have been input in this example, it has 3 charts, one per protein. Clicking the chart button shows the predicted segments and also the analog output of the TMpro algorithm along the sequence. (see Figure B.3).

Standardized TMpro format: The plain text format described earlier is for human interpretation, whereas for computerized programs, to post-process the TMpro predictions, an output format has been standardized (Figure B.2). One text file is created for each protein. The first line of the file contains the protein header. Line 2 contains the primary sequence information, lines 3 and 4 contain TMpro prediction data. To allow the user to compare TMpro prediction with other predictions or sequence annotations, we created the ability for users to enter such information. One additional line is added for every manual submission of segment information by the user (for example, one line per

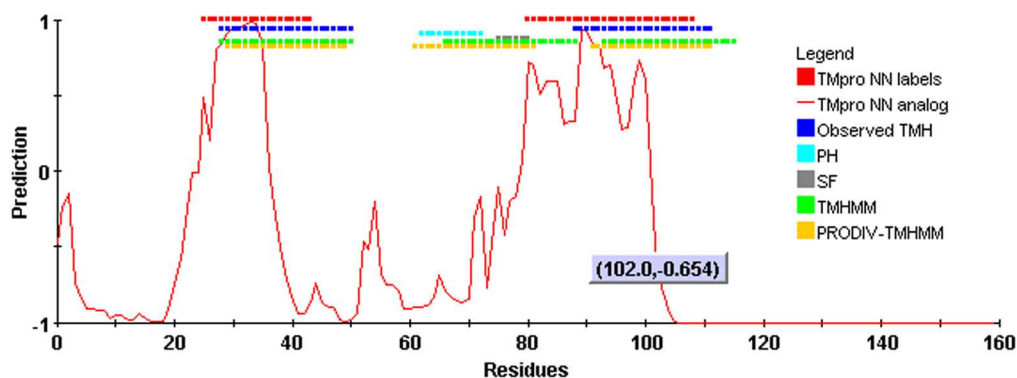
prediction of segments by another method). The standardized TMpro format is useful for computerized processing of TMpro-generated data and additional information input by the user, if any.

```
>POA333|KCSA_STRCO Voltage-gated potassium channel - Streptomyces coelicolor.
Residues && AA && 0 && M, P, P, M, L, S, G, L, L, A, R, L, V, K, L, L, L, G, R, H, G, S, A,
TMpro (NN) Predictions && TMpro NN labels && 1 && 0, 0, 0, 0, 0, 0, 0, 0, 0, 0, 0, 0, 0, 0, 0, 0,
TMpro (NN) Analog && TMpro NN analog && 0 && -0.480, -0.235, -0.153, -0.736, -0.826, -0.914,
Information from SWISSPROT && Observed TMH && 1 && 0, 0, 0, 0, 0, 0, 0, 0, 0, 0, 0, 0, 0, 0, 0, 0,
Pore forming helix && PH && 1 && 0, 0, 0, 0, 0, 0, 0, 0, 0, 0, 0, 0, 0, 0, 0, 0, 0, 0, 0, 0,
Selectivity filter && SF && 1 && 0, 0, 0, 0, 0, 0, 0, 0, 0, 0, 0, 0, 0, 0, 0, 0, 0, 0, 0, 0,
predictions by TMHMM 2.0 && TMHMM && 1 && 0, 0, 0, 0, 0, 0, 0, 0, 0, 0, 0, 0, 0, 0, 0, 0, 0, 0,
Predictions && PRODIV-TMHMM && 1 && 0, 0, 0, 0, 0, 0, 0, 0, 0, 0, 0, 0, 0, 0, 0, 0, 0, 0, 0, 0,
```

Figure B.2: TMpro web server - standardized output of TMpro predictions and additional user-given data

One such file is output for each input protein. It is a plain text file with the following lines: Line 1: Protein header, beginning with a '`'`'. Lines 2 and above have the following fields separated with `&&`: Short name, long descriptive name (of what data the line contains), isBinary (1 if data is binary, 0 otherwise), comma separated values - one value per residue. Line 2 confirms to the above format, but contains residues (single letter codes) instead of numerical values. Its isBinary field is set to 0. When TMpro algorithm finishes, this file has 2 lines after the Residues line (Line 2). Lines 3 and 4 contain predictions of TMpro - analog and binary. See Figure B.3 - the example shown in this figure is what is created when additional information is input by user in creating chart shown in Figure B.3. Analog value is the neural network output at that residue position and binary value is 1 if that residue is in a predicted TM segment. Lines 5 and above are added when user inputs any further information through the user-interactive chart.

User interactive chart: The predictions can be viewed with a user-interactive chart that is generated as a Java Applet or in a standardized TMpro format. The user-interactive chart allows visualizing the positions of the predicted TM segments along the primary sequence. The default view of the chart is the TMpro analog output and predicted TM segments with residue numbers along the X-axis. Any number of sequence annotations provided by the user can be added to the plot. This information could include for example predicted segments from other algorithms, known information from SWISSPROT or other labels such as phosphorylation sites or binding sites, or other predictions, such as secondary structure predictions. Information is appended to the TMpro standard format file and the applet regenerates the chart marking these values on the plot every time a new input is provided (Figure B.3). This feature allows integration of information from diverse sources by visually combining it in a chart for comprehensive analysis. This is a unique feature of our interface and is particularly important in TM structure prediction, where little knowledge is available and user input is particularly valuable in integration of different information sources on a membrane protein of interest.



To change visible series in the chart, click the check boxes next to the name.

- TMpro NN labels TMpro (NN) Predictions
- TMpro NN analog TMpro (NN) Analog
- Observed TMH Information from SWISSPROT
- PH Pore forming helix
- SF Selectivity filter
- TMHMM predictions by TMHMM 2.0
- PRODIV-TMHMM Predictions

Enter Short Legend Name:

Enter Description:

Enter start and end residue numbers of each segment:

Start	End	Start	End	Start	End	Start	End

Be sure to enter TM segments between the start and end bounds (0 and 159)

Figure B.3: TMpro web server - interactive chart

TMpro generates a graphical chart as a Java Applet showing the analog output of TMpro neural network and its predicted TM segments. The user can enter the start and end residue positions of additional features, giving a short name to this additional information. In the figure, predictions by TMpro of the K⁺ channel protein are shown in red. The remaining lines in dark blue, light blue, grey, green and yellow are experimentally known TM segments, experimentally known pore-forming helix, selectivity filter and predicted TM segments by other TM prediction algorithms, TMHMM [117] and PRODIV-TMHMM [119], as examples. Visualization of this information shows that TMHMM and PRODIV-TMHMM confuse the pore-forming helix and selectivity filter together to be an additional TM segment. This visualization can aid researchers of specific proteins in drawing conclusions by integrating information from multiple sources. Check boxes are provided to selectively view specific sources of information from among those entered.

Webservice: For scientists studying a single protein or a few proteins, the interaction with the TMpro tool is likely to be manual through the web interface. But often, it is also of interest to make TM predictions on larger data sets or integrated with other applications, such as other prediction methods. Interoperability with other applications is enabled through a web service, which is made adherent to current W3C standards including Extensible Markup Language (XML) based languages such as Simple Object Access Protocol (SOAP) and Web Services Description Language (WSDL). For instance, users can write client side applications to send protein sequences and receive predictions through SOAP. The web service's operations and the required parameters are described in the WSDL document on the web server, which is openly available to clients.

Appendix C

Error Analysis Figures

See section 7.1.4 for discussion.

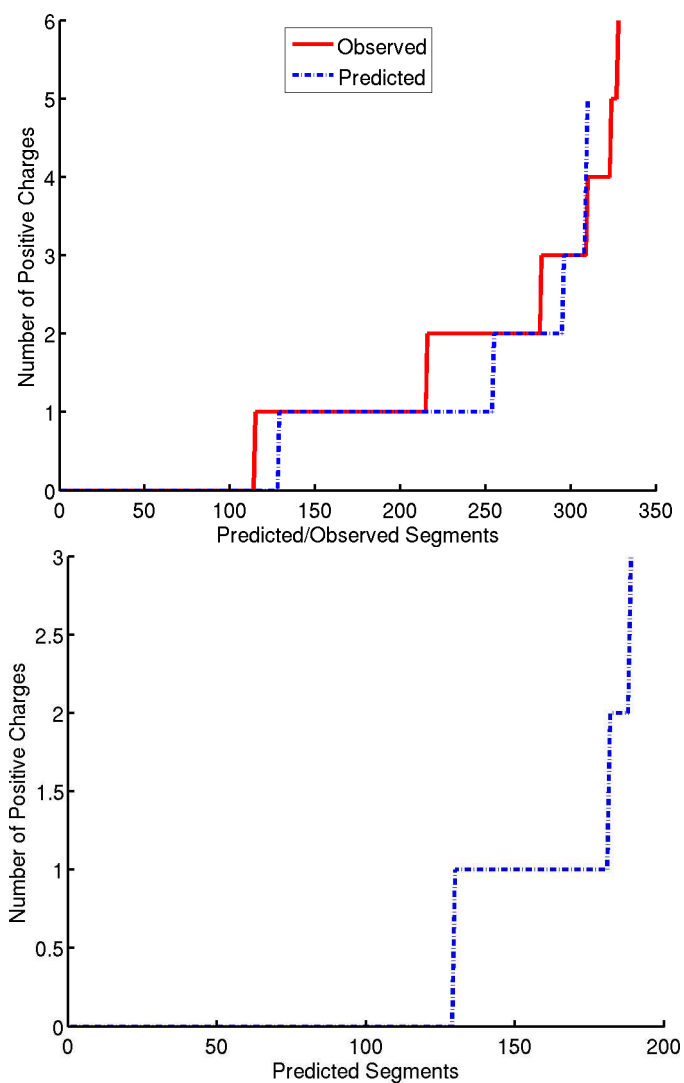


Figure C.1: Number of positively charged residues

TM-glob comparison: positively charged residues in predicted and observed segments in membrane proteins (top) and predicted segments in soluble proteins (bottom)

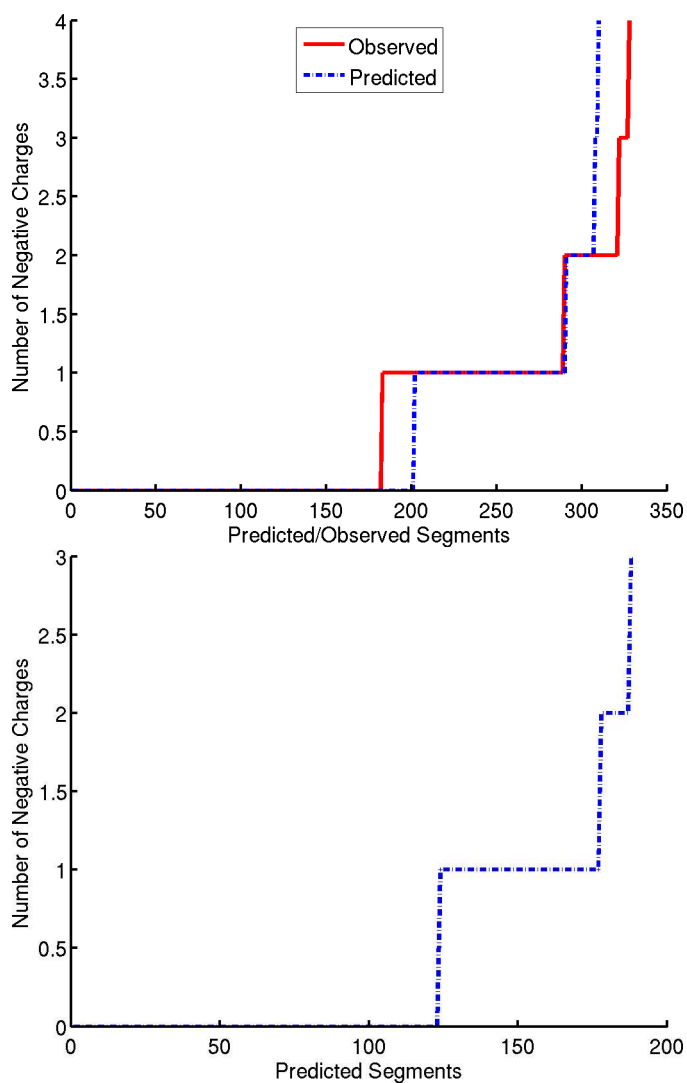


Figure C.2: Number of negatively charged residues

TM-glob comparison: negatively charged residues in predicted and observed segments in membrane proteins (top) and predicted segments in soluble proteins (bottom)

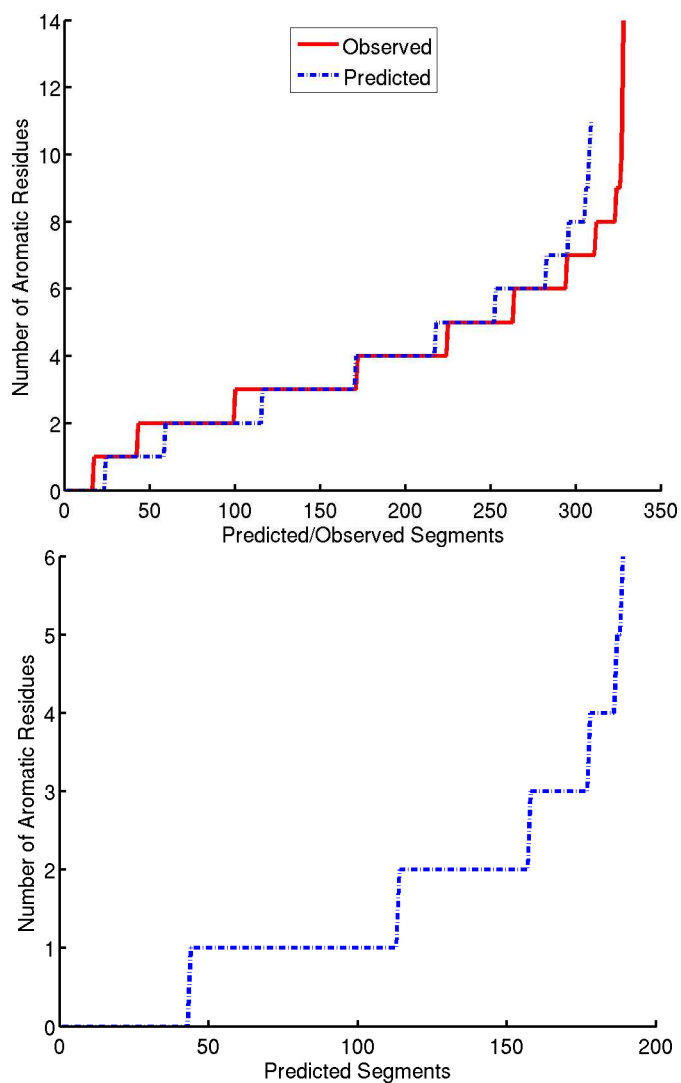


Figure C.3: Number of aromatic residues

TM-glob comparison: aromatic residues in predicted and observed segments in membrane proteins (top) and predicted segments in soluble proteins (bottom)

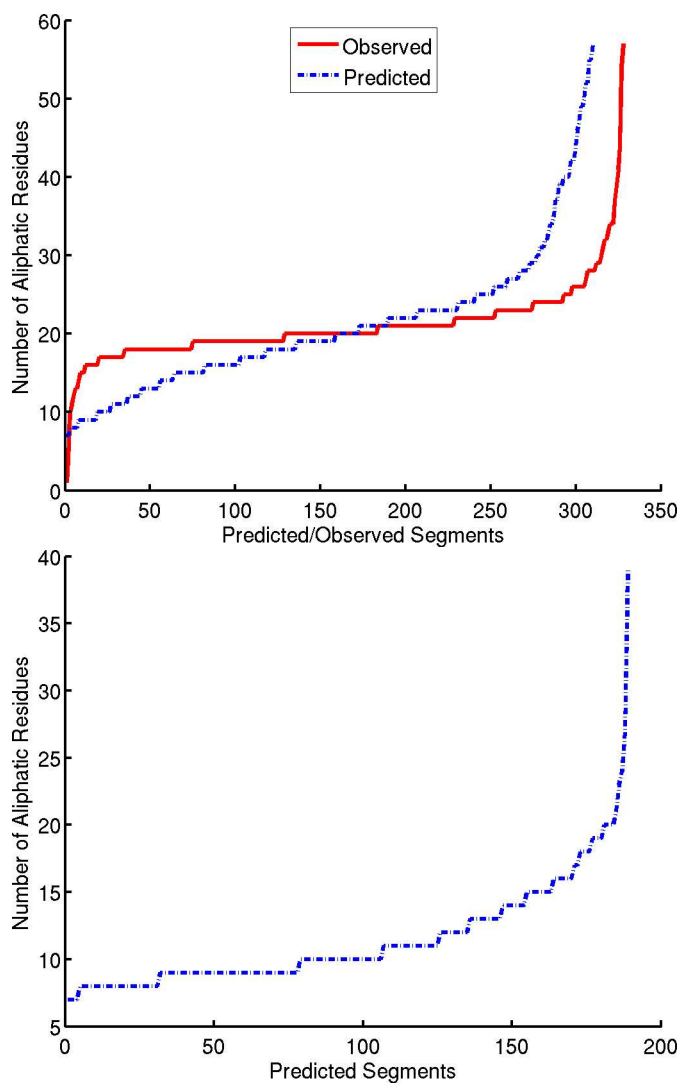


Figure C.4: Number of aliphatic residues

TM-glob comparison: aliphatic residues in predicted and observed segments in membrane proteins (top) and predicted segments in soluble proteins (bottom)

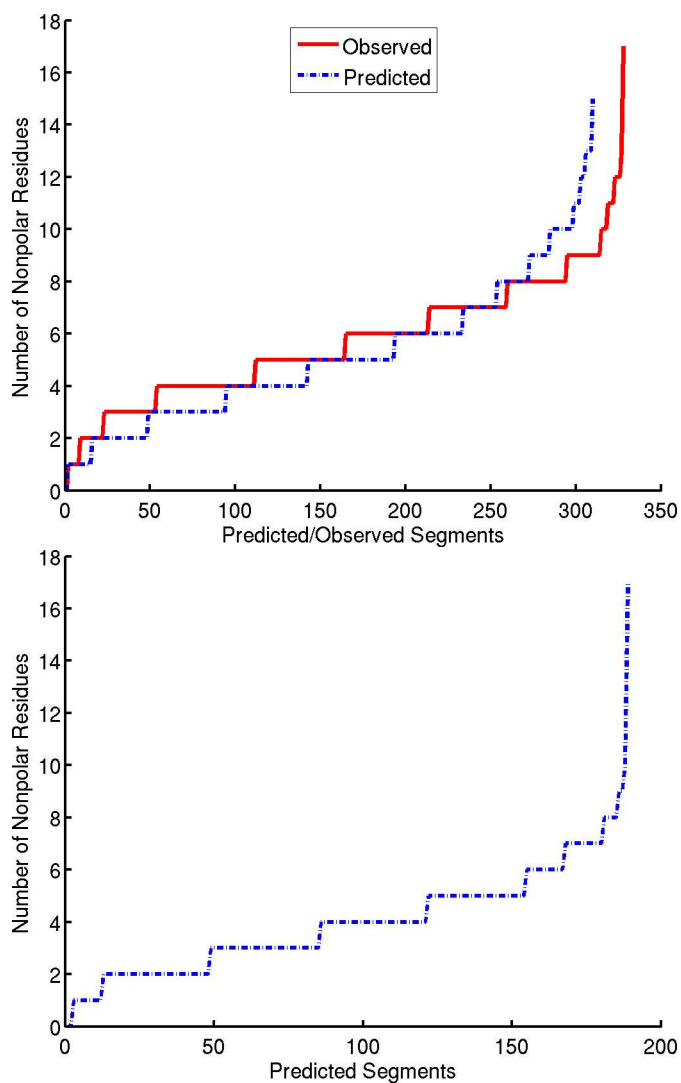


Figure C.5: Number of nonpolar residues

TM-glob comparison: nonpolar residues in predicted and observed segments in membrane proteins (top) and predicted segments in soluble proteins (bottom)

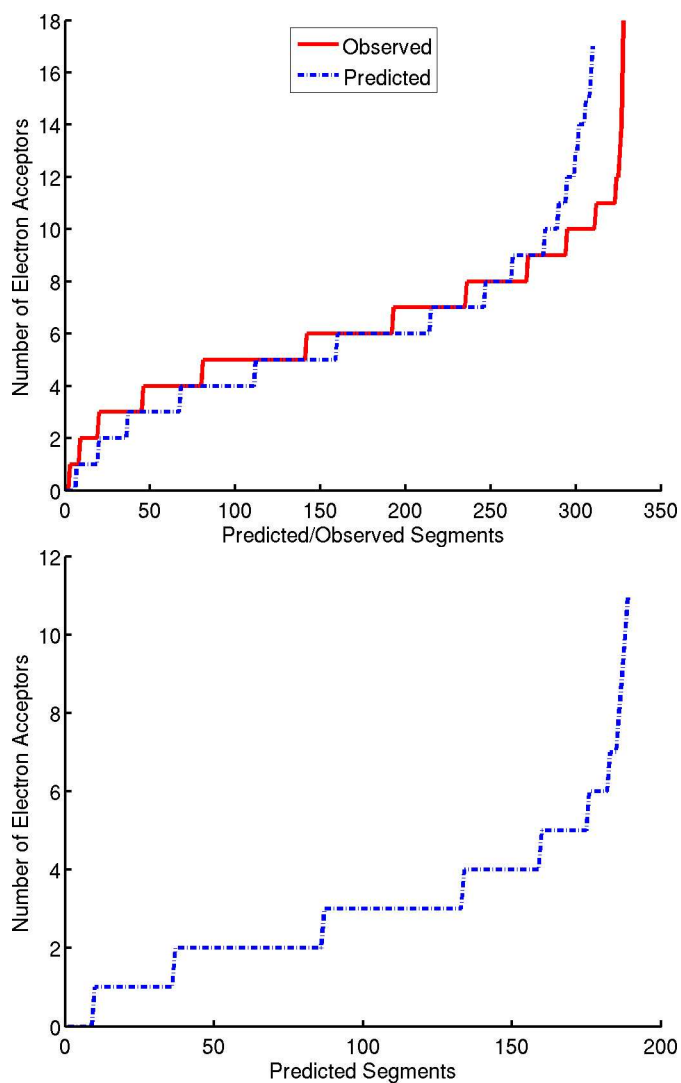


Figure C.6: Number of electron acceptor residues

TM-glob comparison: electron acceptor residues in predicted and observed segments in membrane proteins (top) and predicted segments in soluble proteins (bottom)

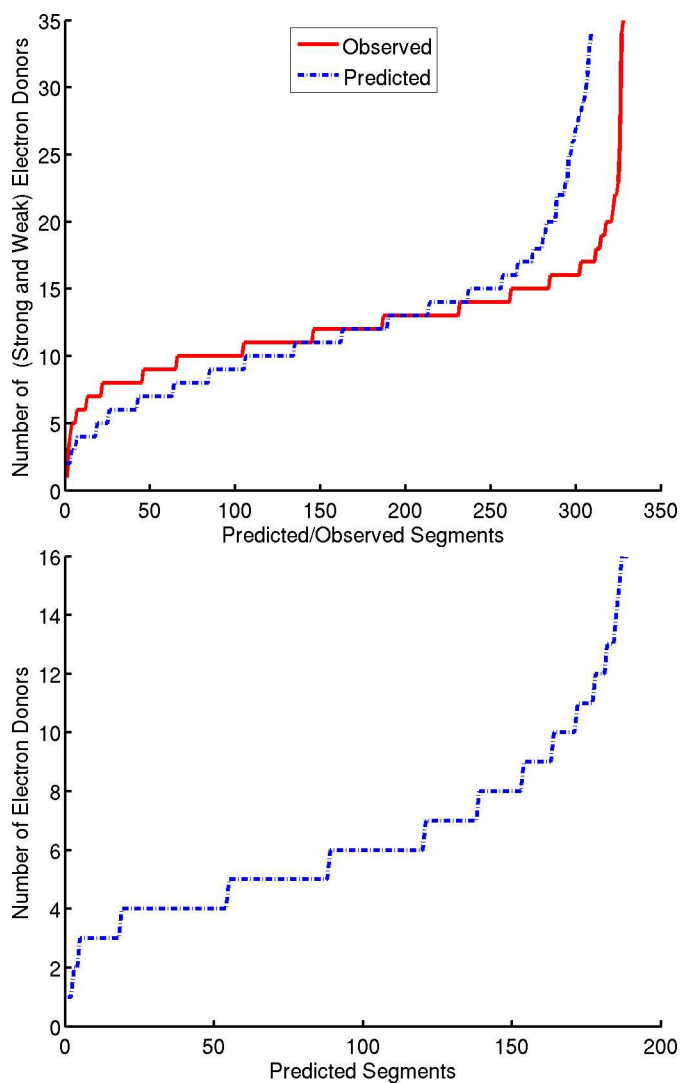


Figure C.7: Number of electron donor residues

TM-glob comparison: electron donor residues in predicted and observed segments in membrane proteins (top) and predicted segments in soluble proteins (bottom)

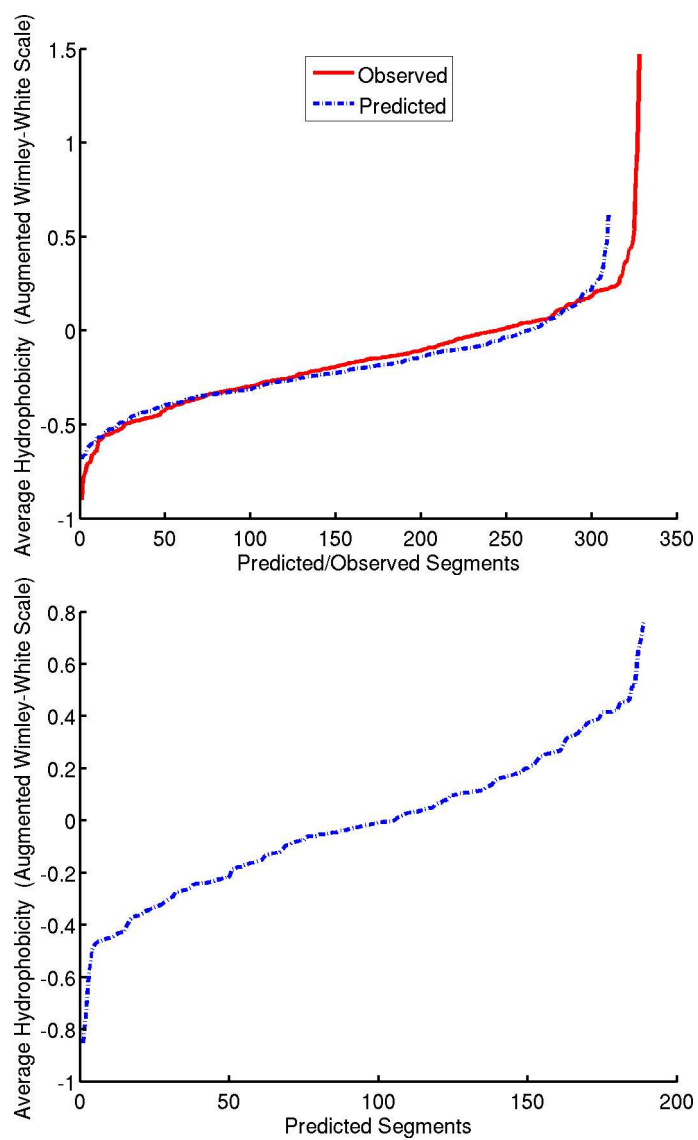


Figure C.8: Average hydrophobicity in the segment
TM-glob comparison: average hydrophobicity in predicted and observed segments in membrane proteins (top) and predicted segments in soluble proteins (bottom)

Bibliography

- [1] Tusnady G, Dosztanyi Z, Simon I: **PDB_TM: selection and membrane localization of transmembrane proteins in the protein data bank.** *Nucleic Acids Research* 2005, **33**.
- [2] Botstein D, Cherry J: **Molecular linguistics: extracting information from gene and protein sequences.** *Proc Natl Acad Sci U S A* 1997, **94**:5506–7.
- [3] Goodfellow P, Sefton L: **Human genetics. Language of the genome.**
- [4] Kay L: **A book of life? How the genome became an information system and DNA a language.** *Perspect Biol Med* 1998, **41**:504–28.
- [5] Muller-Hill B: **Towards a linguistics of DNA and protein.** *Hist Philos Life Sci* 1999, **21**:53–63.
- [6] Zipf G: **Selective Studies and the Principle of Relative Frequency in Language.** In *Hist Philos Life Sci* 1932.
- [7] Israeloff N, Kagalenko M, Chan K: **Can Zipf Distinguish Language from Noise in Noncoding DNA?** *Physical Review Letters* 1996, **76**:1976.
- [8] Konopka A, Martindale C: **Noncoding DNA, Zipf’s Law, and Language.** *Science* 1995, **268**:789.
- [9] Head T: **Formal Language Theory and DNA: An Analysis of the Generative Capacity of Specific Recombinant Behaviors** 1987.
- [10] Rivas E, Eddy S: **The Language of Rna: A Formal Grammar That Includes Pseudoknots.** *Bioinformatics* 2000, **16**:334–40.
- [11] Tsonis A, Elsner J, Tsonis P: **Is DNA a Language?** *J Theor Biol* 1997, **184**:25–9.
- [12] Searls D: **The Language of Genes.** *Nature* 2002, **420**:211–7.
- [13] Troyanskaya O, Arbell O, Koren Y, Landau G, Bolshoy A: **Sequence Complexity Profiles of Prokaryotic Genomic Sequences: A Fast Algorithm for Calculating Linguistic Complexity.** *Bioinformatics* 2002, **18**:679–88.

- [14] Cheng B, Carbonell J, Klein-Seetharaman J: **Protein Classification Based on Text Document Classification Techniques**. *Proteins - Structure, Function and Bioinformatics* 2005, **58**:955–70.
- [15] Coin L, Bateman A, Durbin R: **Enhanced Protein Domain Discovery by Using Language Modeling Techniques from Speech Recognition**. *Proc Natl Acad Sci U S A* 2003, **100**:4516–20.
- [16] Liu Y, Carbonell J, Klein-Seetharaman J, Gopalakrishnan V: **Comparison of Probabilistic Combination Methods for Protein Secondary Structure Prediction**. *Bioinformatics* 2004, **12**:1041–50.
- [17] Cheng B, Carbonell J, Klein-Seetharaman J: **A Machine Text-Inspired Machine Learning Approach for Identification of Transmembrane Helix Boundaries**. In *Bioinformatics* 2004.
- [18] Mantegna R, Buldyrev S, Goldberger A, Havlin S, Peng C, Simons M, Stanley H: **Linguistic Features of Noncoding DNA Sequences**. *Phys Rev Lett* 1994, **73**:3169–72.
- [19] Mantegna R, Buldyrev S, Goldberger A, Havlin S, Peng C, Simons M, Stanley H: **Systematic analysis of coding and noncoding DNA sequences using methods of statistical linguistics**. *Phys. Rev* 1995, **E 52**(3):2939 – 2950.
- [20] Stuart G, Moffett K, Baker S: **Integrated gene and species phylogenies from unaligned whole genome protein sequences**. *Bioinformatics* 2002, **18**:100–8.
- [21] Bussemaker H, Li H, Siggia E: **Building a Dictionary for Genomes: Identification of Presumptive Regulatory Sites by Statistical Analysis**. *Proc Natl Acad Sci U S A* 2000, **97**:10096–100.
- [22] Baldi P: *Bioinformatics*. MIT Press 1998.
- [23] Baxevanis A, Ouellette B: *Bioinformatics. A Practical Guide to the Analysis of Genes and Proteins*. Wiley-Interscience 1998.
- [24] Bolshoy A, Shapiro K, Trifonov E, Ioshikhes I: **Enhancement of the Nucleosomal Pattern in Sequences of Lower Complexity**. *Nucl. Acids. Res.* 1997, **25**:3248–3254.
- [25] Burge C, Karlin S: **Prediction of Complete Gene Structures in Human Genomic DNA**. *J Mol Biol* 1997, **268**:78–94.
- [26] Gibas C, Jambeck P: *Developing Bioinformatics Computer Skills*. O'Reilly & Associates 2001.

- [27] Davis K, Biddulph R, Balashek S: **Automatic Recognition of Spoken Digits.** *The Journal of the Acoustical Society of America* 1952, **24**(6):637–642.
- [28] Eisenberg D, Weiss R, Terwilliger T: **The Helical Hydrophobic Moment: A Measure of the Amphiphilicity of a Helix.** *Nature* 1982, **299**:371–4.
- [29] Eisenberg D, Schwarz E, Komaromy M, Wall R: **Analysis of Membrane and Surface Protein Sequences with the Hydrophobic Moment Plot.** *J Mol Biol* 1984, **179**:125–42.
- [30] Pattini L, Riva L, Cerutti S: **A wavelet based method to predict the alpha helix content in the secondary structure of globular proteins.** In *IEEE* 2002.
- [31] Shepherd A, Gorse G, Thornton J: **A novel approach to the recognition of protein architecture from sequence using Fourier analysis and neural networks.** *Proteins* 2003, **50**:290–302.
- [32] Baker J: **The Dragon System - An Overview.** *IEEE Transactions on Acoustics, Speech and Signal Processing* 1975, **23**:24–29.
- [33] Manning C, Schutze H: *Foundations of Statistical Natural Language Processing.* Cambridge, MA, USA: MIT Press 1999.
- [34] Rabiner L, Juang BH: *Fundamentals of Speech Recognition.* Pearson Education POD 1993.
- [35] Cai C, Rosenfeld R, Wasserman L: **Exponential Language Models, Logistic Regression, and Semantic Coherence.** In *Fundamentals of Speech Recognition* 2000.
- [36] Landauer T, Foltx P, Laham D: **Introduction to Latent Semantic Analysis.** *Discourse Processes* 1998, **25**:259–284.
- [37] Jain A: *Fundamentals of Digital Image Processing.* Prentice Hall 1988.
- [38] Addison P: *The illustrated wavelet transform handbook.* Institute of Physics Publishing 2002.
- [39] Chatzidimitriou-Dreismann C, Streffer R, Larhammar D: **Lack of Biological Significance in the 'Linguistic Features' of Noncoding DNA—a Quantitative Analysis.** *Nucleic Acids Res* 1996, **24**:1676–81.
- [40] Czirok A, Mantegna R, Havlin S, Stanley H: **Correlations in Binary Sequences and a Generalized Zipf Analysis.** *Physical Review. E. Statistical Physics, Plasmas, Fluids, and Related Interdisciplinary Topics* 1995, **52**:446–452.

- [41] Gerstein M: **Patterns of Protein-Fold Usage in Eight Microbial Genomes: A Comprehensive Structural Census.** *Proteins* 1998, **33**:518–34.
- [42] Li W: **Statistical Properties of Open Reading Frames in Complete Genome Sequences.** *Comput Chem* 1999, **23**:283–301.
- [43] Strait B, Dewey T: **The Shannon Information Entropy of Protein Sequences.** *Biophys J* 1996, **71**:148–55.
- [44] Erhan S, Marzolf T, Cohen L: **Amino-Acid Neighborhood Relationships in Proteins. Breakdown of Amino-Acid Sequences into Overlapping Doubles, Triplets and Quadruplets.** *Int J Biomed Comput* 1980, **11**:67–75.
- [45] Karlin S, Blaisdell B, Bucher P: **Quantile Distributions of Amino Acid Usage in Protein Classes.** *Protein Eng* 1992, **5**:729–38.
- [46] Karlin S, Bucher P, Brendel V, Altschul S: **Statistical Methods and Insights for Protein and DNA Sequences.** *Annu Rev Biophys Biophys Chem* 1991, **20**:175–203.
- [47] Karlin S, Burge C: **Trinucleotide Repeats and Long Homopeptides in Genes and Proteins Associated with Nervous System Disease and Development.** *Proc Natl Acad Sci U S A* 1996, **93**:1560–5.
- [48] Altschul S, Gish W, Miller W, Myers E, Lipman D: **Basic Local Alignment Search Tool.** *J Mol Biol* 1990, **215**:403–10.
- [49] Simons K, Bonneau R, Ruczinski I, Baker D: **Ab Initio Protein Structure Prediction of Casp Iii Targets Using Rosetta.** *Proteins* 1999, **Suppl 3**:171–6.
- [50] Hirakawa H, Kuhara S: **Prediction of Hydrophobic Cores of Proteins Using Wavelet Analysis.** *Genome Inform Ser Workshop Genome Inform* 1997, **8**:61–70.
- [51] Hirakawa H, Muta S, Kuhara S: **The hydrophobic cores of proteins predicted by wavelet analysis.** *Bioinformatics* 1999, **15**:141–8.
- [52] Lio P, Vannucci M: **Wavelet Change-Point Prediction of Transmembrane Proteins.** *Bioinformatics* 2000, **16**:376–82.
- [53] Fischer P, Baudoux G, Wouters J: **Wavpred: A Wavelet-Based Algorithm for the Prediction of Transmembrane Proteins.** *Comm. math. sci* 2003, **1**:44 – 56.
- [54] Qiu J, Liang R, Zou X, Mo J: **Prediction of Transmembrane Proteins Based on the Continuous Wavelet Transform.** *J Chem Inf Comput Sci* 2004, **44**:741–7.

- [55] Pashou E, Litou Z, Liakopoulos T, Hamodrakas S: **Wavetm: Wavelet-Based Transmembrane Segment Prediction**. *In Silico Biol* 2004, **4**:127–31.
- [56] de Trad C, Fang Q, Cosic I: **Protein sequence comparison based on the wavelet transform approach**. *Protein Eng* 2002, **15**:193–203.
- [57] Branden CI, Tooze J: *Introduction to Protein Structure*. Garland Publishing 1999.
- [58] ProtScale: **Www.Expasy.Ch/Cgi-Bin/Protscale.Pl**. *In Silico Biol* 1999, **1**:159–62.
- [59] PDBase:
Http://Www.Scsb.Utmb.Edu/Comp_Biol.Html/Venkat/Prop.Html.
Bioinformatics 1998, **14**:749–50.
- [60] Kabsch W, Sander C: **Dictionary of Protein Secondary Structure: Pattern Recognition of Hydrogen-Bonded and Geometrical Features**. *Biopolymers* 1983, **22**:2577–637.
- [61] Doyle D, Cabral J, Pfuetzner R, Kuo A, Gulbis J, Cohen S, Chait B, MacKinnon R: **The Structure of the Potassium Channel: Molecular Basis of K⁺ Conduction and Selectivity**. *Science* 1998, **280**:69–77.
- [62] Arkin I, Brunger A, Engelman D: **Are There Dominant Membrane Protein Families with a Given Number of Helices?** *Proteins* 1997, **28**:465–6.
- [63] Wallin E, von Heijne G: **Genome-Wide Analysis of Integral Membrane Proteins from Eubacterial, Archaeal, and Eukaryotic Organisms**. *Protein Sci* 1998, **7**:1029–38.
- [64] Chen D, Zhao M, Harris S, Mi Z: **Signal Transduction and Biological Functions of Bone Morphogenetic Proteins**. *Front Biosci* 2004, **9**:349–58.
- [65] Kanoh H, Kai M, Wada I: **Phosphatidic Acid Phosphatase from Mammalian Tissues: Discovery of Channel-Like Proteins with Unexpected Functions**. *Biochim Biophys Acta* 1997, **1348**:56–62.
- [66] Kopecek P, Altmannova K, Weigl E: **Stress Proteins: Nomenclature, Division and Functions**. *Biomed Pap Med Fac Univ Palacky Olomouc Czech Repub* 2001, **145**:39–47.
- [67] Ubarretxena-Belandia I, Engelman D: **Helical Membrane Proteins: Diversity of Functions in the Context of Simple Architecture**. *Curr Opin Struct Biol* 2001, **11**:370–6.

- [68] Long S, Campbell E, MacKinnon R: **Crystal Structure of a Mammalian Voltage-Dependent Shaker Family K⁺ Channel**, journal = *Nucleic Acids Res*, volume = **30**, issue = **1**, pages = **264-7** 2005.
- [69] Takeda S, Kadowaki S, Haga T, Takaesu H, Mitaku S: **Identification of G Protein-Coupled Receptor Genes from the Human Genome Sequence**. *FEBS Lett* 2002, **520**:97-101.
- [70] Filipek S, Teller D, Palczewski K, Stenkamp R: **The Crystallographic Model of Rhodopsin and Its Use in Studies of Other G Protein-Coupled Receptors**. *Annu Rev Biophys Biomol Struct* 2003, **32**:375-97.
- [71] Imai T, Fujita N: **Statistical Sequence Analyses of G-Protein-Coupled Receptors: Structural and Functional Characteristics Viewed with Periodicities of Entropy, Hydrophobicity, and Volume**. *Proteins* 2004, **56**:650-60.
- [72] Lomize M, Lomize A, Pogozheva I, Mosberg H: **OPM: Orientations of Proteins in Membranes database**. *Bioinformatics* 2006, **22**.
- [73] O'Donovan C, Apweiler R, Bairoch A: **The human proteomics initiative**. *Trends Biotechnol* 2001, **19**(5):178-81.
- [74] Eyre T, Partridge L, Thornton J: **Computational Analysis of Alpha-Helical Membrane Protein Structure: Implications for the Prediction of 3d Structural Models**. *Protein Eng Des Sel* 2004, **17**:613-24.
- [75] Mitaku S, Hirokawa T: **Physicochemical Factors for Discriminating between Soluble and Membrane Proteins: Hydrophobicity of Helical Segments and Protein Length**. *Protein Eng* 1999, **12**:953-7.
- [76] Engelman D, Zaccai G: **Bacteriorhodopsin Is an inside-out Protein**. *Proc Natl Acad Sci U S A* 1980, **77**:5894-8.
- [77] Rees D, DeAntonio L, Eisenberg D: **Hydrophobic Organization of Membrane Proteins**. *Science* 1989, **245**:510-3.
- [78] Eilers M, Patel A, Liu W, Smith S: **Comparison of Helix Interactions in Membrane and Soluble Alpha-Bundle Proteins**. *Biophys J* 2002, **82**:2720-36.
- [79] Liu W, Eilers M, Patel A, Smith S: **Helix Packing Moments Reveal Diversity and Conservation in Membrane Protein Structure**. *J Mol Biol* 2004, **337**:713-29.
- [80] Eilers M, Shekar S, Shieh T, Smith S, Fleming P: **Internal Packing of Helical Membrane Proteins**. *Proc Natl Acad Sci U S A* 2000, **97**:5796-801.

- [81] Javadpour M, Eilers M, Groesbeek M, Smith S: **Helix Packing in Polytopic Membrane Proteins: Role of Glycine in Transmembrane Helix Association.** *Biophys J* 1999, **77**:1609–18.
- [82] Senes A, Gerstein M, Engelman D: **Statistical Analysis of Amino Acid Patterns in Transmembrane Helices: The Gxxxg Motif Occurs Frequently and in Association with Beta-Branched Residues at Neighboring Positions.** *J Mol Biol* 2000, **296**:921–36.
- [83] Nakai K, Kidera A, Kanehisa M: **Cluster Analysis of Amino Acid Indices for Prediction of Protein Structure and Function.** *Protein Eng* 1988, **2**:93–100.
- [84] Kyte J, Doolittle R: **A Simple Method for Displaying the Hydrophobic Character of a Protein.** *J Mol Biol* 1982, **157**:105–32.
- [85] Engelman D, Steitz T, Goldman A: **Identifying Nonpolar Transbilayer Helices in Amino Acid Sequences of Membrane Proteins.** *Annu Rev Biophys Chem* 1986, **15**:321–53.
- [86] Jones D, Taylor W, Thornton J: **A Model Recognition Approach to the Prediction of All-Helical Membrane Protein Structure and Topology.** *Biochemistry* 1994, **33**:3038–49.
- [87] White S: **The Evolution of Proteins from Random Amino Acid Sequences: Ii. Evidence from the Statistical Distributions of the Lengths of Modern Protein Sequences.** *J Mol Evol* 1994, **38**:383–94.
- [88] White S, Wimley W: **Membrane Protein Folding and Stability: Physical Principles.** *Annu Rev Biophys Biomol Struct* 1999, **28**:319–65.
- [89] Deber C, Wang C, Liu L, Prior A, Agrawal S, Muskat B, Cuticchia A: **Tm Finder: A Prediction Program for Transmembrane Protein Segments Using a Combination of Hydrophobicity and Nonpolar Phase Helicity Scales.** *Protein Sci* 2001, **10**:212–9.
- [90] Wimley W, White S: **Experimentally Determined Hydrophobicity Scale for Proteins at Membrane Interfaces.** *Nat Struct Biol* 1996, **3**:842–8.
- [91] Cid H, Bunster M, Canales M, Gazitua F: **Hydrophobicity and structural classes in proteins.** *Protein Engineering* 1992, **5**(5):373–375.
- [92] Bull H, Breese K: **Surface tension of amino acid solutions: a hydrophobicity scale of the amino acid residues.** *Arch Biochem Biophys* 1974, **16**(2):665–670.
- [93] Fauchere J, Pliska V: **Hydrophobic parameters of amino-acid side chains from the partitioning of N-acetyl-amino-acid amides.** *Eur. J. Med. Chem* 1983, **18**:369375.

- [94] von Heijne G, Blomberg C: **Trans-membrane translocation of proteins. The direct transfer model.** *Eur J Biochem* 1979, **97**:175–181.
- [95] Hopp T, Woods K: **Prediction of Protein Antigenic Determinants from Amino Acid Sequences.** *PNAS* 1981, **78**(6):3824–3828.
- [96] Lawson E, Sadler A, Harmatz D, Brandau D, Micanovic R, MacElroy R, Middaugh C: **A simple experimental model for hydrophobic interactions in proteins.** *J Biol Chem* 1984, **259**(5):2910–2912.
- [97] Levitt M: **A simplified representation of protein conformations for rapid simulation of protein folding.** *J Mol Biol* 1976, **104**:59–107.
- [98] H N, Nishikawa K, Ooi T: **Distinct character in hydrophobicity of amino acid compositions of mitochondrial proteins.** *Proteins* 1990, **8**(2):173–178.
- [99] Radzicka A WR: **Comparing the polarities of the amino acids: side-chain distribution coefficients between the vapor phase, cyclohexane, 1-octanol, and neutral aqueous solution.** *Biochemistry* 1988, **27**(5):1664–1670.
- [100] Roseman M: **Hydrophilicity of polar amino acid side-chains is markedly reduced by flanking peptide bonds.** *J Mol Biol* 1988, **200**(3):513–522.
- [101] Sweet R, Eisenberg D: **Correlation of sequence hydrophobicities measures similarity in three-dimensional protein structure.** *J Mol Biol* 1983, **171**(4):479–488.
- [102] Wolfenden R, Andersson L, Cullis P, Southgate C: **Affinities of amino acid side chains for solvent water.** *Biochemistry* 1981, **20**(4):849–855.
- [103] Jayasinghe S, Hristova K, White S: **Energetics, Stability, and Prediction of Transmembrane Helices.** *J Mol Biol* 2001, **312**:927–34.
- [104] Pilpel Y, Ben-Tal N, Lancet D: **Kprot: A Knowledge-Based Scale for the Propensity of Residue Orientation in Transmembrane Segments. Application to Membrane Protein Structure Prediction.** *J Mol Biol* 1999, **294**:921–35.
- [105] Samatey F, Xu C, Popot J: **On the Distribution of Amino Acid Residues in Transmembrane Alpha-Helix Bundles.** *Proc Natl Acad Sci U S A* 1995, **92**:4577–81.
- [106] Edelman J: **Quadratic minimization of predictors for protein secondary structure. Application to transmembrane alpha-helices.** *J Mol Biol* 1993, **232**:165–91.

- [107] Wallace J, Daman O, Harris F, Phoenix D: **Investigation of Hydrophobic Moment and Hydrophobicity Properties for Transmembrane Alpha-Helices.** *Theor Biol Med Model* 2004, **1**:5.
- [108] von Heijne G: **Membrane Protein Structure Prediction. Hydrophobicity Analysis and the Positive-inside Rule.** *J Mol Biol* 1992, **225**:487–94.
- [109] Needleman S, Wunsch C: **A general method applicable to the search for similarities in the amino acid sequence of two proteins.** *J Mol Biol* 1970, **48**:443–53.
- [110] Hirokawa T, Boon-Chieng S, Mitaku S: **Sosui: Classification and Secondary Structure Prediction System for Membrane Proteins.** *Bioinformatics* 1998, **14**:378–9.
- [111] Chen C, Kernytsky A, Rost B: **Transmembrane Helix Predictions Revisited.** *Protein Sci* 2002, **11**:2774–91.
- [112] Pasquier C, Promponas V, Palaios G, Hamodrakas J, Hamodrakas S: **A Novel Method for Predicting Transmembrane Segments in Proteins Based on a Statistical Analysis of the Swissprot Database: The Pred-Tmr Algorithm.** *Protein Eng* 1999, **12**:381–5.
- [113] Liu L, Deber C: **Combining Hydrophobicity and Helicity: A Novel Approach to Membrane Protein Structure Prediction.** *Bioorg Med Chem* 1999, **7**:1–7.
- [114] Tusnady G, Simon I: **Principles Governing Amino Acid Composition of Integral Membrane Proteins: Application to Topology Prediction.** *J Mol Biol* 1998, **283**:489–506.
- [115] Sonnhammer E, von Heijne G, Krogh A: **A Hidden Markov Model for Predicting Transmembrane Helices in Protein Sequences.** *Proc Int Conf Intell Syst Mol Biol* 1998, **6**:175–82.
- [116] Nilsson J, Persson B, von Heijne G: **Consensus Predictions of Membrane Protein Topology.** *FEBS Lett* 2000, **486**:267–9.
- [117] Krogh A, Larsson B, von Heijne G, Sonnhammer E: **Predicting Transmembrane Protein Topology with a Hidden Markov Model: Application to Complete Genomes.** *J Mol Biol* 2001, **305**:567–80.
- [118] Yuan Z, Mattick J, Teasdale R: **Svmtm: Support Vector Machines to Predict Transmembrane Segments.** *J Comput Chem* 2004, **25**:632–6.

- [119] Viklund H, Elofsson A: **Best Alpha-Helical Transmembrane Protein Topology Predictions Are Achieved Using Hidden Markov Models and Evolutionary Information.** *Protein Sci* 2004, **13**:1908–17.
- [120] Xu E, Kearney P, Brown D: **The Use of Functional Domains to Improve Transmembrane Protein Topology Prediction.** *J Bioinform Comput Biol* 2006, **4**:109–23.
- [121] Bagos P, Liakopoulos T, Hamodrakas S: **Algorithms for Incorporating Prior Topological Information in Hmms: Application to Transmembrane Proteins.** *BMC Bioinformatics* 2006, **7**:189.
- [122] Sadka T, Linial M: **Families of Membranous Proteins Can Be Characterized by the Amino Acid Composition of Their Transmembrane Domains.** *Bioinformatics* 2005, **21 Suppl 1**:i378–86.
- [123] Rost B, Casadio R, Fariselli P, Sander C: **Transmembrane Helices Predicted at 95% Accuracy.** *Protein Sci* 1995, **4**:521–33.
- [124] Manber U, Meyers G: **A New Method for on-Line String Searches.** *SIAM Journal on Computing* 1993, **22**:935–948.
- [125] Kasai T, Lee G, Arimura H, Arikawa S, Park K: **Linear-Time Longest-Common-Prefix Computation in Suffix Arrays and Its Applications.** In *SIAM Journal on Computing* 2001.
- [126] Taylor W: **The classification of amino acid conservation.** *J Theor Biol* 1986, **119**:205–18.
- [127] Haykin S: *Neural Networks: A Comprehensive Foundation.* Prentice Hall 1998.
- [128] NCBI: <http://www.ncbi.nlm.nih.gov/entrez/query.fcgi?db=Genome>. In *Neural Networks: A Comprehensive Foundation*.
- [129] JPRED: **Jpred** **Distribution** **Material:**
[Http://Www.Compbio.Dundee.Ac.Uk/~Www-Jpred/Data/](http://Www.Compbio.Dundee.Ac.Uk/~Www-Jpred/Data/).
- [130] Page **SWMPR:**
http://blanco.biomol.uci.edu/Membrane_Proteins_xtal.html.
- [131] Bank PD: <http://www.rcsb.org/pdb/>.
- [132] Pfam: <http://pfam.wustl.edu/>.
- [133] Swiss-Prot: <http://us.expasy.org/sprot/>.
- [134] GPCRDB: <http://www.gpcr.org/>.

- [135] Kernytsky A, Rost B: **Static Benchmarking of Membrane Helix Predictions.** *Nucleic Acids Res* 2003, **31**:3642–4.
- [136] Apostolico A: **The Myriad Virtues of Subword Trees, Combinatorial Algorithms on Words.** *NATO ASI series in Computer and System Sciences* 1985, **12**:85–96.
- [137] Weiner P: **Linear Pattern Matching Algorithms.** In *NATO ASI series in Computer and System Sciences* 1973.
- [138] Grossi R, Vitter J: **Compressed Suffix Arrays and Suffix Trees, with Applications to Text Indexing and String Matching.** In *NATO ASI series in Computer and System Sciences* 2000.
- [139] Larsson N: **Extended Application of Suffix Trees to Data Compression.** In *NATO ASI series in Computer and System Sciences* 1996.
- [140] Burkhardt S, Crauser A, Ferragina P, Lenhof HP, Rivals E, Vingron M: **Q-Gram Based Database Searching Using a Suffix Array (Quasar).** In *NATO ASI series in Computer and System Sciences* 1999.
- [141] Bishop Y, Fienberg S, Holland P: *Discrete Multivariate Analysis.* MIT Press 1975.
- [142] Penel S, Morrison R, Mortishire-Smith R, Doig A: **Periodicity in Alpha-Helix Lengths and C-Capping Preferences.** *J Mol Biol* 1999, **293**:1211–9.
- [143] Beuming T, Weinstein H: **A Knowledge-Based Scale for the Analysis and Prediction of Buried and Exposed Faces of Transmembrane Domain Proteins.** *Bioinformatics* 2004, **20**:1822–35.
- [144] Zhou X, Alber F, Folkers G, Gonnet G, Chelvanayagam G: **An Analysis of the Helix-to-Strand Transition between Peptides with Identical Sequence.** *Proteins* 2000, **41**:248–56.
- [145] Kuznetsov I, Rackovsky S: **On the Properties and Sequence Context of Structurally Ambivalent Fragments in Proteins.** *Protein Sci* 2003, **12**:2420–33.
- [146] Rost B, Fariselli P, Casadio R: **Topology Prediction for Helical Transmembrane Proteins at 86% Accuracy.** *Protein Sci* 1996, **5**:1704–1718.
- [147] Cserzo M, Eisenhaber F, Eisenhaber B, Simon I: **Tm or Not Tm: Transmembrane Protein Prediction with Low False Positive Rate Using Das-Tmfilter.** *Bioinformatics* 2004, **20**:136–7.
- [148] Cserzo M, Wallin E, Simon I, von Heijne G, Elofsson A: **Prediction of Transmembrane Alpha-Helices in Prokaryotic Membrane Proteins: The Dense Alignment Surface Method.** *Protein Eng* 1997, **10**:673–6.

- [149] Murata K, Mitsuoka K, Hirai T, Walz T, Agre P, Heymann J, Engel A, Fujiyoshi Y: **Structural Determinants of Water Permeation through Aquaporin-1.** *Journal of Molecular Biology* 2000, **407**:599–605.
- [150] Hollier M, Dimmock N: **The C-Terminal Tail of the Gp41 Transmembrane Envelope Glycoprotein of Hiv-1 Clades a, B, C, and D May Exist in Two Conformations: An Analysis of Sequence, Structure, and Function.** *Virology* 2005, **337**:284–96.
- [151] Leitner T, Foley B, Hahn B, Marx P, McCutchan F, Mellors J, Wolinsky S, B K: **HIV Sequence Compendium 2005.** Tech. Rep. LA-UR 06-0680, Theoretical Biology and Biophysics Group, Los Alamos National Laboratory 2005.
- [152] Data LA: <http://www.hiv.lanl.gov/content/hiv-db>. In *Virology*.
- [153] Bagos P, Liakopoulos T, Spyropoulos I, Hamodrakas S: **PRED-TMBB: a web server for predicting the topology of beta-barrel outer membrane proteins.** *Nucleic Acids Res* 2004, **32**(Web Server issue):W400–4.
- [154] Dutzler R, Campbell E, MacKinnon R: **Gating the Selectivity Filter in Clc Chloride Channels.** *Science* 2003, **300**:108–112.
- [155] Bennett P, Carbonell J: **Combining Probability-Based Rankers for Action-Item Detection.** In *Proceedings of HLT-NAACL* 2007.
- [156] Vries J, Munshi R, Tobi D, Klein-Seetharaman J, Benos P, Bahar I: **A Sequence Alignment-Independent Method for Protein Classification.** *Appl. Bioinformatics* 2004, **in press**:483–92.
- [157] Wu C, Whitson G, McLarty J, Ermongkonchai A, Chang T: **Protein Classification Artificial Neural System.** *Protein Sci* 1992, **1**:667–77.
- [158] Liu Y, Carbonell J, Klein-Seetharaman J, Gopalakrishnan V: **Comparison of Probabilistic Combination Methods for Protein Secondary Structure Prediction.** *Bioinformatics* 2004, **20**:3099–3107.
- [159] Li MH, Wang XL, Lin L, Guan Y: **Protein secondary structure pattern discovery and its application in secondary structure prediction.** In *Proceedings of the Third International Conference on Machine Learning and Cybernetics* 2004:1435–40.
- [160] Zhou Y, Mishra B: **Models of Genome Evolution.** *Lecture Notes in Computer Science* 2004, :287–304.

- [161] Zhou H, Zhang C, Liu S, Zhou Y: **Web-based toolkits for topology prediction of transmembrane helical proteins, fold recognition, structure and binding scoring, folding-kinetics analysis and comparative analysis of domain combinations.** *Nucleic Acids Res* 2005, **33**:W193–197.
- [162] Mishra B, Daruwala R, Zhou ea Y: **A sense of life: computational and experimental investigations with models of biochemical and evolutionary processes.** *Omic* 2003, **7**:253–268.
- [163] Tomovic A, Janicic P, Keselj V: **n-gram-based classification and unsupervised hierarchical clustering of genome sequences.** *Comput Methods Programs Biomed* 2006, **81**:137–53.
- [164] Dong Q, Lin L, Wang X: **A Pattern-Based SVM for Protein Remote Homology Detection.** In *Comput Methods Programs Biomed, Volume 6* 2005:3363–3368.
- [165] Singh G, Singh H: **Functional proteomics with biolinguistic methods.** *IEEE Engineering in Medicine and Biology Magazine* 2005, **24**:73–80.
- [166] Dong Q, Wang X, Lin L: **Application of latent semantic analysis to protein remote homology detection.** *Bioinformatics* 2006, **22**:285–90.
- [167] Kurgan L, Homaeian L: **Prediction of Secondary Protein Structure Content from Primary Sequence Alone A Feature Selection Based Approach.** *Lecture Notes in Computer Science* 2005, **3587**:334–345.
- [168] Ruan J, Wang K, Yang J, Kurgan L, Cios K: **Highly accurate and consistent method for prediction of helix and strand content from primary protein sequences.** *Artificial Intelligence in Medicine* 2005, **35**:19–35.
- [169] Zhang B, Chen Z, Murphey Y: **Protein Secondary Structure Prediction Using Machine Learning.** In *Proceedings of International Joint Conference on Neural Networks* 2005.

Index

- α -helix, 24
- amino acids, 20
- aquaporin, 109
- backbone, 22
- BLMT, 39
- cell membrane, 26
- child wavelet, 17
- coil, 24
- cosine similarity, 16
- dilation, 17
- DSSP, 24
- gp41, 111
- helix, 24
- hydrogen bond, 24
- jpred, 60
- k nearest neighbor, 46
- KcsA, 108
- kNN, 46
- latent semantic analysis, 14
- LSA, 14
- main chain, 22
- membrane proteins, 26
- mother wavelet, 17
- multimer, 25
- n-grams, 13
- palh, 110
- PDB, 3
- peptide, 22
- potassium channel, 108
- precision, 66
- primary sequence, 25
- primary structure, 25
- property-segment matrix, 45
- protein data bank, 3
- protein sequence, 25
- protein vocabulary, 45
- proteome, 28
- Q2, 65
- quaternary structure, 25
- recall, 66
- residue, 22
- Secondary structure, 23
- secondary structure, 23, 25
- sequence, 25
- sheet, 24
- side chain, 20
- similarity, 16
- singular value decomposition, 15
- soluble proteins, 26
- superfamily, 27
- SVD, 15
- tertiary structure, 25
- TMpro, 97
- transmembrane proteins, 26
- turn, 24
- vector space model, 15
- VSM, 15
- word-document matrix, 15

Yules q -statistic, 14